NAVAL POSTGRADUATE SCHOOL

MONTEREY, CALIFORNIA

THESIS

NOVEL PARADIGM SUPERCAPACITORS V: SIGNIFICANCE OF ORGANIC POLAR SOLVENTS AND SALT IDENTITIES

by

David A. Backer

June 2017

Thesis Advisor: Jonathan Phillips
Second Reader: Claudia Luhrs

THIS PAGE INTENTIONALLY LEFT BLANK

REPORT DOCUMENTATION PAGE			Form Approved OMB No. 0704-0188

1. AGENCY USE ONLY *(Leave blank)*	2. REPORT DATE June 2017	3. REPORT TYPE AND DATES COVERED Master's thesis

4. TITLE AND SUBTITLE
NOVEL PARADIGM SUPERCAPACITORS V: SIGNIFICANCE OF ORGANIC POLAR SOLVENTS AND SALT IDENTITIES

5. FUNDING NUMBERS

6. AUTHOR(S) David A. Backer

7. PERFORMING ORGANIZATION NAME(S) AND ADDRESS(ES)
Naval Postgraduate School
Monterey, CA 93943-5000

8. PERFORMING ORGANIZATION REPORT NUMBER

9. SPONSORING /MONITORING AGENCY NAME(S) AND ADDRESS(ES)
N/A

10. SPONSORING / MONITORING AGENCY REPORT NUMBER

11. SUPPLEMENTARY NOTES The views expressed in this thesis are those of the author and do not reflect the official policy or position of the Department of Defense or the U.S. Government. IRB number ____N/A____.

12a. DISTRIBUTION / AVAILABILITY STATEMENT
Approved for public release. Distribution is unlimited.

12b. DISTRIBUTION CODE

13. ABSTRACT (maximum 200 words)

This thesis is part of an ongoing program exploring the means to improve the performance, particularly energy and power density, of super dielectric materials (SDM)–based Novel Paradigm (NP) Supercapacitors. The underlying hypothesis is that replacing aqueous solutions with higher-voltage breakdown organic polar solvents (OPS) can increase energy density. Combinations of three different OPS and four salts were studied, as well as mixtures of OPS and aqueous solvents and organic salts. The NP Supercapacitors were tested for capacitor performance as a function of frequency. The effectiveness of the OPS solutions was determined by evaluating the energy density, power density, capacitance and dielectric constant as a function of time.

The three OPS evaluated in this study successfully attained operating voltages in the range of 3.0–5.0 volts. These results are significantly higher than realized in previous studies, which maxed out at 2.3 volts. However, the higher voltages did not result in higher energy and power densities, as the best results attained were in the range of 90–155 J/cm^3 and 700–950 W/cm^3, respectively. These results are significantly lower than realized in previous studies by our team but still higher than the results presented in the general literature for all capacitor types, with the exception of a few prototype graphene-based supercapacitors.

14. SUBJECT TERMS
capacitor, super dielectric material, titanium dioxide, nanotube, sodium chloride, potassium nitrate, boric acid, sodium nitrate, n-methyl-2-pyrrolidone, dimethyl sulfoxide, propylene carbonate, ethylenediaminetetraacetic acid

15. NUMBER OF PAGES
179

16. PRICE CODE

17. SECURITY CLASSIFICATION OF REPORT	18. SECURITY CLASSIFICATION OF THIS PAGE	19. SECURITY CLASSIFICATION OF ABSTRACT	20. LIMITATION OF ABSTRACT
Unclassified	Unclassified	Unclassified	UU

NSN 7540-01-280-5500 Standard Form 298 (Rev. 2-89)
Prescribed by ANSI Std. 239-18

THIS PAGE INTENTIONALLY LEFT BLANK

Approved for public release. Distribution is unlimited.

NOVEL PARADIGM SUPERCAPACITORS V: SIGNIFICANCE OF ORGANIC POLAR SOLVENTS AND SALT IDENTITIES

David A. Backer
Commander, United States Navy
B.S., United States Naval Academy, 2001
M.A., Naval Postgraduate School, 2007
MEM, Old Dominion University, 2011

Submitted in partial fulfillment of the
requirements for the degree of

MASTER OF SCIENCE IN MECHANICAL ENGINEERING

from the

NAVAL POSTGRADUATE SCHOOL
June 2017

Approved by: Jonathan Phillips, Ph.D.
Thesis Advisor

Claudia Luhrs, Ph.D.
Second Reader

Garth Hobson, Ph.D.
Chair, Department of Mechanical and Aerospace Engineering

THIS PAGE INTENTIONALLY LEFT BLANK

ABSTRACT

This thesis is part of an ongoing program exploring the means to improve the performance, particularly energy and power density, of super dielectric materials (SDM)–based Novel Paradigm (NP) Supercapacitors. The underlying hypothesis is that replacing aqueous solutions with higher-voltage breakdown organic polar solvents (OPS) can increase energy density. Combinations of three different OPS and four salts were studied, as well as mixtures of OPS and aqueous solvents and organic salts. The NP Supercapacitors were tested for capacitor performance as a function of frequency. The effectiveness of the OPS solutions was determined by evaluating the energy density, power density, capacitance and dielectric constant as a function of time.

The three OPS evaluated in this study successfully attained operating voltages in the range of 3.0–5.0 volts. These results are significantly higher than realized in previous studies, which maxed out at 2.3 volts. However, the higher voltages did not result in higher energy and power densities, as the best results attained were in the range of 90–155 J/cm^3 and 700–950 W/cm^3, respectively. These results are significantly lower than realized in previous studies by our team but still higher than the results presented in the general literature for all capacitor types, with the exception of a few prototype graphene-based supercapacitors.

THIS PAGE INTENTIONALLY LEFT BLANK

TABLE OF CONTENTS

LIST OF FIGURES

THIS PAGE INTENTIONALLY LEFT BLANK

LIST OF TABLES

LIST OF ACRONYMS AND ABBREVIATIONS

$BaTiO_3$	Barium Titanate
C	Capacitance
DI	Deionzed Water
DMSO	Dimethyl Sulfoxide
ED	Energy Density
EDLC	Electric Double Layer Capacitors
EDTA	Ethylenediaminetetraacetic acid
EMALS	Electromagnetic Aircraft Launch System
F	Farad
FEL	Free Electron Laser
HSA	High School Area
Hz	Hertz
J	Joules
J/cm^3	Joules per Cubic Centimeter
kg	Kilograms
KOH	Potassium Hydroxide
LaWS	Laser Weapons System
m	Meters
m^3	Cubic Meters
mm	Millimeter
m/s	Meters per Second
MW	Megawatt
NaCl	Sodium Chloride
$NaNO_3$	Sodium Nitrate
NaOH	Sodium Hydroxide
NH_4Cl	Ammonium Chloride
NH_4F	Ammonium Fluoride
NMP	N-Methyl-2-Pyrrolidone
NP	Novel Paradigm
NTSDM	Nanotube Super Dielectric Material

PC	Polypropylene Carbonate
Q	Electrical Charge
RC	Resistor-Capacitor
SDM	Super Dielectric Material
SEM	Scanning Electron Microscope
TiO	Titanium (II) Oxide
TiO_2	Titanium (II) Dioxide (aka Titania)
USN	United States Navy
V	Volts
W	Watts
W-h	Watt-hour

ACKNOWLEDGMENTS

“Great thesis data, but the scientific world will yawn.”

Dr. Phillips, thank you for affording me unlimited freedom to make this two-year research endeavor extremely enjoyable and satisfying. The occasional “rudder” to get me back on course and the confidence boosting were invaluable when the results were not going our way. In the end, I am confident that we have positively contributed to the literature.

Dr. Luhrs, thank you for ensuring my work was centered on sound engineering principles. Attaining your high standards for academic work is possible because your passion and drive inspires your students to do their best.

Dr. Menon, thank you for all the characterization assistance despite my extremely short timelines. The Naval Postgraduate School is going to miss your guidance and expertise. Congratulations and enjoy your well-deserved retirement.

To my wife: Our dual-military relationship has kept us apart for yet another tour. Despite the 5600-mile separation, you provided unwavering support and encouragement. I love you.

THIS PAGE INTENTIONALLY LEFT BLANK

I. INTRODUCTION

This thesis is part of a larger effort conducted in facilities around the world to meet an urgent need in advancing energy storage techniques. Various uses, from automobiles to satellites, require the creation of electric capacitors that are inexpensive, yet have higher energy and power densities than those presently available. The Navy has a unique need to provide high energy/power density capacitors that operate in a very short amount of time. The power shipboard systems, like the free electron lasers, Railguns and Electromagnetic Aircraft Launch System (EMALS), are termed short pulse systems. The Navy needs capacitors that can provide the necessary power, yet have a footprint compatible with the limited space aboard a navy ship.

Four years ago our team at the Naval Postgraduate School invented a new class of materials, Super Dielectric Materials (SDM) that when used as the dielectric in capacitors of novel design, Novel Paradigm (NP) Supercapacitors, may provide the power and energy density required to address the demand for energy storage. Building and characterizing a new class of materials, and assembling them into a useful form, is generally a daunting task, and SDM and associated NP Supercapacitors are not an exception. To date, three different families of NP Supercapacitors have been invented and tested based on variations of SDM: powder based SDM (P-SDM), tube based SDM (T-SDM) and fabric based SDM (F-SDM).

The fundamental SDM theory is that solvents containing dissolved ions should have dielectric constants, much higher than any previously discovered form of dielectric material. Therefore, capacitors built with these materials should have higher capacitance and energy densities than any other type of capacitor. As noted, this very general formulation has many particular forms. Also, there is not a sufficient theoretical basis for predicting behavior, hence detailed, exacting laboratory studies and analysis are required.

Among the parameters that must be studied experimentally for their impact on the key parameters of energy and power density, dielectric constant, and reliability are different i) ‘containment’ strategies, ii) salts, iii) layer thicknesses, and iv) polar solvents.

So far, three different ‘containments’ have been developed and partially tested, i) high surface area, highly porous refractory oxide powders (P-SDM), ii) micron scale, non-electrically conductive tubes created on a titanium metal base (T-SDM) and iii) woven fabrics (F-SDM) [1]. Each of these containments has also been tested in different forms. The powders tested include alumina, silica and fumed silica while aqueous solutions containing dissolved ions have been tried. This includes trying aqueous solutions in different concentrations and salts, including NaCl, boric acid, KOH and NH_3OH. The significance of empirical testing was demonstrated by some surprising findings that in fact, the highest salt concentration solutions are not the best dielectrics. Silica proved better than alumina for no clear reason. Also, the theory had to be revised to explain that the energy density of T-SDM is not a function of tube length.

In addition to empirical testing of variations of the physical structure and chemical composition of the SDM, it was also necessary to invent a reliable method to test performance as a function of frequency. Existing methods for testing capacitors are not adequate for predicting some key behaviors required for engineering design such as actual power delivery over short intervals.

This thesis is focused on a piece of the bigger picture. Specifically, the work done herein is the first study of the efficacy of replacing aqueous salt solutions with non-aqueous polar solvents containing dissolved salts in T-SDM. This class of solvents found in batteries and some other applications is generally referred to as ‘organic solvents.’ For our work, we prefer the term ‘polar organic polar solvents’ (OPS) because it reflects the needs of SDM theory. That is, for a solvent to be useful for SDM it must have a high concentration of mobile ions and only polar solvents are capable of dissolving salts, hence creating high densities of mobile ions in solution [2].

OPS were selected for study because they have higher ‘breakdown’ voltages than water and therefore may have higher energy densities. That is, energy density of capacitors is roughly a function of two parameters, the maximum operating voltage squared and the dielectric constant, as show in Equation 1.

$$Energy\ Density_{General} = \frac{\varepsilon\varepsilon_o A}{2t} V^2 \qquad (1)$$

Some OPS reportedly have breakdown voltages in excess of twice that of water. Given that the energy density is proportional to the square of voltage the potential for significant increase in energy density based on switching to OPS salt solutions from aqueous salt solutions is readily apparent. In short, this thesis was designed to test the following hypothesis*: Super dielectric materials based on organic polar salt (OPS) solutions will operate to a higher maximum voltage that, in turn, will produce higher energy densities than aqueous salt solution based super dielectric materials.*

In order to test this hypothesis, this thesis presents the results of testing T-SDM prepared by anodization containing three OPS, each with four different salts, and at several salt concentrations. In addition, based on some serendipitous observations, mixtures of aqueous saturated salt solutions and OPS were studied as well. The result of this work indicated that *the hypothesis is not correct*. It was found that although the operating voltages did increase, significantly in some cases, the capacitance decreased significantly in all cases. The product of these two factors led to a net decrease in energy density relative to the best aqueous salt solution based SDM. Another significant finding was that OPS/aqueous salt solution mixtures were better than pure OPS solutions. Finally, an explanation for the significant lowering of the capacitance of the OPS salt solutions relative to the aqueous salt solution work was postulated, and is consistent with the data collected: *All of the OPS dissolved far less salt than the water. The explanation for the impact of reduced salt in solution on performance is provided in the SDM theory section*.

A. MOTIVATION

It is now clear that a thorough investigation of this new class of materials and capacitors based on these materials is an effort that will take many years. Is further study of SDM a reasonable investment? The answer based on the work to date is a resounding yes. The best prototypes developed, using simple, inexpensive materials, and easy assembly, are far better than commercial Electric Double Layer Supercapacitors (EDL Supercapacitors) which are undoubtedly the best presently available to the Navy and other organizations. NP Supercapacitors tested by our team rival the best graphene based

EDL Supercapacitors for power and energy density, but clearly the NP Supercapacitors are assembled from far less expensive materials. The race to create the next generation of commercial supercapacitors is on, and NP Supercapacitors are a definite entry.

This work addresses the Navy's need to obtain a more effective means to power such high-energy systems as the Railgun, Electromagnetic Aircraft Launch System (EMALS) and the Free Electron Laser (FEL) [3]–[5]. The common thread amongst these weapons systems is the need for a large and instantaneous delivery of power with the capability for fast recharge. The current directed energy needs are fulfilled with ship's electricity system, which is already responsible for running propulsion, support equipment and vital ship systems [4]. Specific to capacitors, the technology does exist to relieve, and with a lot of concessions, replace the overburdened energy systems. However, in order for current capacitor technology to replace current energy systems would require an enormous amount of space.

The Railgun is a high-energy weapons system that can launch a 3 kg projectile such that it strikes a target at a distance of 111 miles at a velocity of Mach 7 (~2,401 m/s) [6]. A major problem with creating and integrating such a system is few existing ships can deliver the energy required to make this a viable weapon to replace what is considered competent, reliable and sufficient weapons systems [7]. The new Zumwalt class of destroyers can produce 78 megawatts of power but a properly functioning Railgun system requires 25 megawatts [8]. However, it is not feasible to take one-third of a ship's available power and the addition of a battery or capacitor bank assigned directly to the Railgun would require a lot of space [2]. Studies have shown that a capacitor bank capable of providing the required energy to fire a single shot of the Railgun would require 30 m^3 of space [9].

EMALS is designed to replace the conventional steam catapults used onboard aircraft carriers by using an electromagnetic field to accelerate aircraft to launch speeds. EMALS contains multiple subsystems that are responsible for storing, converting, delivering and distributing energy to the launching system [10]. Of particular interest to this research is the energy storage subsystem (ESS), specifically the motor generator [11]. The USS GERALD FORD (CVN-78) is the first carrier selected for EMALS installation

with the biggest physical items being the 12 motor generators that are responsible for creating and storing the energy [12]. This is a significant requirement considering a motor generator produces 60 mega joules, weighs over 36,000 kilograms (80,000 pounds) and requires a 30-m^3 space. Utilizing current capacitor technology, a capacitor bank the size of 750 m^3 is required to produce the same amount of energy [2].

The FEL is a weapons system that generates a high-intensity laser light sourced from the collection of unbounded accelerated high-energy electrons [13]. The FEL initially required 14 kilowatts [14] but technological advances and studies place current requirements at 100 kilowatts [15]. However, the 100-kilowatt requirement is based on the power of the released energy beam, the support equipment will add additional burdens to an already taxed ship's electrical system. If capacitors were designed to alleviate some of the electrical responsibility of the FEL, a comparable sized bank of capacitors would require .15 m^3 of space [2].

The Navy has invested a significant amount of time and money in the technological advancement of the Railgun, EMALS and FEL systems. The procurement and implementation of these power-hungry systems are unique in that they provide the warfighter with the ability to counter emerging threats while also adhering to policy changes focused on making the Navy use energy more efficiently [16].

B. BACKGROUND

1. Technologies

Capacitors are fundamental electric circuit elements that store electrical energy [17]. Current capacitor technology is categorized as an electric double layer supercapacitor (EDLC) or advanced dielectric based supercapacitors [18]. EDLC's, regardless of the subcategory, provided large power densities but low energy densities relative to batteries, ca 10% by volume [17]. Current EDLC research focuses on implementing transition metal oxides for the electrode material in an effort to increase the energy density output while maintaining a favorable high power output density [17]. Capacitors are classified by dielectric class and include ceramic, polymer, mixed metal or insulating, colossal and SDM [18]. The dielectric class capacitors are commonly used in

low energy demand applications like rectifiers, filters, computer memory and consumer electronic devices [2]. This is due to the devices inability to effectively store energy [19].

Another method to classify capacitors, which is the preferred method for this thesis, is by interpreting capacitor performance parameters based on the standard parallel plate capacitor equation [20] expressed in Equation 2.

$$C = \frac{\varepsilon \varepsilon_o A}{t} \tag{2}$$

where C is capacitance, ε is dielectric constant of the material, ε_o is the permittivity of air, 8.85E-12 [Farad/m], A is the area of the electrode and t is the thickness of the dielectric [2], [18]. From Equation 2, there are only three variables that can change–ε, A and t. Coincidentally, there are three competing capacitor types that have attempted to increase the capacitor performance parameters by changing one of those three variables. Figure 1 shows how the best capacitors from this thesis fared against the competing electronic storage devices. Additionally, a commercial supercapacitor was analyzed with the same testing equipment and the results are also displayed in Figure 1.

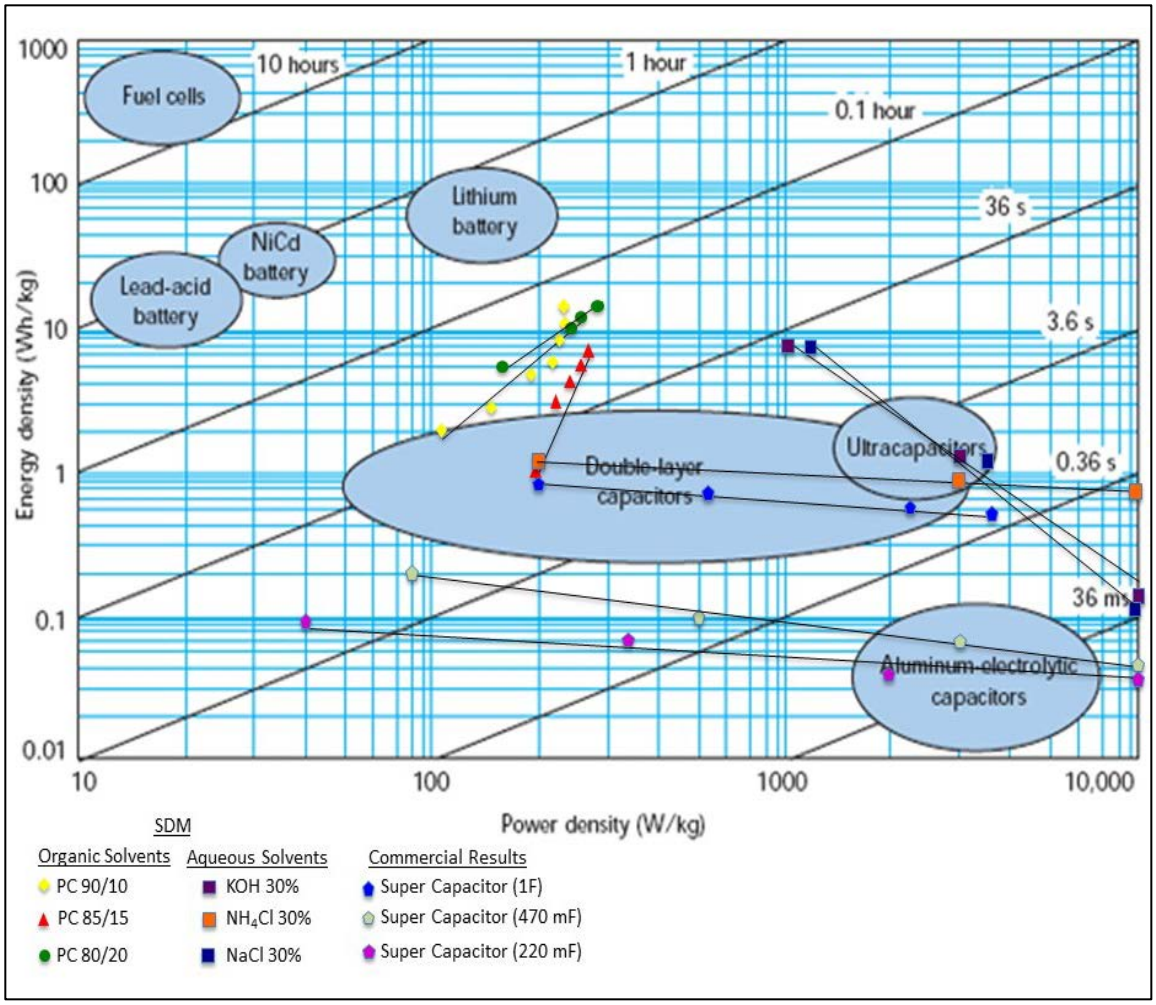

Figure 1. Comparison of Competing Electronic Storage Devices. Adapted from: [2], [21].

a. Type I

This method increases capacitor performance parameters by changing the area of the electrode. A. Changing the area exploits conductive materials that possess the highest surface area per unit mass, or unit volume [22]. Examples of this material include carbon, conductive clays, some metal and oxides and graphene. These are the same materials that were generally considered for use as the electrode material in EDLCs. They benefit from high power densities while suffering from low energy densities. Additionally, capacitors of this type possess relatively low dielectric constants but these low values are not indicative of the overall performance of the capacitor.

b. Type II

This method increases capacitor performance parameters by decreasing the thickness of the dielectric material, t. This method has experienced significant challenges because of the difficulty involved with shrinking existing dielectric materials that already measure in the 1E-6 range [2]. Additionally, it appears that a non-linear relationship exists between decreasing the thickness of the dielectric material and the resulting performance results. This makes subsequent testing difficult, unpredictable and undesirable [18] and a major reason why this method has garnered little attention.

c. Type III

This method increases capacitor performance parameters by changing the dielectric constant, ε. As stated earlier, there are four subcategories associated with this type of capacitor. The first subcategory involves working with a derivative of barium titanate because of the historically high dielectric constants of up to 1E5 [23]. However, research in this subcategory has plateaued and attention has been redirected towards other subcategories. The second subcategory mixes barium titanate with ceramic or metal particles. This has seen limited success with results not significantly greater than values obtained with isolated barium titanate and barium titanate derivatives [24]. The third subcategory creates solid dielectric materials possessing dipoles based on surface state defects [18]. Extensive work has been conducted by Lunkenheimer [25]–[27] which produced dielectric constants in the range of 1E4. These dielectric constants are classified colossal dielectric constants (CDC) [27]. The fourth subcategory focuses on the newly discovered Super Dielectric Materials (SDM). SDM materials are unique in that the dielectric value is a function of both the thickness of the material and the material itself [18]. Research utilizing this method has reported extremely positive results with capacitor performance parameters far exceeding existing values [2], [23], [28], [29].

2. Capacitor Theory

This section discusses general capacitor theory as it pertains to the hypothesis presented in this thesis, specifically parallel plate capacitor theory. Generalizing the theory provides a baseline from which to compare the capacitors based on the Type I, Type II and Type III methods for increasing the capacitor performance parameters. The first capacitor was called the Leyden jar and invented by Pieter van Musschenbroek in 1746 at the University of Leyden in Holland [30]. Its design consisted of a jar wrapped in a thin conductive metal foil. Two layers were formed inside and outside the jar. The key to this design, and the basis for subsequent designs was the separation of the metal foil by a non-conductive material. In this case, the glass was the non-conductive material.

A capacitor is an electrical device [2] used to store energy while capacitance is the ability of a device to store an electric charge. In a capacitor, a dipole field is created when equal and opposite charges are placed on two electrodes of a parallel plate capacitor [18]. Figure 2 shows the formation of an electric field between the parallel plates in a parallel plate capacitor.

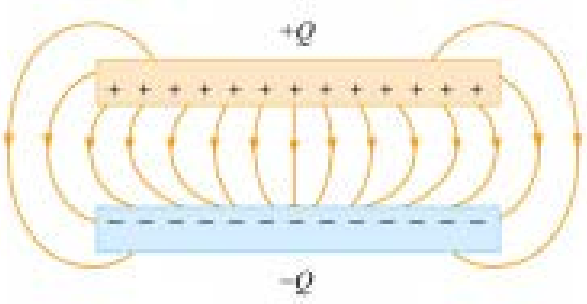

Figure 2. Electric Field between Plates of a Parallel Capacitor. Source: [20].

The size of the dipole and the strength of the field depend on the distance of the charge points and are independent of the amount of charge on the plates [18]. There is a dipole field created by the dielectric material and this reduces the net magnitude of the field created by the capacitor at every point in space [2]. Equation 3 explains how to bring a charge from a point in space to the electrode surface.

$$V = \int E \cdot dl \tag{3}$$

where V is the voltage, E is the electric field and l is the distance measured along a path. As the electrodes get closer the dipole field, energy, is smaller at every point in space and due to the direct relationship between energy and voltage from Equations 1 and 3, the voltage will decrease [18]. It is also important to present Equation 4 because it is the next step to understanding parallel plate capacitor theory.

$$C = q/\mathrm{V} \tag{4}$$

where C is the capacitance, q is the number of charges on the electrodes and V is the net voltage between electrodes. Continuing the above scenario, when the voltage is decreased the capacitance is increased. In the case of Equation 3, voltage is changed as a function of energy, while the charge current stays constant-there is no value to change current [18]. This important concept is the basis for the testing schedules created for this thesis-hold current constant and changes in voltage will change the capacitance. As demonstrated in Equation 1, the ability of the device to store energy is a function of the type of material, the area of the material or the distance between the conductive materials.

Equation 5 provides the ability to compare the energy and power densities between the three types of capacitors. This is necessary because the three types of capacitors are a different size, shape and composition. Dividing Equation 1 by the volume of the respective capacitor did this.

$$Energy\ Density_{Comparison} = \frac{\varepsilon\varepsilon_o A}{2t*Volume}V^2 = \frac{\varepsilon\varepsilon_o A}{2t*A*t}V^2 = \frac{\varepsilon\varepsilon_o}{2t^2}V^2 \tag{5}$$

3. SDM Theory

This thesis focused on increasing the capacitor performance parameters by increasing the dielectric value and decreasing the distance between the electrodes. The dielectric value changed because of the increase in size and concentration of salt dipoles present in the ionic salt solution. The larger the salt dipoles of the dielectric, the better the capacitor. This is because larger dipoles of the dielectric material are more effective in canceling the dielectric field of the charges on the electrode [18]. The first SDMs postulated that the largest dipoles would come from solutions containing dissolved salts subjected to an electric field [18]. Conversely, if a solution does not contain a sufficient amount of dissolved salts, the formed dipoles are small and lack mobility and therefore

not as effective in canceling the field created by the charges placed on the capacitive plates. This concept is illustrated in Figure 3.

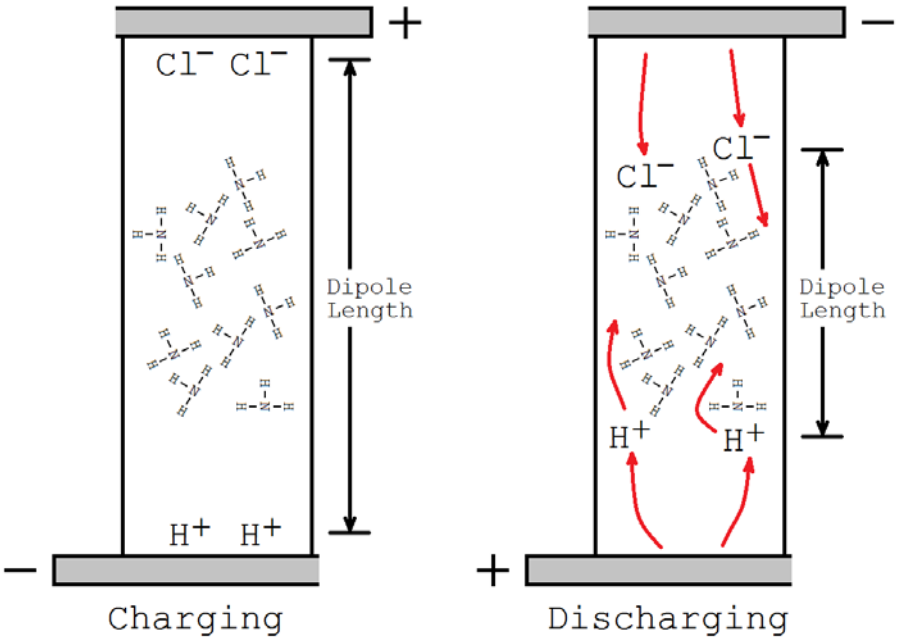

Figure 3. Visual Description of SDM Theory and Dipole Lengths

Barium titanate was initially selected for SDM testing because of the high dielectric constants obtained from their use in other types of capacitors. Results were in the range of 1E5 [23]. However, the energy density results for the barium titanate SDM testing were not spectacular because researchers were not able to sufficiently decrease the thickness between the electrodes [18].

This led to the development of the Novel Paradigm Supercapacitor (NPS) and presents the second area of study this thesis attempted to exploit - minimizing the distance between the electrodes. The NPS were made from anodized titanium films that consisted of an insulating material of titanium dioxide [2]. The NPS minimized the distance between the electrodes by creating an array of nanotubes that placed the electrodes at a distance of 8E-6 microns. The nanotubes were a matrix of symmetric, hollow and tubular array of straight columns. The hollow tubes allowed for more of the salt ionic solution to exist between the electrodes plates and also served as the insulating

material to keep the electrodes apart. The combination of the minimized distance between electrodes and the dense ionic salt solution would produce capacitors with high energy and power densities. Table 1 shows how the TiO_2 samples compared to other types of SDMs.

Table 1. Dielectric Materials with Dielectric Constants Greater Than 10^7. Source: [18].

Super Dielectric Material	Highest dielectric constant
Nylon fabric saturated with aqueous NaCl	$1.2x10^{11}$
Fumed silica powder with aqueous NaCl	$1x10^{11}$
TiO_2 nanotubes with aqueous NaCl	$7x10^9$
Porous alumina powder with aqueous NaCl	$1x10^{11}$
TiO_2 nanotubes with aqueous $NaNO_3$	$7x10^9$
Porous alumina powder with boric acid	$5x10^9$
Illuminated perovskite	$1x10^7$
Wet perovskite	$1x10^7$
Li/Na ion solid electrolytes	$1x10^7$

C. FOCUS OF PRESENT STUDY

1. Thesis Theory

This thesis continues the Naval Postgraduate School's SDM work completed by Gandy [23], Fromille [1], Jenkins [29] and Lombardo [2]. Fromille and Jenkins employed the first generation SDM that utilized a circular plate parallel capacitor filled with a powder-based SDM paste. Their dielectric values far exceeded previously established values that peaked at 1E5. Jenkins reported dielectric values as high as 1E9 [29] and Fromille reported dielectric values as high as of 1E8 [28]. Gandy and Lombardo employed the second generation SDM that studied the effects of aqueous salt solutions placed in-between flat parallel plate capacitors. These structures were composed of TiO_2 and created on titanium metal using anodization. They tested the TiO_2 samples on various salt solutions, at different concentrations [2] and placed in the same aqueous solvent, distilled water. All researchers reported dielectric values as high as 1E7 and energy densities as high as 400 J/cm^3 [23].

2. Outline

This study will help determine if the NPS constructed of titanium based SDM can provide power delivery and capacity to new weapons such as the Railgun and laser weapons. This is in addition to the excellent scientific value obtained from the frequency performance data that indicates any improvements in the model of SDM. These NPS will be tested for capacitive performance as a function of a number of parameters including solvent identity, salt concentration, titania tube length, voltage and frequency. The engineering goal is to create a second-generation T-SDM that can operate at a higher voltage than the first-generation T-SDM and thus will have higher energy and power delivery at ~1Hz than achieved previously.

This was accomplished using the following outline. The Experimental Methods section discusses the anodization process, capacitor construction, Galvanostat operation, constant current analysis and characterization utilizing the scanning electron microscope. This section also explains the selection of the organic solvents and salt solution combinations. Lastly, this section presents the testing schedules used to determine the

capacitive performance parameters of the selected non-aqueous solvent and salt ionic solution combinations.

The Results section presents the analysis of the capacitor performance parameters. The results will include graphs that analyze power and energy densities versus discharge time. Tabular results display the dielectric values, capacitance, power and energy densities and discharge time. Particular attention will be given to the graphical results of the charge and discharge cycles and the energy and power density compared to discharge time. The Conclusions section compares the energy and power densities of the selected non-aqueous solvent and salt ionic solutions as a function of frequency.

II. EXPERIMENTAL METHODS

This chapter discusses the methods required to create the second-generation T-SDM and test its capacitive performance. The first section discusses how the TiO_2 samples were created, characterized and tested. Due to the many tests conducted in support of this thesis, concerted efforts were made to ensure each test was carried out in a similar manner in order to control as many variables as possible. The efforts made to control as many variables as possible provided a sense of confidence that the results obtained were a direct effect of intended changes. The second section explains the selection process of the solvents and salts and the final solutions used for testing. The third section outlines the testing schedules, parameters and requirements.

A. CREATING TIO_2 SAMPLES

This procedure produced an 8-µm long titania nanotube array that served two purposes. It provides the spacing between the two-capacitor plates and it also serves as a vessel to hold the ionic salt solution. The titania array was created in a two-step process that consisted of a preliminary setup and an electrochemical anodization process. The preliminary setup focused on establishing equipment parameters and preparing the sample and chemical solution. The electrochemical process places a strip of 95% pure titanium in an Ammonium Fluoride (NH_4F), distilled water and ethylene glycol solution and applying a constant voltage for a set time.

1. Creating Samples

The titania sample was prepared by cutting an anode and cathode from a 95%, .05 mm sheet of titanium. The anode strip was cut into a 3x1 cm^2 rectangle while the cathode strip was cut a bit larger at 3.5x1.6 cm^2. Both pieces were rinsed with distilled water and placed in a 100% ethanol (ethyl alcohol) bath for 10 minutes to remove contaminants. Concurrently, three power supplies were set to 60 volts. This voltage was essential as it meets the voltage and current requirements that guarantee the aforementioned morphology [31]. Lastly, a number of beakers, pipets and cylinders were cleaned with

distilled water and allowed to air dry. These vessels were used to hold the chemical solution that supported the reaction process.

The clean titanium anode and cathode were placed in a mixture of 80-mL of ethylene glycol, 1.6-mL of distilled water and 0.1358-g of NH_4F. It was important to quickly add the NH_4F to the distilled water and ethylene glycol to minimize the amount of moisture absorbed from the air.[1] Once the anode and cathode were placed in the solution, a constant 60 volts was applied for 46 minutes.

Figure 4 shows how the anode and cathode are placed in the solution. The anode and cathode are separated at a distance of 2 cm and submerged until approximately 2 cm are sticking out of the solution. Indication of proper setup occurs when bubbles form on the cathode and the anode turns a bronze/gold color. The TiO_2 sample is rinsed in distilled water, air-dried and placed in a test tube for future use or post analysis testing.

Figure 4. Anode and Cathode Sitting in Solution. Source: [2].

[1] There were issues with deteriorated TiO_2 samples that stemmed from NH_4F that was found out of the desiccant bottle for an unknown amount of time. It was assumed that the NH_4F had absorbed a significant amount of moisture from the air.

2. Characterization

Characterization was conducted using the scanning electron microscope (SEM). Figure 5 displays the Zeiss SEM Neon 40 with 2 keV electron beam. It was selected for characterization and imagery because of its high resolution, ability to control magnification and a large depth of field [32]. The SEM was used to observe three samples in order to verify lengths and inspect structural integrity of the titania array elements. This was important for two reasons. The first was to validate that the TiO_2 procedure produced a straight, tubular and 8-um long titania nanotube array. The second reason was to investigate the titania nanotube array of some burned samples. This was important because some of the samples exhibited burned marks. It was assumed that the burning led to a decrease in dielectric constant and capacitance values during the longer tests.

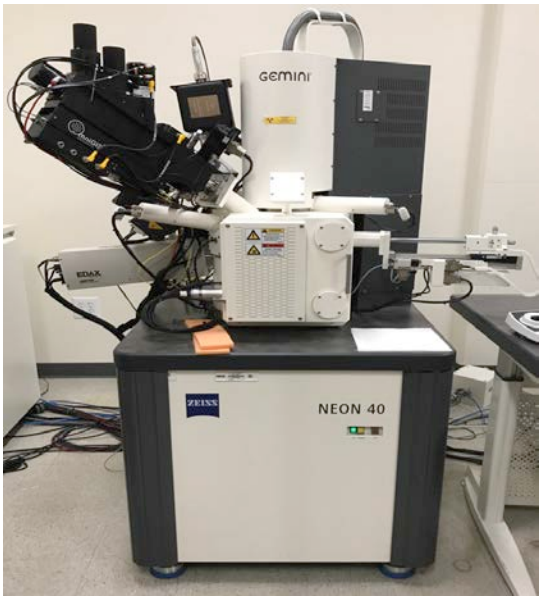

Figure 5. Zeiss 40 Neon SEM

Three samples were selected for SEM imagery. The first sample was tested in a solution of PC and Boric acid salt solution. The second sample was tested in a solution of NMP and NaCl salt solution. The final sample was tested in a solution of DMSO and NaCl salt solution. All three samples are from post testing. A sample from post testing is

first subjected to a 20-minute soak in the selected solvent and salt solution. The sample was then run at the Low Frequency, High Frequency and FHS testing schedules. After testing, the sample was rinsed in DI water and soaked in ethyl alcohol for four hours to remove as much salt as possible from the TiO_2 sample. To remove the moisture from the sample it was placed in the vacuum chamber for six days.

Figure 6 shows how the samples were mounted for the SEM and depicts the various zones associated with a sample. SEM imagery concentrated on the 2-cm^2 testing area since it possessed the greater amount of well-formed and straight nanotube array. The area near the transition zone and the edges were generally avoided for imagery because of possible damage incurred during sample creation due to crimping. Alligator clips were used to hold the samples in the NH_4F solution and caused uneven and not well-formed nanotube array to form in the vicinity of the clips.

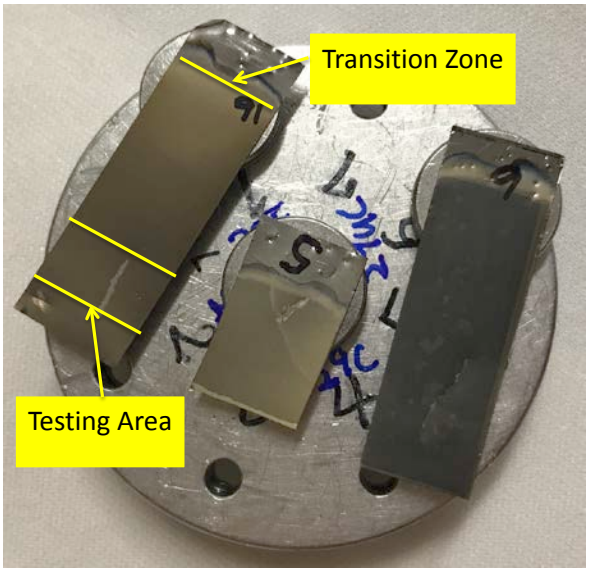

Figure 6. Samples Mounted for SEM Characterization

In order to expose the edges of nanotube array in the 2-cm^2 area, a scratch was created in the TiO_2 using a sharp set of tweezers. Table 2 shows the lengths of the nanotube array taken at various sites on all three samples. These results validated the processes utilized in [31] and created TiO_2 samples that conform to the desired morphology.

Table 2. Lengths of Nanotubes at Various Sites in Micrometers (μm)

	Sample 1 (μm)	Sample 2 (μm)	Sample 3 (μm)
	8.312	7.469	8.169
	8.409	7.401	8.036
	8.399	7.339	7.271
	8.736	7.497	7.834
	8.386	7.519	7.494
	8.333	7.327	8.151
Average	8.43	7.43	7.83

Figure 7 shows how the lengths were determined using the SEM. In order to obtain accurate lengths, it was ideal to find a sample site that was perpendicular to the viewing plane. It was difficult to find a sample site that was not skewed or tilted at a certain angle.

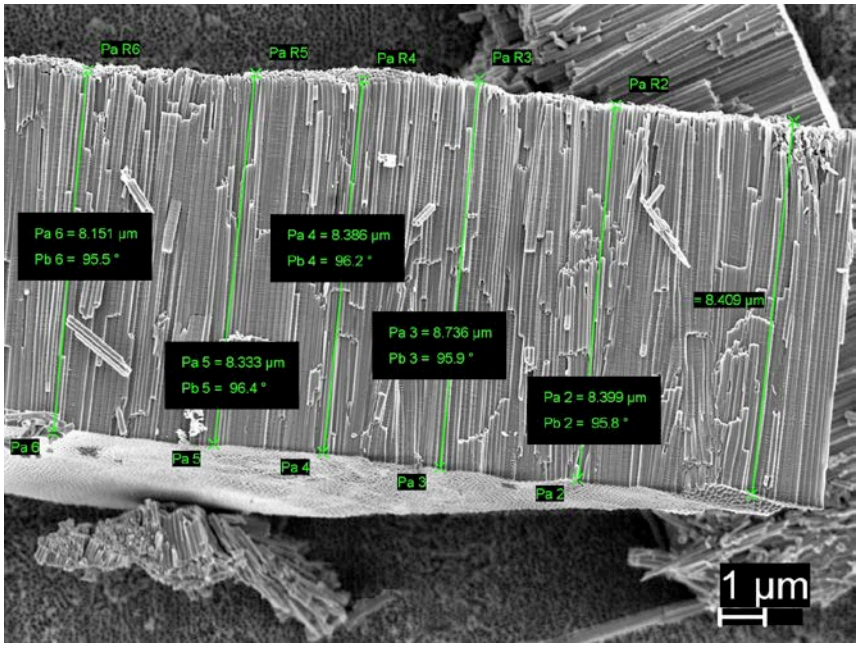

Figure 7. Length Determination with SEM

Figure 8 shows that the nanotubes are straight and close formed, creating a symmetric anodized matrix. The broken pieces of the nanotubes display a near perfect diameter and are of the ideal thickness of 0.9 µm [2]. Finally, the area circled in yellow presents the bottom of the nanotubes and displays the near perfect rounded ends associated with the desired morphology.

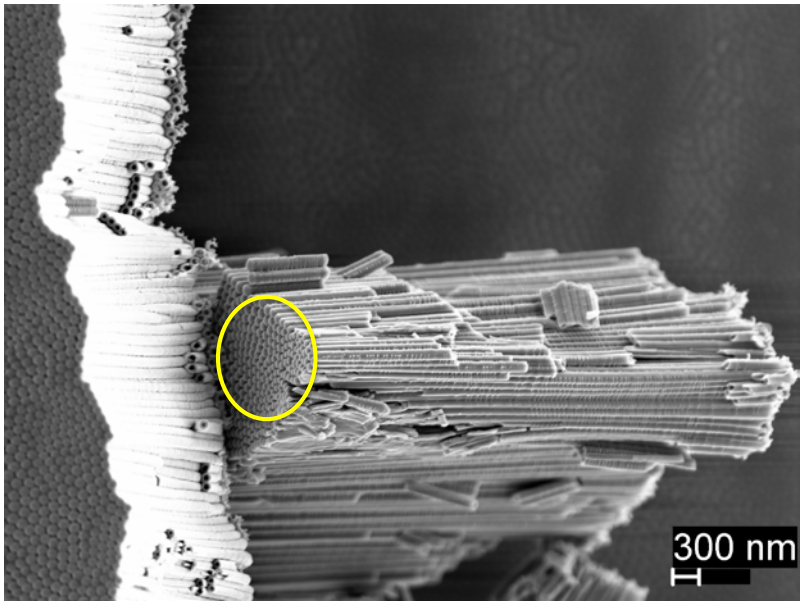

Figure 8. Bottom Formation of TiO_2 Samples

Figure 9 shows the surface of a TiO_2 sample that possesses the wear and tear associated with testing and prepping for SEM imagery. The anodized matrix is still relatively well formed but the nanotubes are at different heights, which indicates heavy deterioration of the ends. Also, this was the sample that suffered from burn damage after testing but the SEM images do not show discoloration or evidence of burning. This surface image is consistent with the surface images of the other two observed samples that did not suffer from burn damage.

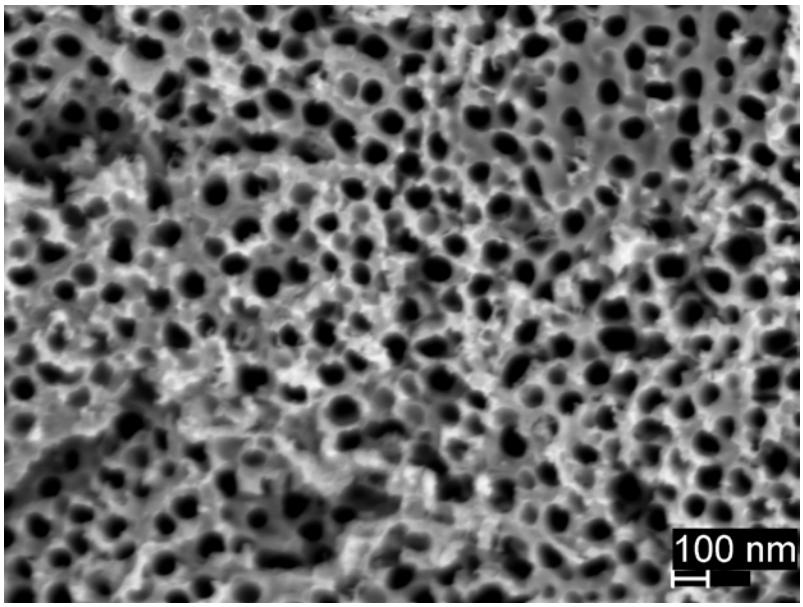

Figure 9. SEM Image of TiO_2 Sample Surface

3. Capacitor Testing

The TiO_2 sample was placed in the testing device shown in Figure 10. The testing device ensured consistent placement of the TiO_2 in order to maximize the performance of the capacitor.[2] The setup consisted of two-5x10 cm glass plates separated by two pieces of Grafoil. One more piece of Grafoil was affixed to the bottom plate to connect the capacitor to the positive testing lead of the testing machine. The negative lead of the testing device was connected to the free end of the TiO_2 sample.

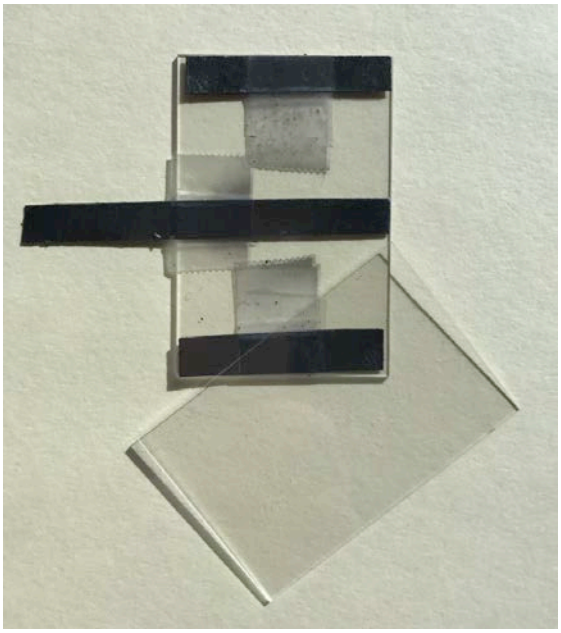

Figure 10. Testing Rig with Cover Off

[2] A number of testing devices were used before finally settling on the shown setup. Previous setups were notorious for short-circuiting capacitors or damaging the nanotube array. This was due to the different clamping devices (clothespins and forceps) used to solidify the connection between the capacitor and the testing device.

A small weight, approximately 35 g, was placed on the top plate to ensure a solid connection was made with the capacitor and the testing galvanostat computer, the Bio-Logic VSP 300 system. Figure 11 shows the complete testing rig.

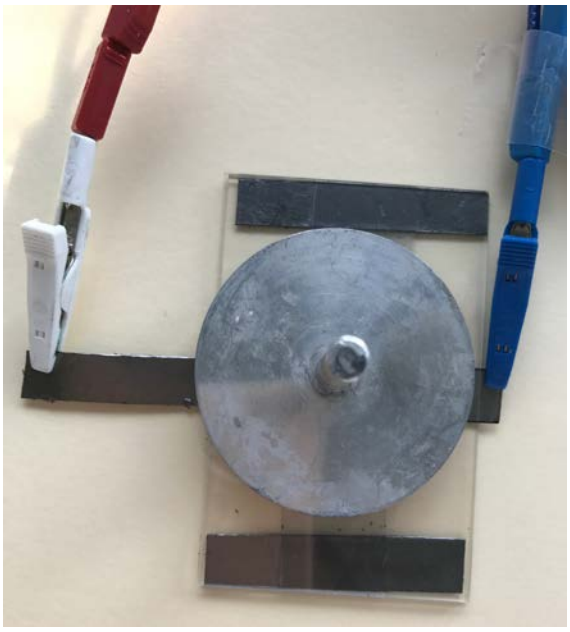

Figure 11. Testing Rig with Top On, Connected to Testing Galvanostat Computer

4. Galvanostat Computer and EC Lab Software

The Bio-Logic VSP 300 system with the EC Lab Software was the testing suite used to conduct and record capacitor performance. The “Big Blue Computer,” Figure 12, is a flexible multipotentiostat that can provide highly accurate reference voltages, reference control signals, filtering and currents [33]. When coupled with the EC Lab software, the user is able to conduct a wide array of capacitor testing.

Figure 12. Bio-Logic VSP 300 Multichannel Potentiostat / Galvanostat

The typical performance test consisted of charging and discharging the capacitor multiple times at a specified current or voltage. Figure 13 shows the control screen for the charging evolution (denoted as “0” at the top of the figure). In this particular test, the charging current is held constant at 100 mA. The conditional statement, outlined in the “Limits” section, is met when the capacitor is charged to a voltage of 5 volts. Once this occurs, the program will move to the second task (denoted as “1” at the top of the figure).

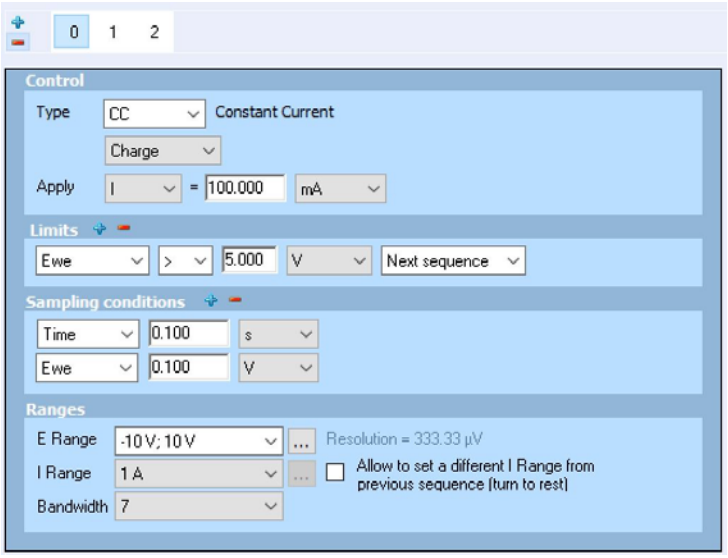

Figure 13. Charging Screen for Capacitor Testing

Figure 14 shows the second task of this cycle, the discharge test. In this example, the current is still 100 mA but now this is the discharge rate. The conditional statement, outlined in the "Limits" section, is met when the capacitor is discharged to a voltage of 0.1 V. Once this occurs, the program will move to the third task (denoted as "2" at the top of the figure).

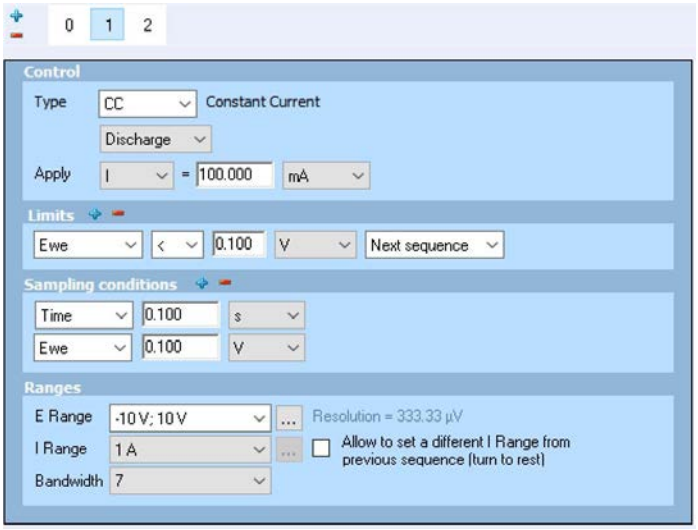

Figure 14. Discharging Screen for Capacitor Testing

Figure 15 shows the last task of this cycle, the loop function. In this example, the cycle will return to the first test, charge, and run sequentially through the remaining tasks. In this case, the charge and discharge tasks will repeat 10 times.

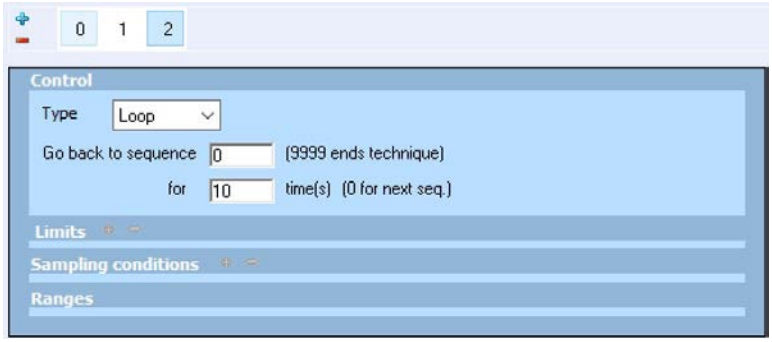

Figure 15. Loop Screen for Capacitor Testing

The EC-Lab software also contains post-test analysis tools used to determine capacitor performance parameters. The integral and the linear fit functions were the primary analysis tools used to determine capacitor performance parameters like energy density, power density, capacitance, discharge time and dielectric constant. The integral method uses the trapezoidal rule to approximate the area under a curve. The example in Figure 16 shows the integral method applied to one waveform of a completed graph. In this case, only one waveform is shown, but each test contained between 10–20 waveforms. Integrals were taken on 3–5 waveforms and averaged to obtain a single value used for subsequent results and analysis. The resulting units are V.s.

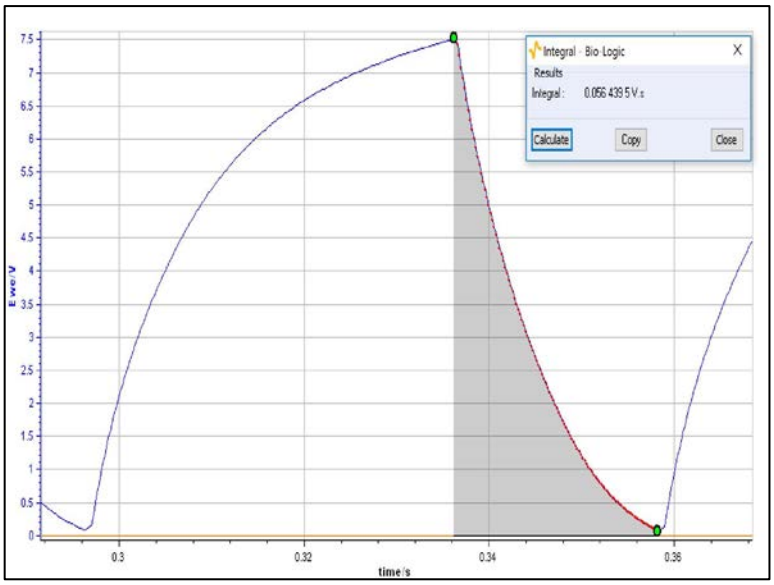

Figure 16. EC Lab Software Integral Analysis Tool Function

The linear-fit tool, shown in Figure 17, was used to determine the slope of the line between 0.8–0.1 volts. This range was selected based on the past performance of NPS capacitors that yielded the most stable discharge characteristics between 0.8 volts and 0.1 volts. The resulting units are V/s.

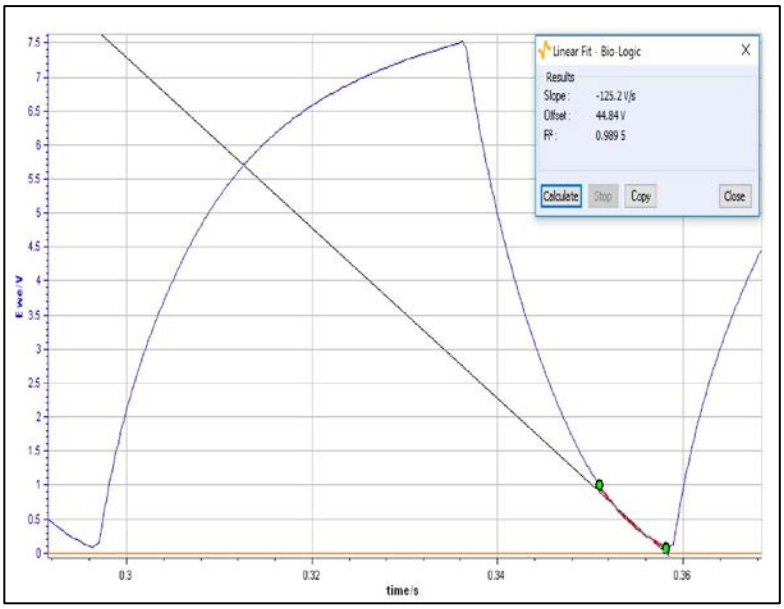

Figure 17. EC Lab Software Linear Fit Tool Function

B. CHEMICAL DECISION PROCESS

Early NPS capacitor work focused on using an ionic species that consisted of distilled water and NaCl. Subsequent research explored new ionic solutions, electrolytes, which focused on different salts with distilled water. The problem encountered with distilled water, in the absence of salt, is that breakdown voltage occurs at 1.23 volts [2]. The highest breakdown voltage achieved was 2.3 volts for the distilled water and salt solution [2], [23].

This thesis focused on increasing the breakdown voltage by selecting electrolytes that are present in current battery and capacitor technologies. Specifically, the research was interested in the electrolytic components of lithium batteries and high performance non-nanotube SDM (NTSDM) capacitors. This is because these energy sources exhibit

the type of performance traits desired for the NTSDM capacitors. Table 3 lists the electrolytes associated with different lithium batteries and various commercial non-NTSDM capacitors.

Table 3. List of Lithium Battery and Electrolytic Capacitors.
Adapted from [34]–[36].

Type	Cathode	Electrolyte
Lithium	Manganese Dioxide	Lithium perchlorate, Propylene Carbonate, and Dimethoxyethane
Lithium	Carbon monofluoride	Lithium tetrafluoroborate in propylene carbonate, dimethoxyethane, gamma-butyrolactone
Lithium	Iron sulfide	Propylene carbonate, dioxolane, dimethoxyethane
Lithium	Iron disulfide	Propylene carbonate, dioxolane, dimethoxyethane
Rechargeable Lithium Batteries	Various	Dimethyl sulfoxide (DMSO)
Lithium	Various	N-methyl pyrrolidone (NMP)
Aluminum	Electrolytic capacitor etched foils	Borax, glycol, gamaa-butyrolactone, dimethylformamide, dimethylacetamide
Tantalum	N/a	Sulfuric acid, manganese dioxide
Niobium oxide	N/a	Manganese dioxide

The solvents selected for testing are DMSO, NMP, and propylene carbonate. The solvents were selected based on their performance characteristics, breakdown voltages, and availability. Concerning salts, previous research by the NPS super capacitor group focused on NaCl, NH_4Cl, $NaNO_3$ and KOH [2], [22]. This thesis expanded the list of salts to include KNO_3 and Boric Acid but eventually settled on the salts for testing down to NaCl, KNO_3, $NaNO_3$ and Boric Acid. The final group of salts was chosen based on their apparent ability to dissolve in the selected solvents, their availability and their proximity to known successful salts on the periodic table. Proximity on the periodic table stems from the idea that salts close to the Fluorine, the primary salt used in lithium batteries, would yield similar performance characteristics.

Tables 4 through 6 show the solvent and salt solution combinations and the associated weights, in grams. Each solvent was mixed with each salt, yielding 15 tests. The control solution was the solvent with no addition of salts. Based on the exploratory research, all the solvents were able to attain a voltage of at least 3 volts with a constant charging current of 10 mA. Of significant note, the propylene carbonate reached 7 volts without adding salt.

Table 4. Components of DMSO Electrolytic Salt Solutions

Solvent	**Wt (g / %)**	**Solute**	**Wt (g / %)**
DMSO	10 / 100	Control	0 / 0
	11.71 / 93.1	NaCl	1.02 / 8.7
	10.67 / 94.8	KNO_3	.56 / 5.2
	10.62 / 94.8	$NaNO_3$	.55 / 5.2
	10.27 / 83.9	Boric Acid	1.65 / 16.1

Table 5. Components of NMP Electrolytic Salt Solutions

Solvent	**Wt (g / %)**	**Solute**	**Wt (g / %)**
NMP	10 / 100	Control	0 / 0
	15.06 / 93.1	NaCl	1.04 / 6.9
	10.15 / 90.1	KNO_3	1.00 / 9.8
	10.09 / 89.6	$NaNO_3$	1.05 / 10.4
	10.17 / 88.5	Boric Acid	1.17 / 11.5

Table 6. Components of NMP Electrolytic Salt Solutions

Solvent	**Wt (g / %)**	**Solute**	**Wt (g / %)**
Propylene Carbonate	10 / 100	Control	0 / 0
	10.06 / 89.5	NaCl	1.06 / 10.5
	10.90 / 89.8	KNO_3	1.11 / 10.2
	10.77 / 89.6	$NaNO_3$	1.12 / 10.4
	10.13 / 89.9	Boric Acid	1.02 / 10.1

During the exploratory testing, it was discovered that the salts selected for the electrolytic solution only partially dissolved in each of the three solvents. The issue was the lack of documentation concerning the salt solubility and salt saturation amounts required to make salt saturated electrolytic solutions. However, testing proved that some salt did dissolve in the solvents as evidenced by the increased energy density yielded by the salt electrolyte solution when compared to the control solvent, or non-salt solution. Additionally, the maximum obtained voltage decreased with the salt electrolyte solution when compared to the control solvent.

It was postulated that taking a saturated NaCl electrolyte solution and adding it to the Propylene Carbonate would increase the likelihood of testing a solution that possessed a saturated electrolyte. The propylene carbonate was selected because it yielded the highest obtained voltage when tested without salt. The idea is to maintain as high a voltage as possible while adding ionic salt solution to increase the energy density. This was achieved by varying the concentration of the solute to the NaCl electrolyte solution. Table 7 shows percentage of propylene carbonate to NaCl solution.

Table 7. Schedule for Testing Propylene Carbonate and NaCl Electrolyte Solution

Propylene Carbonate (%)	**Distilled Water / NaCl Solution (%)**
95	05
90	10
85	15
80	20
75	25

C. LOW/HIGH FREQUENCY AND FHS TESTS

In an effort to compare the results of this thesis with previous work done by the NPS energy group, the following testing schedules were used to determine NTSDM capacitor performance traits over a wide range of frequencies [2]. Table 8 and Table 9 show the low and high testing schedules. These schedules are representative of the various load demands required by the Navy and commercial applications—examples include: Railgun launch, EMALS, FEL, battery driven cars and small device operations [9]–[11]. The tests were conducted using the same charge and discharge current.

Table 8. Schedule of Low Frequency Testing

Current (mA)
5
8
10
12
15
18
20

Table 9. Schedule for High Frequency Testing

Current (mA)
10
20
30
50
80
100
150
200
250

Recent capacitor testing and research has yielded a new method to extract what seems to be the highest performance out of capacitors. The Murata technique charges a capacitor to a rated voltage, holds the voltage with a varying current and discharges the capacitor to a set voltage [37]. The Murata technique, renamed Fast-Hold-Slow (FHS), was used on super capacitors but the theory and test method can be directly applied to the NTSDM capacitors. The idea is that charging to a maximum voltage and allowing the salt dipoles time to align at that voltage will produce the highest energy density possible for a given electrolytic solution.

Table 10 shows the FHS testing schedule that was conducted on all the DMSO, NMP, Propylene Carbonate and Propylene Carbonate (with the distilled water + NaCl) electrolyte solutions. Each solution was tested at all hold times and discharged at the same current. The charge current and hold voltage were specific to each solution.

Table 10. Sample Schedule for FHS Testing

Solvent	Solute	Voltage (volts)	Hold Time (s)	Discharge Current (mA)
DMSO	Control	3.0	1	1
	NaCl	3.0	10	
	KNO3	3.0	30	
	NaNO3	3.0	60	
	Boric Acid	3.0	100	
			200	
			300	
			1000	

THIS PAGE INTENTIONALLY LEFT BLANK

III. RESULTS

For this thesis the dielectric constant, capacitance, energy density and power density (resolved as a function of discharge time/frequency) were determined for 20 capacitors. In all cases, nearly identical anodized titania foils were used. The difference between each capacitor was the polar fluid and salts employed as the "polarizable" phase, filling the hollow vertical, electrically insulating tubes of the anodized titania. In particular, the following polar fluids were used: NMP, DMSO and Propylene Carbonate. These were used in conjunction with the following salts: NaCl, KNO_3, Boric Acid and $NaNO_3$. In some cases, the salt concentration was changed as well, specifically when tested with the Propylene Carbonate.

The key discoveries were that each fluid and salt concentration yielded higher breakdown voltages when compared with previously tested aqueous based solutions [2], [22]. However, none of the fluid and salt concentrations yielded energy densities as high as pure aqueous salt solutions. This chapter presents the solvent and salt solution combinations tested in the Low Frequency, High Frequency and FHS testing schedules.

A. PC + (DISTILLED WATER / SODIUM CHLORIDE)

Figure 18 shows the complete testing schedule for the selected solvent.

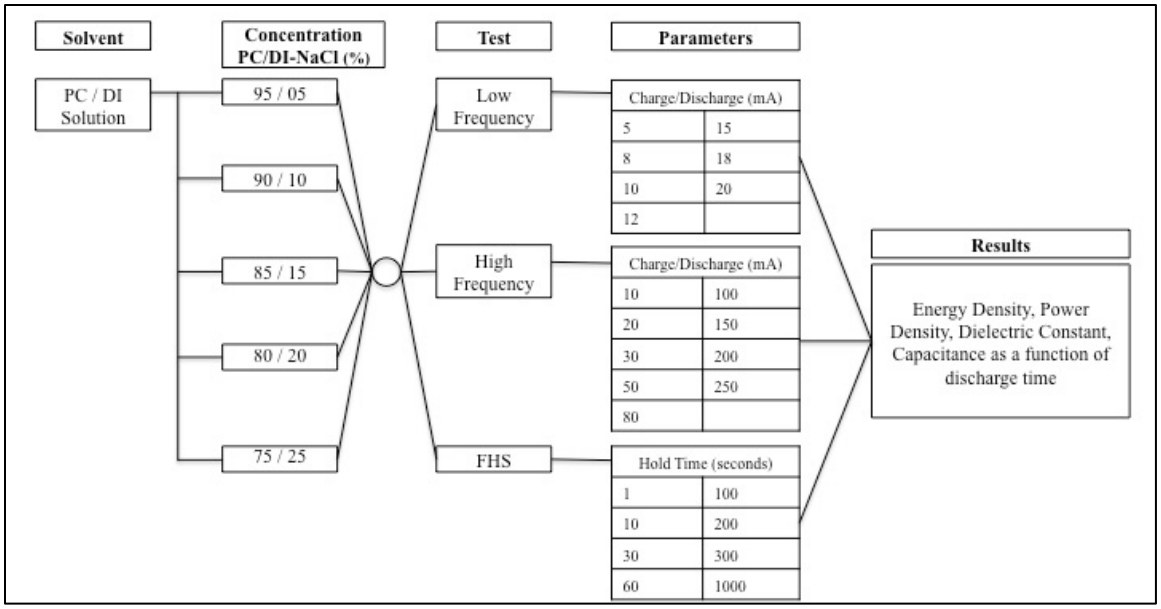

Figure 18. Complete Testing Schedule for PC + DI/NaCl

1. PC + DI/NaCl [95/05]

a. Low Frequency Tests (PC + DI/NaCl [95/05])

Figure 19 shows the wave shapes of the PC + DI/NaCl control solution for the Low Frequency frequencies. Although seven frequencies were tested, only the 10 mA and 20 mA current waveforms are shown. The shapes for all waveforms are smooth on both the charge and the discharge phase for all cycles. There is no evidence of aliasing nor sharp declines at the onset of the discharge phase. This indicates that there was no wasted energy and the capacitor was performing at its fullest potential for the given charge rate. The initial charge rate took an abnormally long time to achieve the 4 volts but subsequent cycles did not take as long. It was assumed that the additional time was needed for the salt dipoles to align. Once the 4 volts was achieved, the salt dipoles were in the optimum position for capacitor performance.

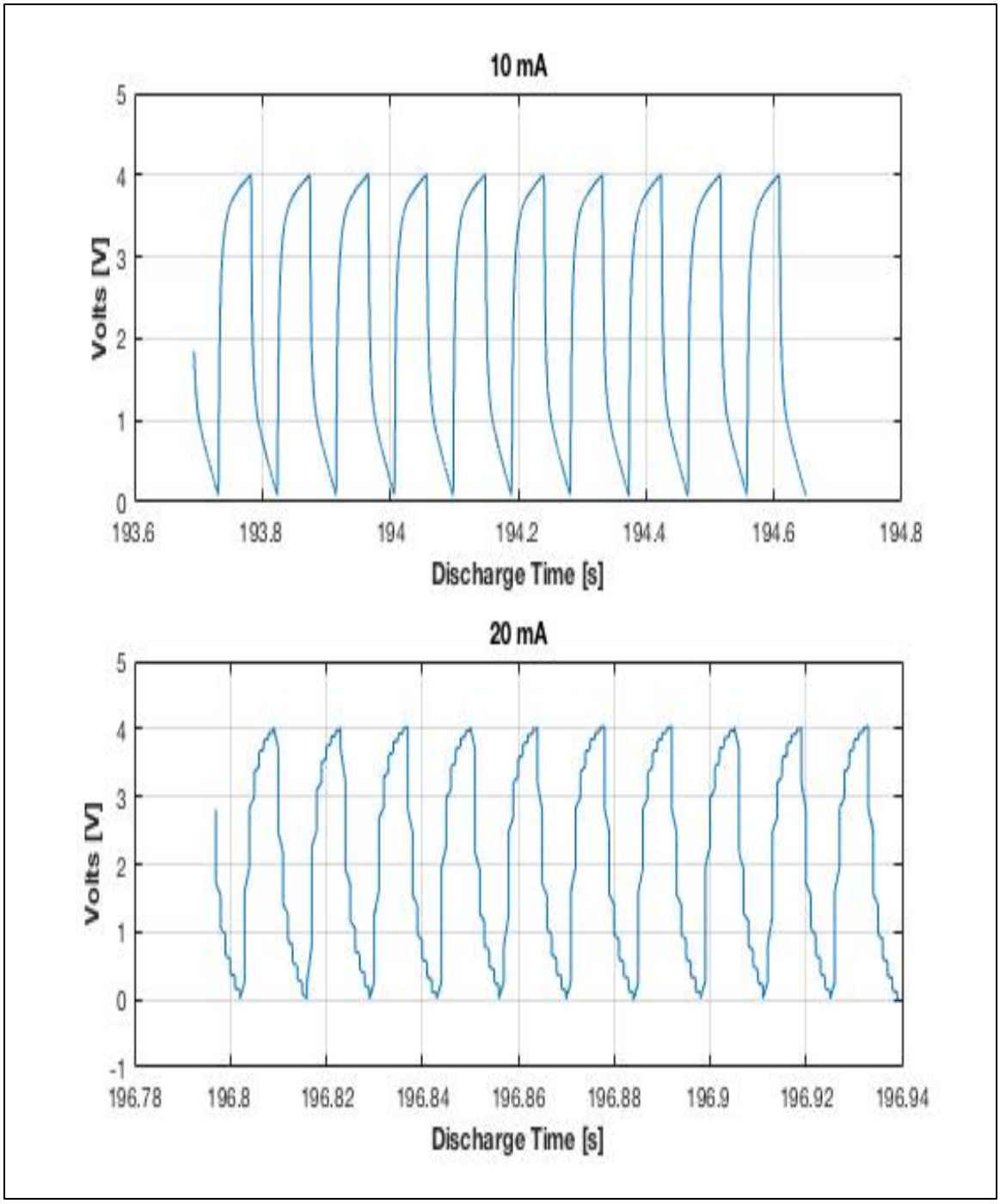

Figure 19. PC+DI/NaCl Solution for Select Low Frequency Tests Frequencies

Table 11 contains the performance data for the PC + DI/NaCl solution. The results are the average of 10–20 cycles and tests for all currents were completed satisfactorily.

Table 11. Performance Data for PC + DI/NaCl Solution, Low Frequency Tests

Amperage (mA)	Voltage (V)	Discharge Time (s)	Power Density (W/cm^3)	Dielectric Constant	Capacitance (F)
5	4.0	0.44	2.75	5.84 E 06	1.40 E -03
8	4.0	0.084	3.95	2.16 E 06	5.16 E -04
10	4.0	0.041	4.94	1.38 E 06	3.31 E -04
12	4.0	0.024	6.22	9.30 E 05	2.22 E -04
15	4.0	0.012	9.07	5.64 E 05	1.35 E -04
18	4.0	0.008	12.2	3.87 E 05	9.25 E -05
20	4.0	0.006	14.3	3.22 E 05	7.69 E -05

Figure 20 shows the energy density for PC + DI/NaCl solution. Further examination of the power trend line and the resulting equation predicts an energy density of 28 J/cm^3 at 100 seconds.

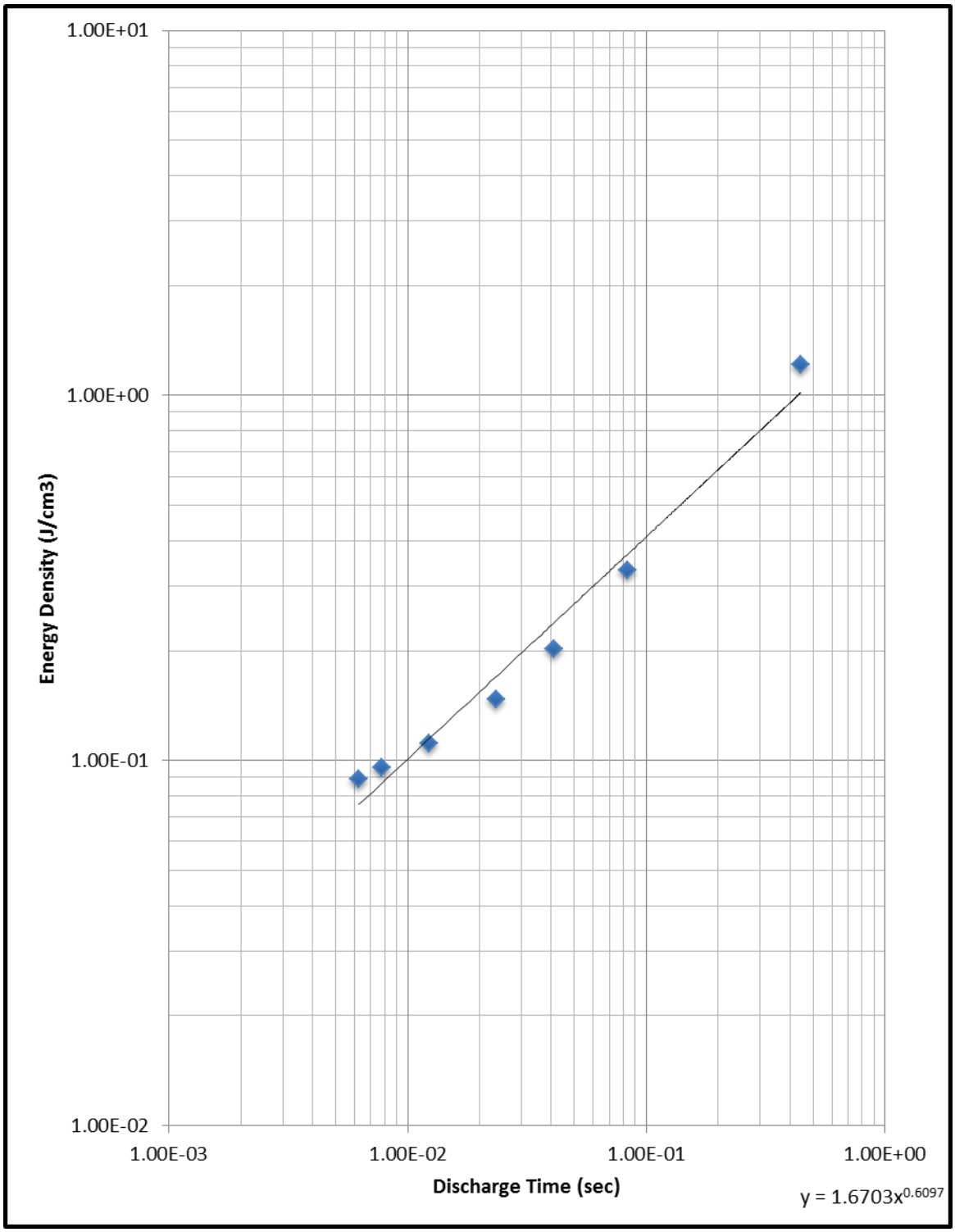

Figure 20. Energy Density for PC + DI/NaCl Solution, Low Frequency Tests

b. High Frequency Tests (PC + DI/NaCl [95/05])

Figure 21 shows the wave shapes of the PC + DI/NaCl solution for the High Frequency Tests. Although ten frequencies were tested, only the 50 mA and 200 mA constant current waveforms are shown. The shapes for all waveforms are smooth and connected on both the charge and the discharge phase for all cycles; however, there is evidence of dramatic aliasing on both the charge and discharge phases on all cycles for the higher frequencies-constant currents greater than 50 mA. Paying particular attention to the bottom 200 mA graph in Figure 21, the current only reaches (and then overshoots) the intended voltage every other cycle. It was postulated that the machine was unable to fully discharge the capacitor. When it was time to turn the current, from discharge to charge, residual energy in the capacitor provided a false indication of actual energy. The software was unable to process the fast charge and discharge current and this particular salt solution did not retard the process. In other words, the salt solution was not allowed sufficient time to establish the optimum ion dipole arrangement for energy capacity. This indicates that there was wasted energy or less area under the curve when utilizing the integral analysis tool during post-analysis processing.

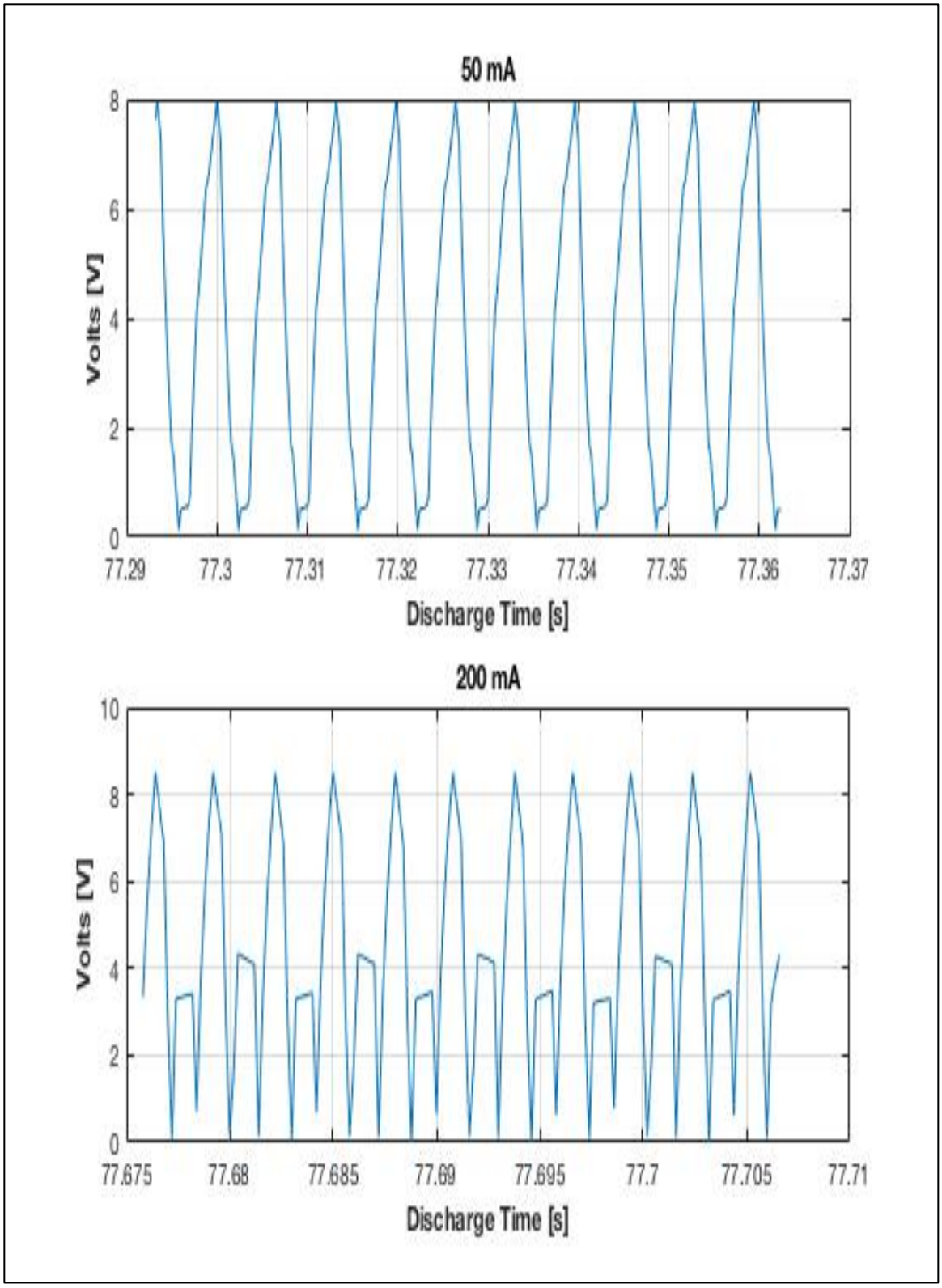

Figure 21. PC+DI/NaCl Solution for Select High Frequency Tests

Table 12 contains the performance data for the PC + DI/NaCl solution for all the High Frequency Tests. The results are the average of 10–20 cycles and tests for all currents were completed satisfactorily but with significant inconsistencies due to the aliasing.

Table 12. Performance Data for PC + DI/NaCl Solution, High Frequency Tests

Amperage (mA)	Voltage (V)	Discharge Time (s)	Power Density (W/cm^3)	Dielectric Constant	Capacitance (F)
10	7.0	0.052	6.03	1.83 E 06	4.37 E -04
20	7.0	0.0072	26.11	2.38 E 05	5.70 E -05
30	7.2	0.0038	50.66	1.38 E 05	3.30 E -05
40	7.3	0.0028	75.80	1.22 E 05	2.91 E -05
50	8.0	0.0024	104.2	7.70 E 04	1.84 E -05
80	8.3	0.0016	217.2	1.16 E 05	2.78 E -05
100	8.5	0.001	220.8	7.96 E 04	1.90 E -05
150	8.5	0.001	455.1	6.77 E 04	1.62 E -05
200	8.5	0.0008	566.7	5.97 E 04	1.43 E -05
250	8.5	0.001	914.3	6.09 E 04	1.45 E -05

Figure 22 shows the energy density for PC + DI/NaCl solution. Further examination of the power trend line and the resulting equation predicts an energy density of 0.061 J/cm^3 at 100 seconds. Energy density normally decreases as discharge time decreases. Figure 22 shows the opposite. This was due to the extremely small discharge times and the small range of energy density (.188–.914 J/cm^3) that does not span a decade on the log-log plot. In general, experience suggests data obtained for discharge times of less than 0.002 seconds are not reliable and is a shortcoming of the testing machine and software analysis tools.

Figure 22. Energy Density for PC + DI/NaCl Solution, High Frequency Tests

c. FHS Tests (PC + DI/NaCl [95/05])

Figure 23 shows the wave shapes of the PC + DI/NaCl solution for the FHS testing. The hold times were 1, 10, 100 and 1000 seconds but only the graphs for 10 and 1000 seconds are shown. The shapes for all waveforms are smooth on both the charge and the discharge phase for all cycles.

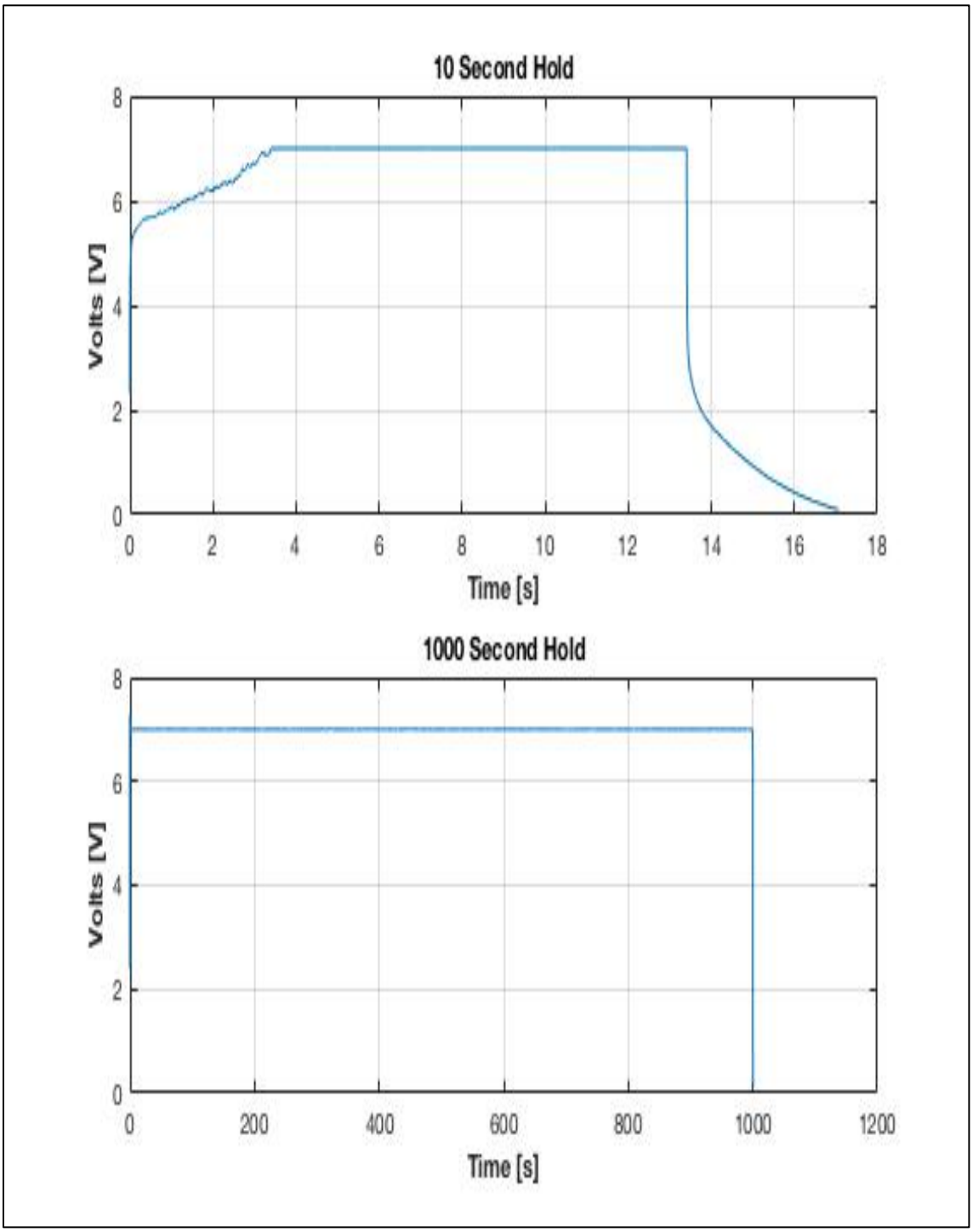

Figure 23. PC + DI/NaCl Solution for FHS Testing

Table 13 contains the performance data for the PC + DI/NaCl solution for all FHS hold times.

Table 13. Performance Data for PC + DI/NaCl Solution, FHS Testing

Hold Time (s)	Voltage (V)	Discharge Time (s)	Power Density (W/cm^3)	Dielectric Constant	Capacitance (F)
1	7.0	8.64	0.511	3.00 E 07	7.16 E -03
10	7.0	3.65	0.560	1.76 E 07	4.20 E -03
30	7.0	2.10	0.523	7.00 E 06	1.67 E -03
60	7.0	1.33	0.640	4.37 E 06	1.04 E -03
100	7.0	1.02	0.492	2.70 E 06	6.45 E -03
200	7.0	0.60	0.588	1.92 E 06	4.69 E -03
300	7.0	0.20	0.976	5.75 E 05	1.37 E -03
1000	7.0	0.20	0.820	9.40 E 04	2.25 E -03

Figure 24 shows the energy density for PC + DI/NaCl solution. FHS testing makes it difficult to predict the performance parameters at a specific discharge time because the trend line equation is based on the hold times. Conversely, the trend line equations from the Low and High Frequency testing schedules are based on discharge times so the predictions are defensible and relevant. Consideration was given to basing the FHS testing on discharge times, but the point of the Murata technique was to exploit the supposed positive effects that hold times had on the NTSDM capacitor performance parameters. To that end, FHS testing was based on the hold times and the charts that follow are valuable for highlighting energy density trends as the hold times are increased. Energy density normally decreases as discharge time decreases. Figure 24 shows the opposite. Since the FHS tests focused on hold times (vice discharge times) the reasons for this phenomenon are not comparable to the results obtained from the Low and High Frequency Tests that focused on discharge times.

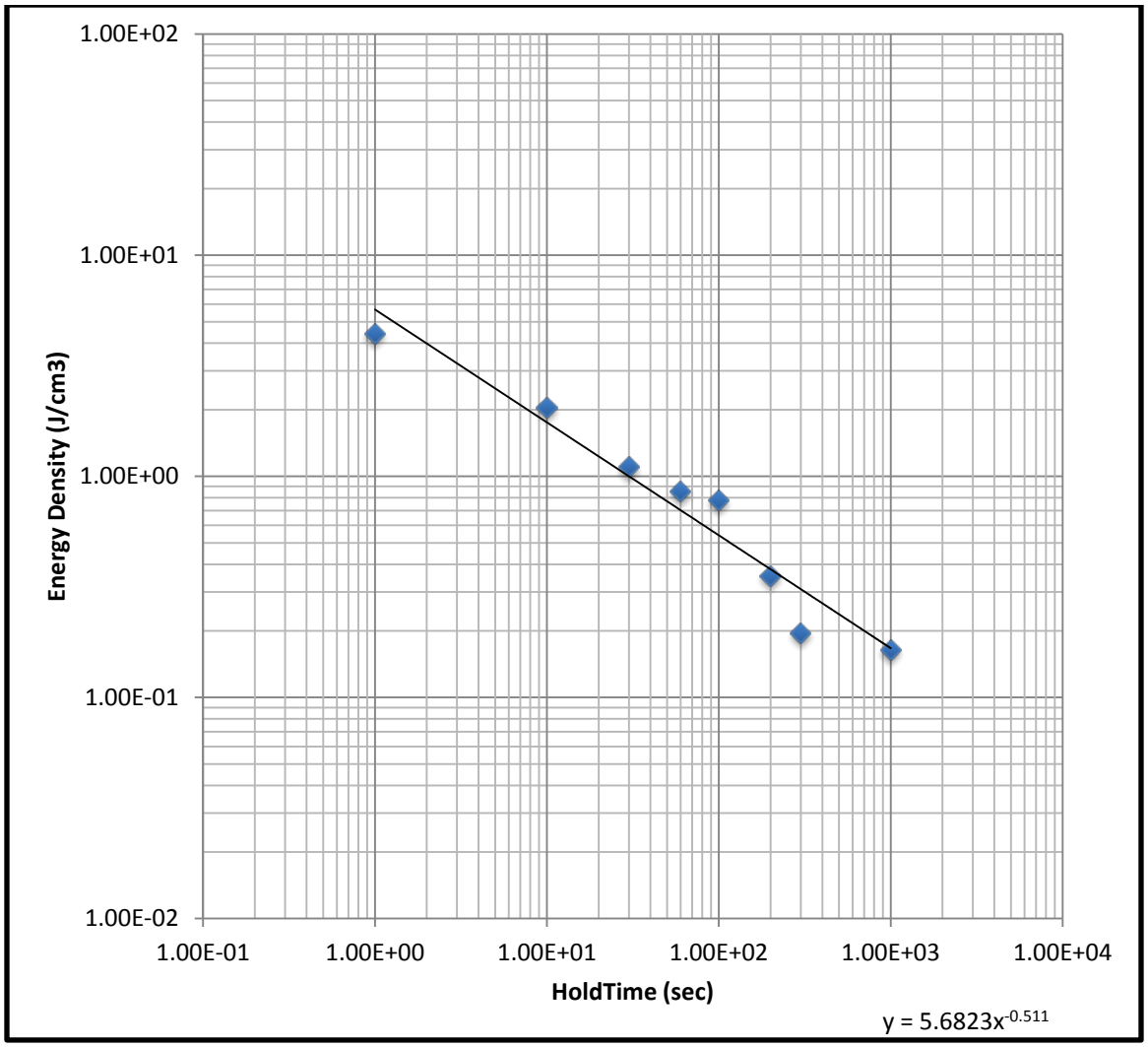

Figure 24. Energy Density for PC + DI/NaCl Solution, FHS Testing

2. PC + DI/NaCl [90/10]

a. Low Frequency Tests (PC + DI/NaCl [90/10])

Figure 25 shows the wave shapes of the PC + DI/NaCl solution for the Low Frequency Tests. Although seven frequencies were tested, only the 10 mA and 20 mA constant current waveforms are two shown below. The shapes for all waveforms are smooth on both the charge and the discharge phase for all cycles. There is no evidence of aliasing nor sharp declines at the onset of the discharge phase. This indicates that there

was no wasted energy and the capacitor was performing at its fullest potential for the given the charge rate.

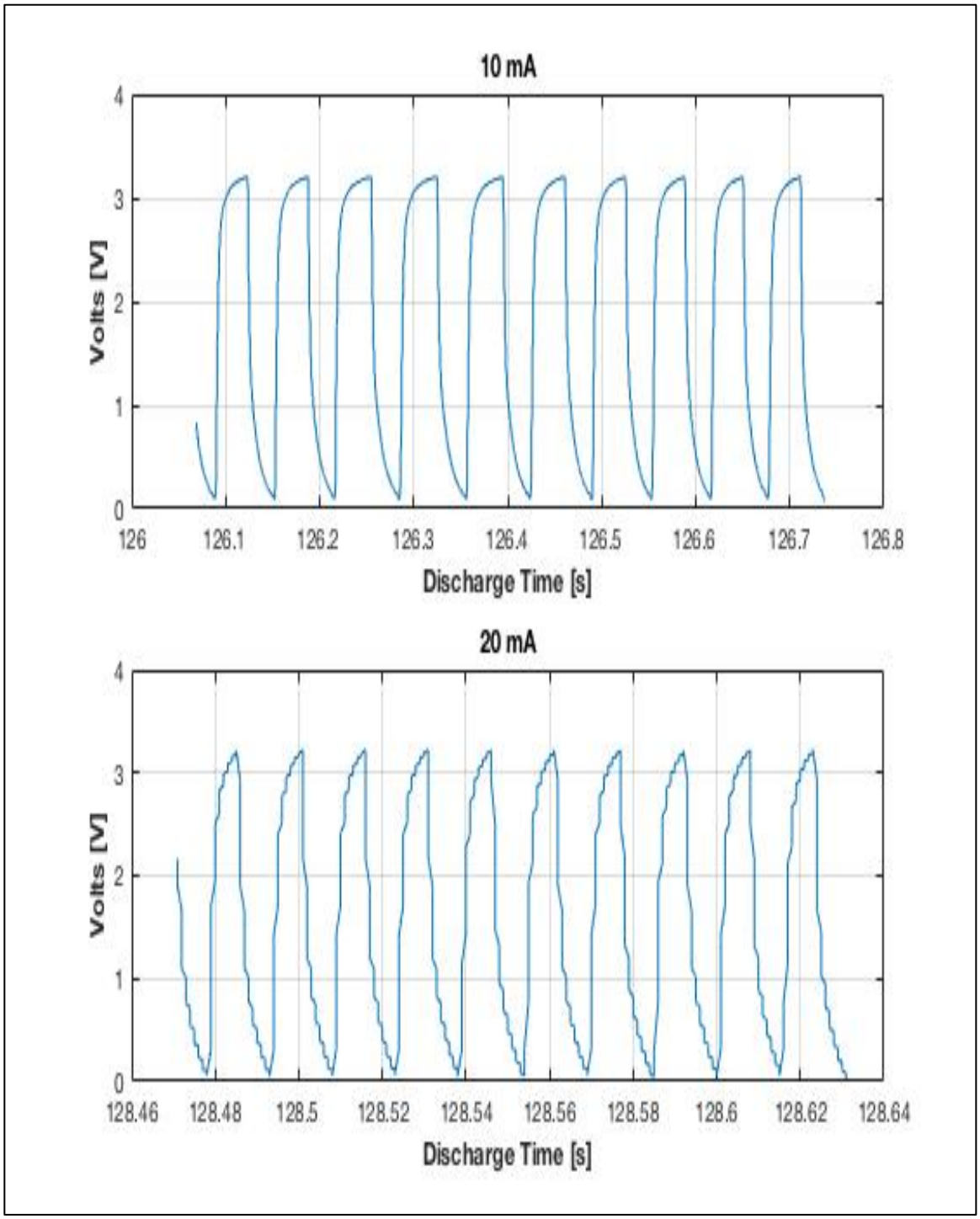

Figure 25. PC + DI/NaCl Solution for Select Low Frequency Tests

Table 14 contains the performance data for the PC + DI/NaCl solution. The results are the average of 10–20 cycles and tests for all currents were completed satisfactorily.

Table 14. Performance Data for PC + DI/NaCl Solution, Low Frequency Tests

Amperage (mA)	Voltage (V)	Discharge Time (s)	Power Density (W/cm^3)	Dielectric Constant	Capacitance (F)
5	3.2	0.250	0.934	7.39 E 06	1.77 E -03
8	3.2	0.092	2.16	3.81 E 06	9.10 E -03
10	3.2	0.027	3.88	1.16 E 06	2.77 E -04
12	3.2	0.014	5.76	6.03 E 05	1.44 E -04
15	3.2	0.015	6.20	9.82 E 05	2.35 E -04
18	3.2	0.010	8.43	7.04 E 05	1.68 E -04
20	3.2	0.008	10.1	5.62 E 05	1.34 E -04

Figure 26 shows the energy density for PC + DI/NaCl solution. Further examination of the power trend line and the resulting equation predicts an energy density of 2 J/cm^3 at 100 seconds.

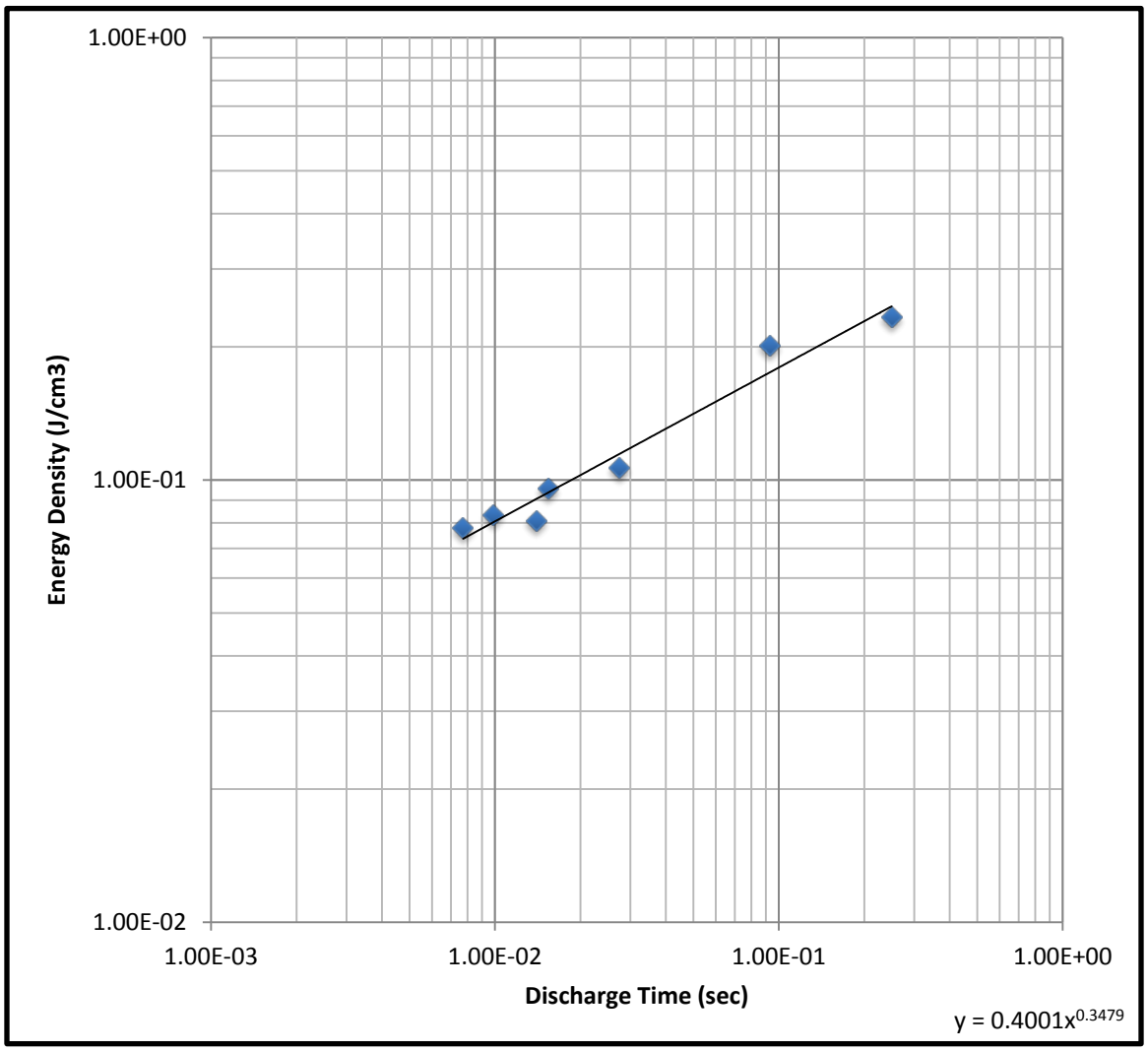

Figure 26. Energy Density for PC + DI/NaCl Solution, Low Frequency Tests

b. High Frequency Tests (PC + DI/NaCl [90/10])

Figure 27 shows the wave shapes of the PC + DI/NaCl solution for the High Frequency Tests. Although ten frequencies were tested, only the 50 mA and 200 mA current waveforms are shown below. The shapes for all waveforms are smooth and connected on both the charge and the discharge phase for all cycles. However, there is evidence of dramatic aliasing on both the charge and discharge phases on all cycles for the higher frequencies (> 100 mA). Additionally, there were sharp declines at the onset of the discharge phase. This indicates that there was wasted energy or less area under the curve when utilizing the integral analysis tool during post-analysis processing.

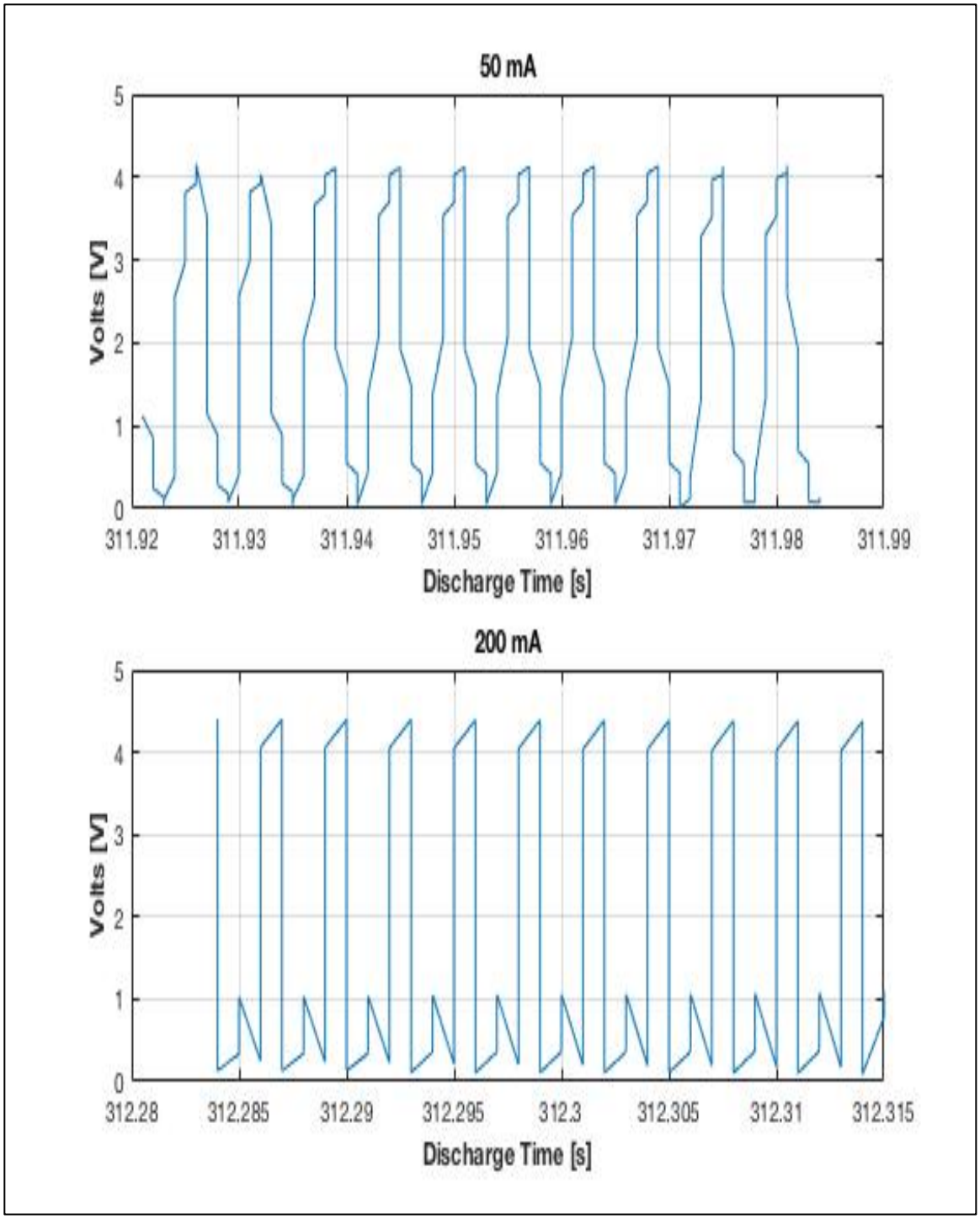

Figure 27. PC + DI/NaCl Solution for Select High Frequency Tests

Table 15 contains the performance data for the PC + DI/NaCl solution for all the High Frequency Tests. The results are the average of 10–20 cycles and tests for all currents were completed satisfactorily but with significant inconsistencies due to the aliasing.

Table 15. Performance Data for PC + DI/NaCl Solution, High Frequency Tests

Amperage (mA)	Voltage (V)	Discharge Time (s)	Power Density (W/cm^3)	Dielectric Constant	Capacitance (F)
10	4.0	3.22	3.28	1.77 E 08	4.23 E -02
20	4.0	0.030	7.83	2.99 E 06	7.15 E -04
30	4.0	0.0073	17.9	6.51 E 05	1.56 E -04
40	4.1	0.0042	27.7	4.37 E 05	1.05 E -04
50	4.2	0.0028	40.6	3.22 E 05	7.69 E -05
80	4.2	0.0023	60.3	5.08 E 05	1.21 E -04
100	4.2	0.0016	96.4	3.76 E 05	8.98 E -05
150	4.4	0.0010	185.1	2.86 E 05	6.84 E -05
200	4.4	0.0008	268.6	2.21 E 05	5.29 E -05
250	4.5	0.0008	318.8	2.48 E 05	5.93 E -05

Figure 28 shows the energy density for PC + DI/NaCl solution. Further examination of the power trend line and the resulting equation predicts an energy density of 27 J/cm^3 at 100 seconds.

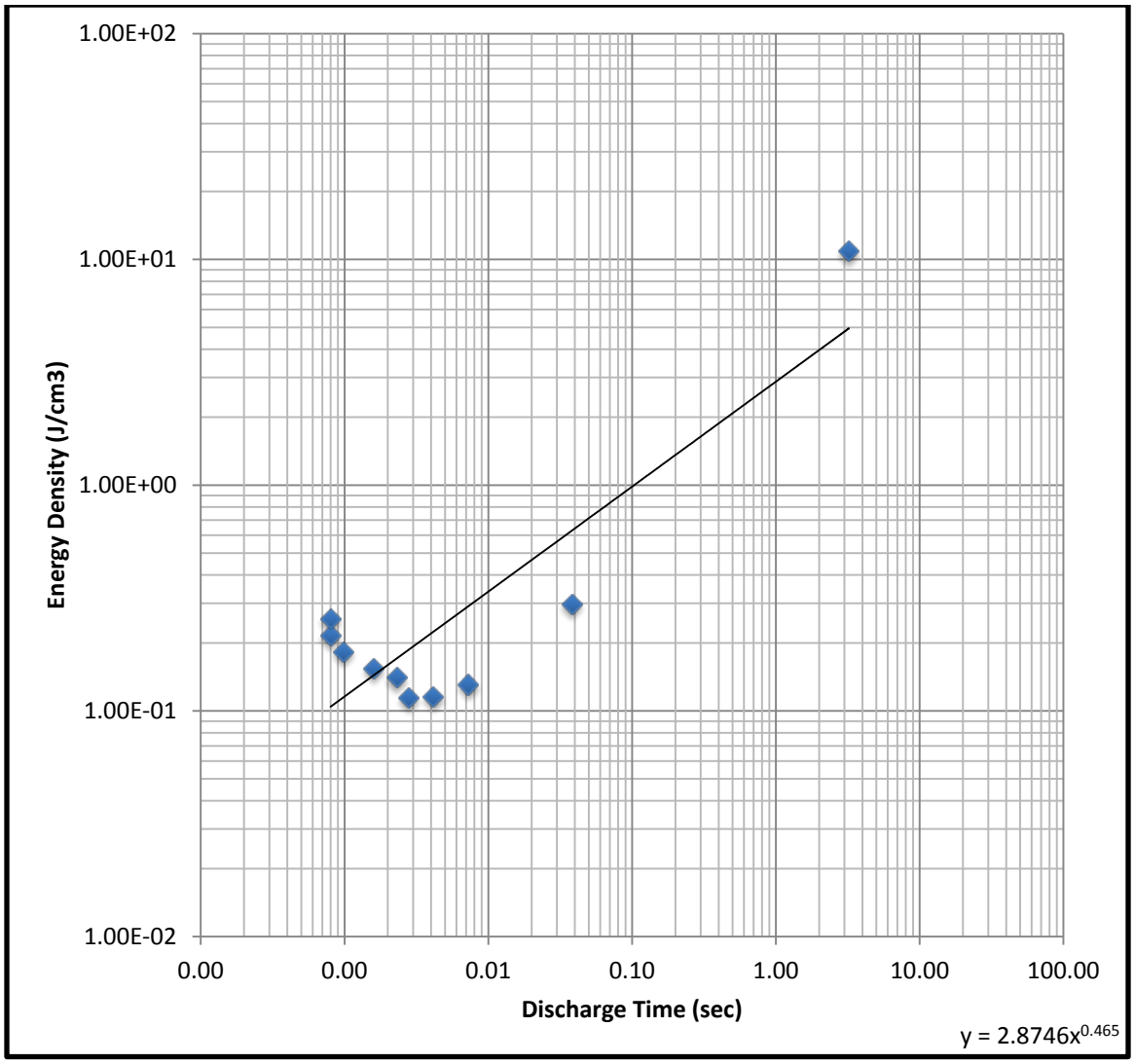

Figure 28. Energy Density for PC + DI/NaCl Solution, High Frequency Tests

c. FHS Tests (PC + DI/NaCl [90/10])

Figure 29 shows the wave shapes of the PC + DI/NaCl solution for the FHS testing. The hold times were 1, 10, 100 and 1000 seconds but only the graphs for 10 and 300 seconds are shown. The bump in voltage during the charge phase on the first graph was due to a manual increase in hold voltage. The shapes for all waveforms are smooth on both the charge and the discharge phase for all cycles.

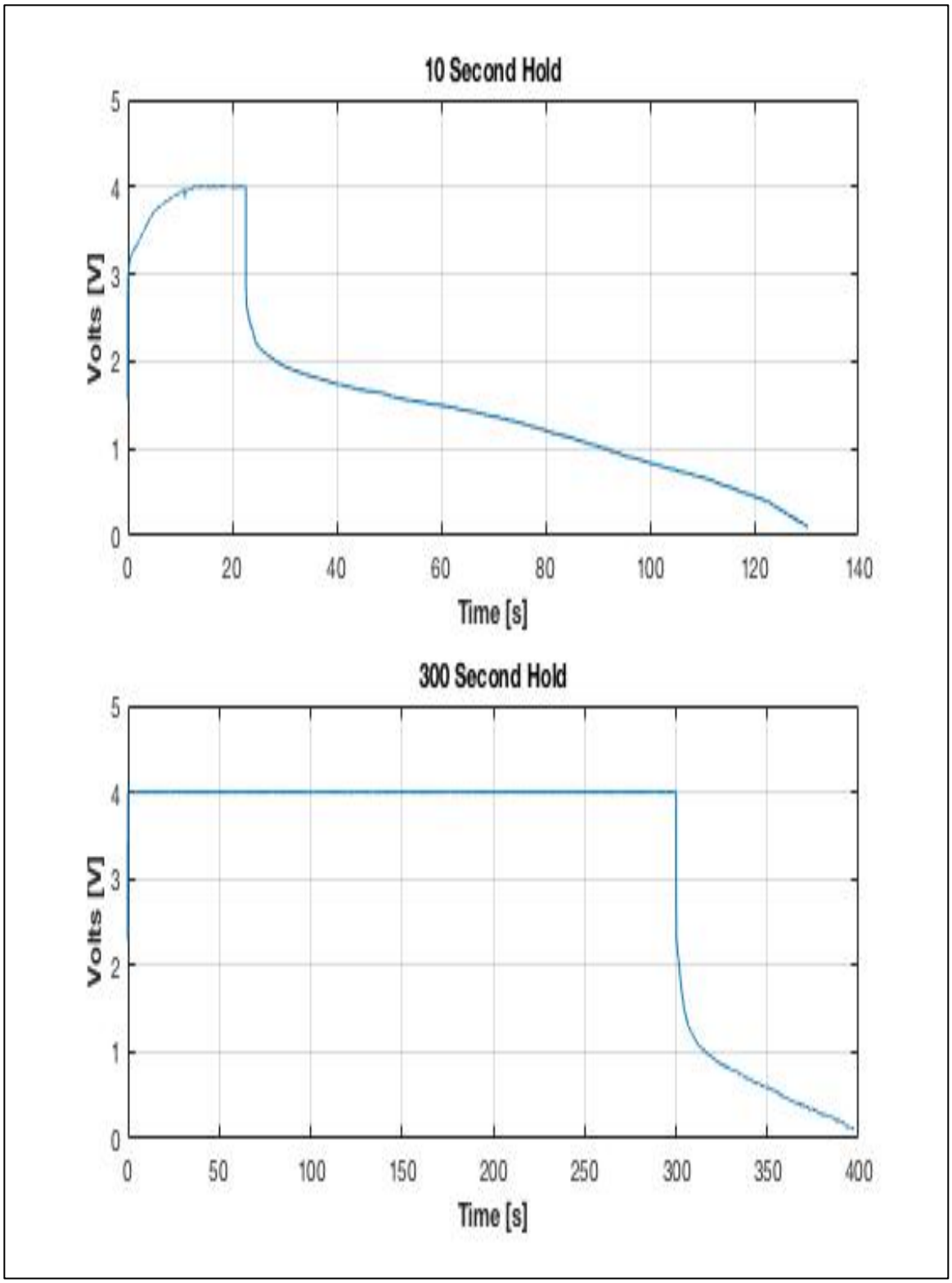

Figure 29. PC + DI/NaCl Solution for FHS Testing

Table 16 contains the performance data for the DMSO and NaCl solution for all FHS hold times.

Table 16. Performance Data for PC + DI/NaCl Solution, FHS Testing

Hold Time (s)	Voltage (V)	Discharge Time (s)	Power Density (W/cm^3)	Dielectric Constant	Capacitance (F)
1	4.0	195.4	0.734	3.03 E 08	0.072
10	4.0	107.8	0.703	1.77 E 08	0.024
30	4.0	135.0	0.683	2.62 E 08	0.063
60	4.0	153.8	0.702	2.45 E 08	0.058
100	4.0	115.3	0.451	3.79 E 08	0.091
200	4.0	162.0	0.576	1.72 E 08	0.041
300	4.0	137.3	0.450	4.67 E 08	0.009
1000	4.0	175.0	0.578	3.64 E 08	0.087

Figure 30 shows the energy density for the PC + DI/NaCl solution. FHS testing makes it difficult to predict the performance parameters at a specific discharge time because the trend line equation is based on the hold times. Conversely, the trend line equations from the Low and High Frequency Tests are based on discharge times so the predictions are defensible and relevant. Consideration was given to basing the FHS testing on discharge times but the point of the Murata technique was to exploit the supposed positive effects that hold times had on the NTSDM capacitor performance parameters. To that end, FHS testing was based on the hold times and the charts that follow are valuable for highlighting energy density trends as the hold times increased.

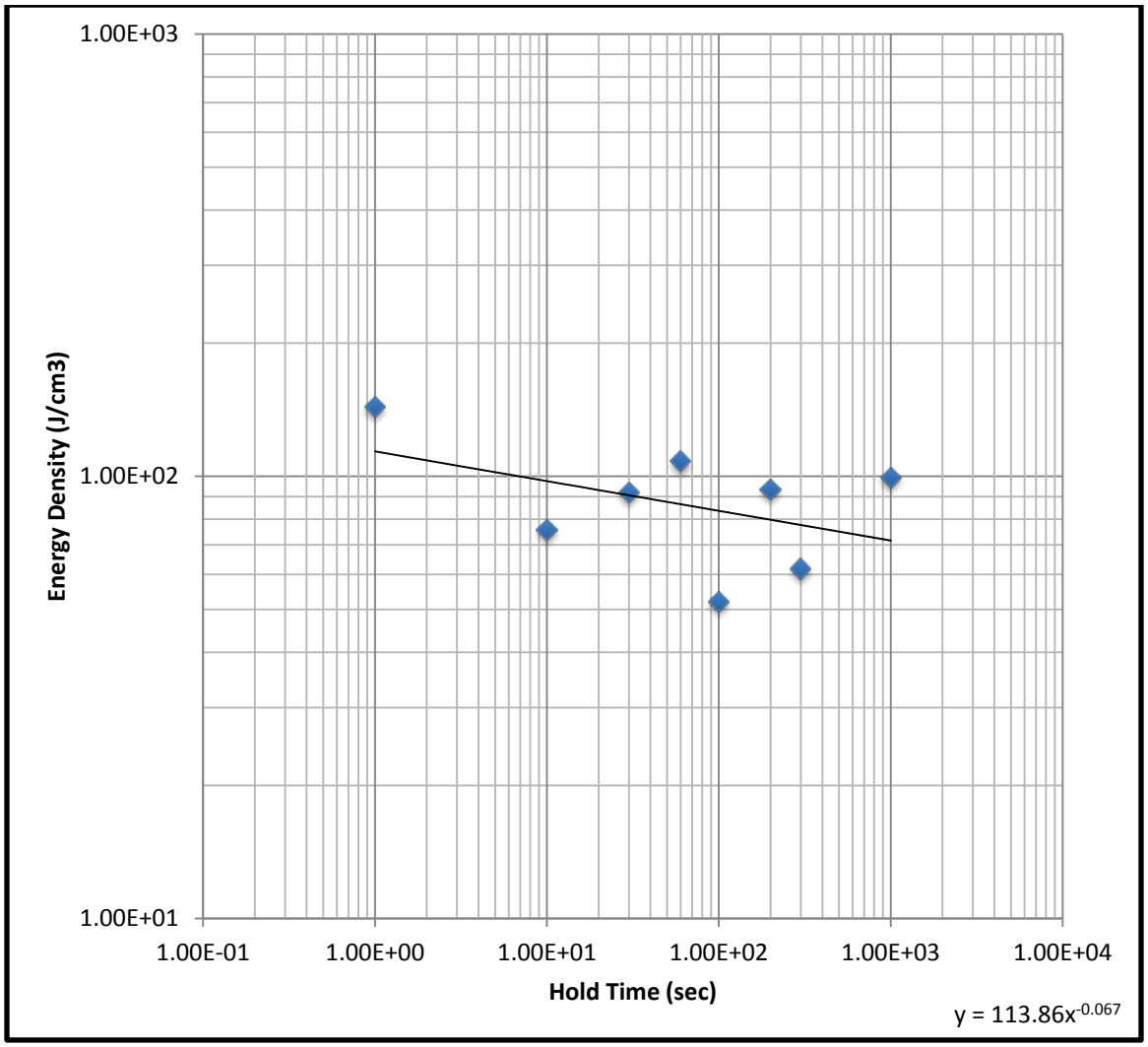

Figure 30. Energy Density for PC + DI/NaCl Solution, FHS Testing

3. PC + DI/NaCl [85/15]

a. Low Frequency Tests (PC + Di/NaCl [85/15])

Figure 31 shows the wave shapes of the PC + DI/NaCl solution for the Low Frequency Tests. Although ten frequencies were tested, only the 10 mA and 20 mA current waveforms are shown below. The shapes for all waveforms are smooth on both the charge and the discharge phase for all cycles. There is no evidence of aliasing nor sharp declines at the onset of the discharge phase. This indicates that there was no wasted

energy and the capacitor was performing at its fullest potential for the given the charge rate.

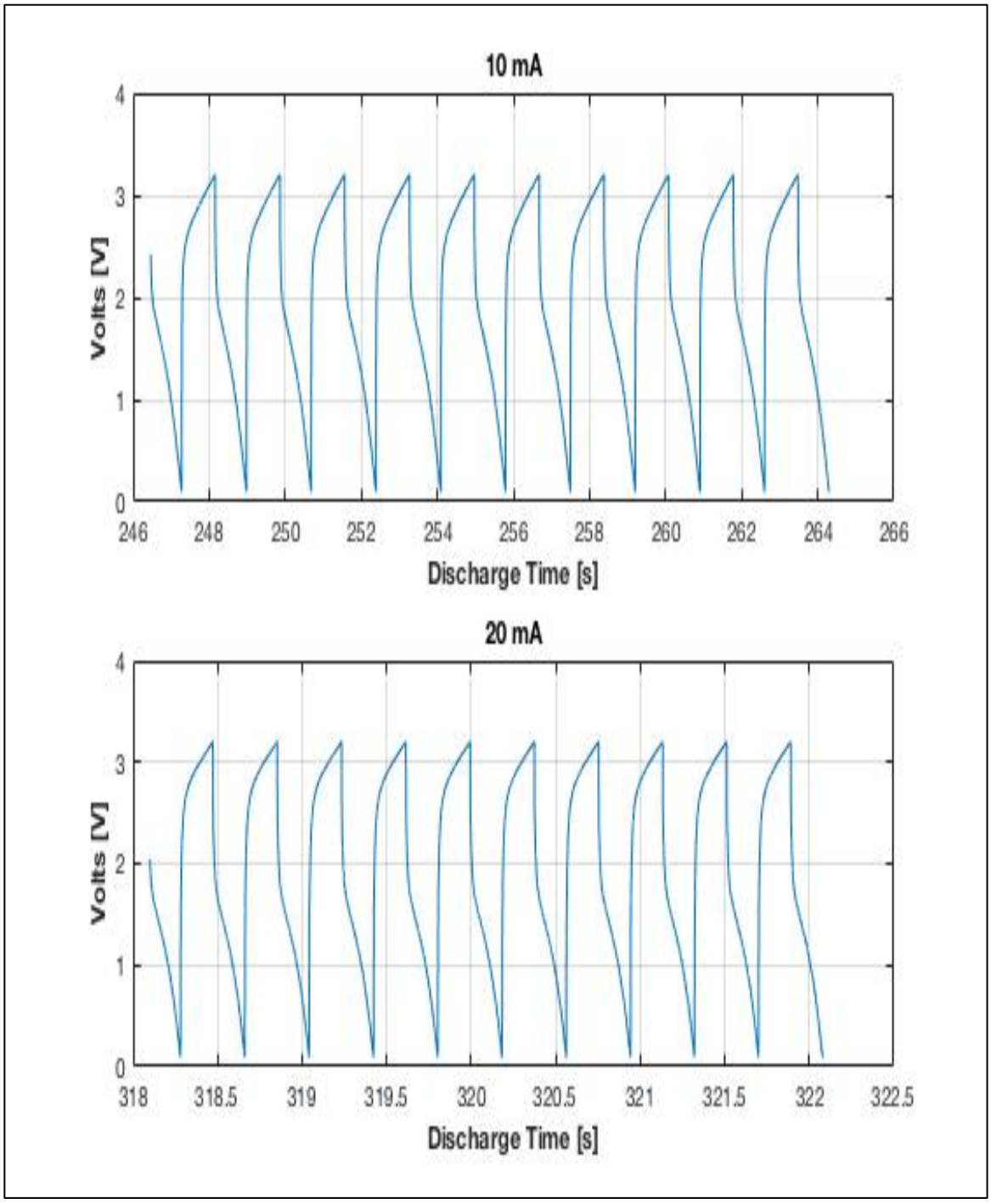

Figure 31. PC + DI/NaCl Solution for Select Low Frequency Tests.

Table 17 contains the performance data for the PC + DI/NaCl solution. The results are the average of 10–20 cycles and tests for all currents were completed satisfactorily.

Table 17. Performance Data for PC + DI/NaCl Solution, Low Frequency Tests

Amperage (mA)	Voltage (V)	Discharge Time (s)	Power Density (W/cm^3)	Dielectric Constant	Capacitance (F)
5	3.2	5.366	3.2	6.04 E 07	1.44 E -02
8	3.2	1.345	5.68	1.79 E 07	4.28 E -03
10	3.2	0.820	7.19	1.23 E 07	2.94 E -03
12	3.2	0.562	8.69	9.64 E 06	2.30 E -03
15	3.2	0.352	10.6	7.70 E 06	1.84 E -03
18	3.2	0.238	12.2	6.60 E 06	1.58 E -03
20	3.2	0.188	13.2	6.02 E 06	1.44 E -03

Figure 32 shows the energy density for PC + DI/NaCl solution. Further examination of the power trend line and the resulting equation predicts an energy density of 90 J/cm^3 at 100 seconds.

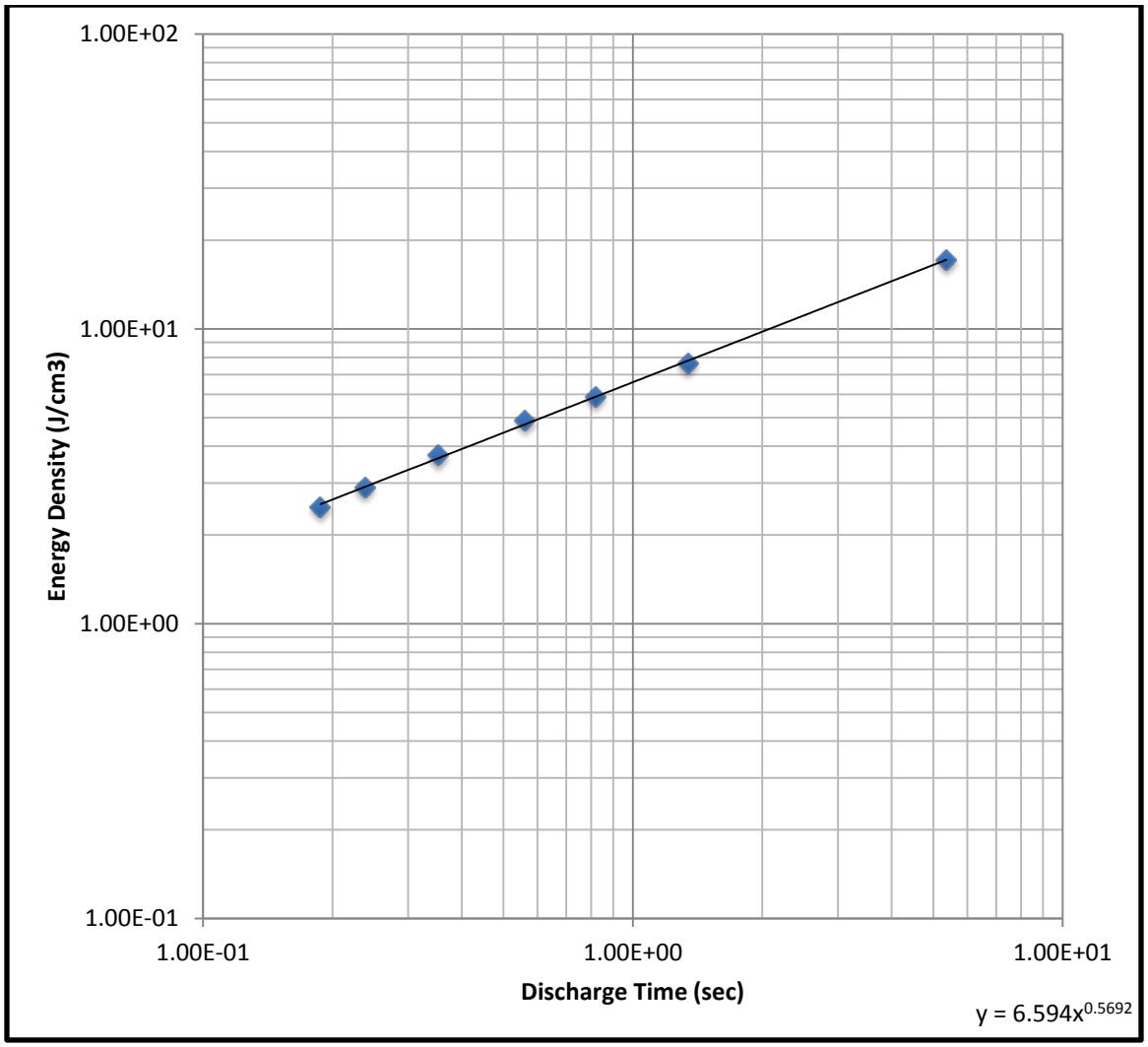

Figure 32. Energy Density for PC + DI/NaCl Solution, Low Frequency Tests

b. High Frequency Tests (PC + DI/NaCl [85/15])

Figure 33 shows the wave shapes of the PC + DI/NaCl solution for the High Frequency Tests. Although ten frequencies were tested, only the 50 mA and 200 mA current waveforms are shown below. The shapes for all waveforms are smooth and connected on both the charge and the discharge phase for all cycles. However, there is evidence of dramatic aliasing on both the charge and discharge phases on all cycles for the higher frequencies (> 100 mA). Additionally, there were sharp declines at the onset of the discharge phase. This indicates that there was wasted energy or less area under the curve when utilizing the Integral analysis tool during post-analysis processing.

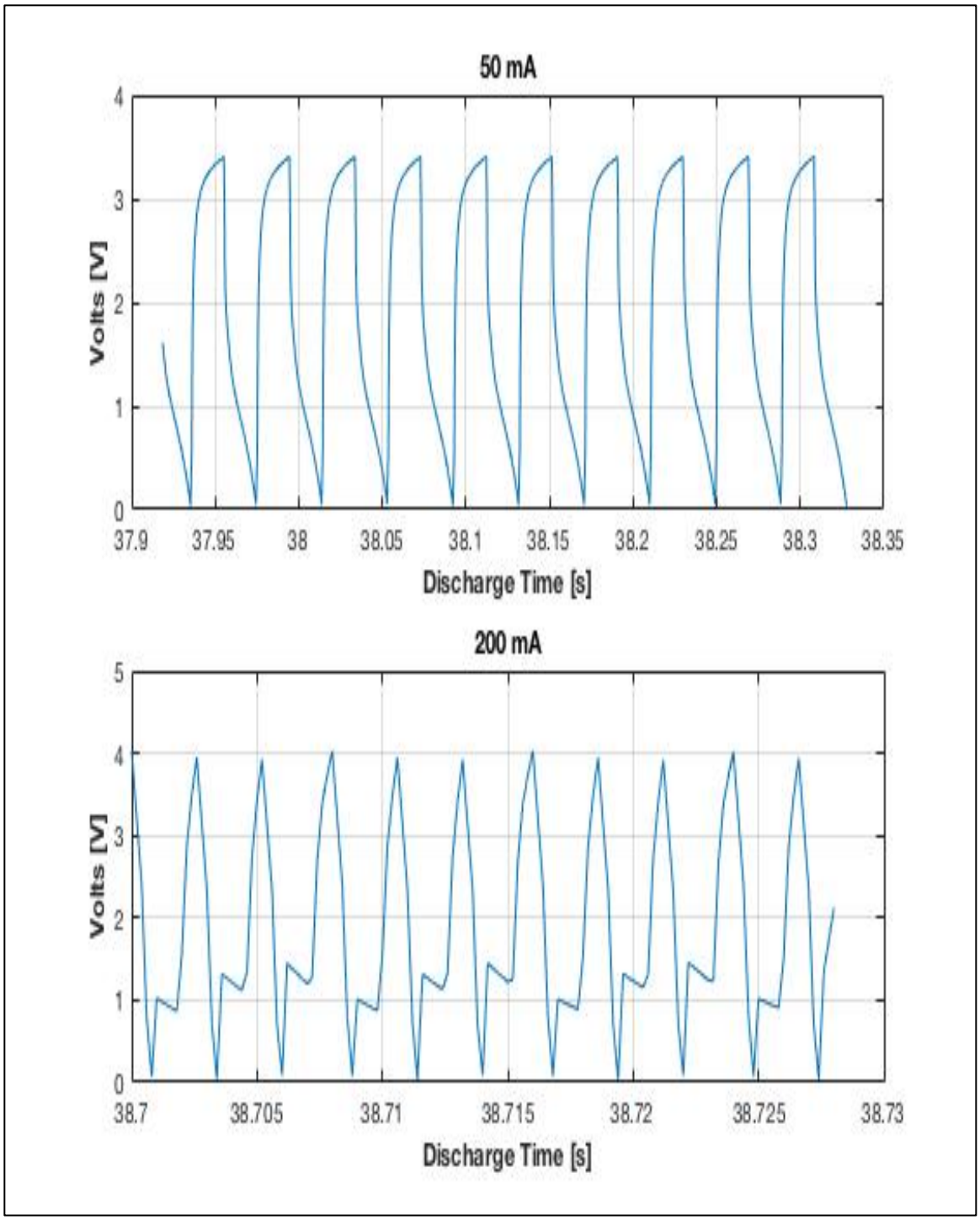

Figure 33. PC + DI/NaCl Solution for Select High Frequency Tests

Table 18 contains the performance data for the PC + DI/NaCl solution for all the High Frequency Tests. The results are the average of 10–20 cycles and tests for all currents were completed satisfactorily but with significant inconsistencies due to the aliasing.

Table 18. Performance Data for PC + DI/NaCl Solution, High Frequency Tests

Amperage (mA)	Voltage (V)	Discharge Time (s)	Power Density (W/cm^3)	Dielectric Constant	Capacitance (F)
10	3.4	0.956	7.23	1.56 E 07	3.72 E -03
20	3.4	0.236	14.1	7.20 E 06	1.72 E -03
30	3.4	0.0960	19.5	5.42 E 06	1.29 E -03
40	3.4	0.0418	23.9	3.86 E 06	9.22 E -04
50	3.4	0.0192	28.8	2.35 E 06	5.62 E -04
80	3.4	0.0035	52.4	6.86 E 05	1.64 E -04
100	3.5	0.0018	82.5	3.96 E 05	9.47 E -05
150	3.7	0.001	237.4	3.04 E 05	7.26 E -05
200	4.0	0.0008	239.1	2.24 E 05	5.36 E -05
250	4.1	0.0007	315.3	2.42 E 05	5.79 E -05

Figure 34 shows the energy density for PC + DI/NaCl solution. Further examination of the power trend line and the resulting equation predicts an energy density of 74 J/cm^3 at 100 seconds.

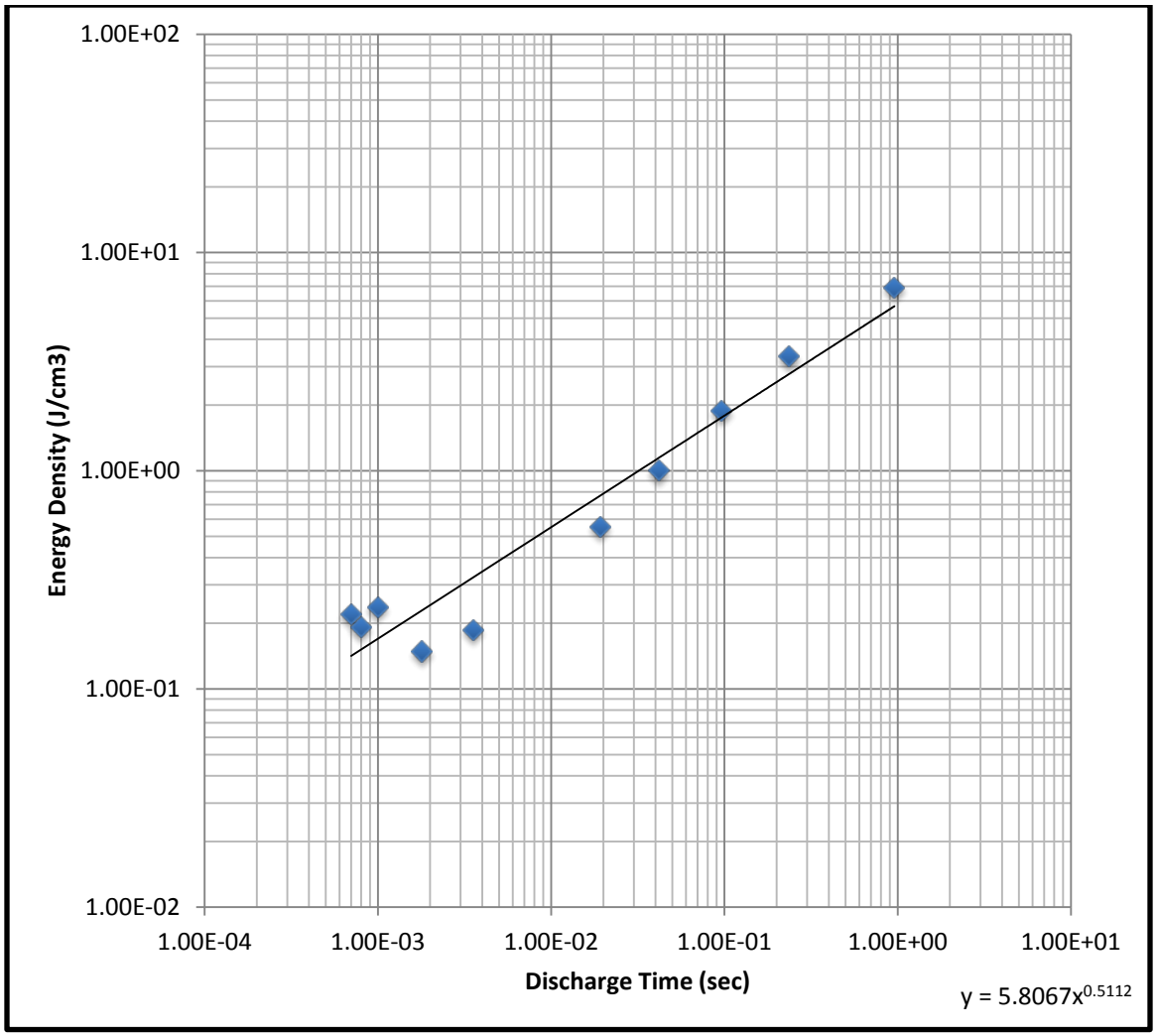

Figure 34. Energy Density for PC + DI/NaCl Solution, High Frequency Tests

c. FHS Tests (PC + DI/NaCl [85/15])

Figure 35 shows the wave shapes of the PC + DI/NaCl solution for the FHS testing. The hold times were 1, 10, 100 and 1000 seconds but only the graphs for 10 and 300 seconds are shown. The shapes for all waveforms are smooth on both the charge and the discharge phase for all cycles.

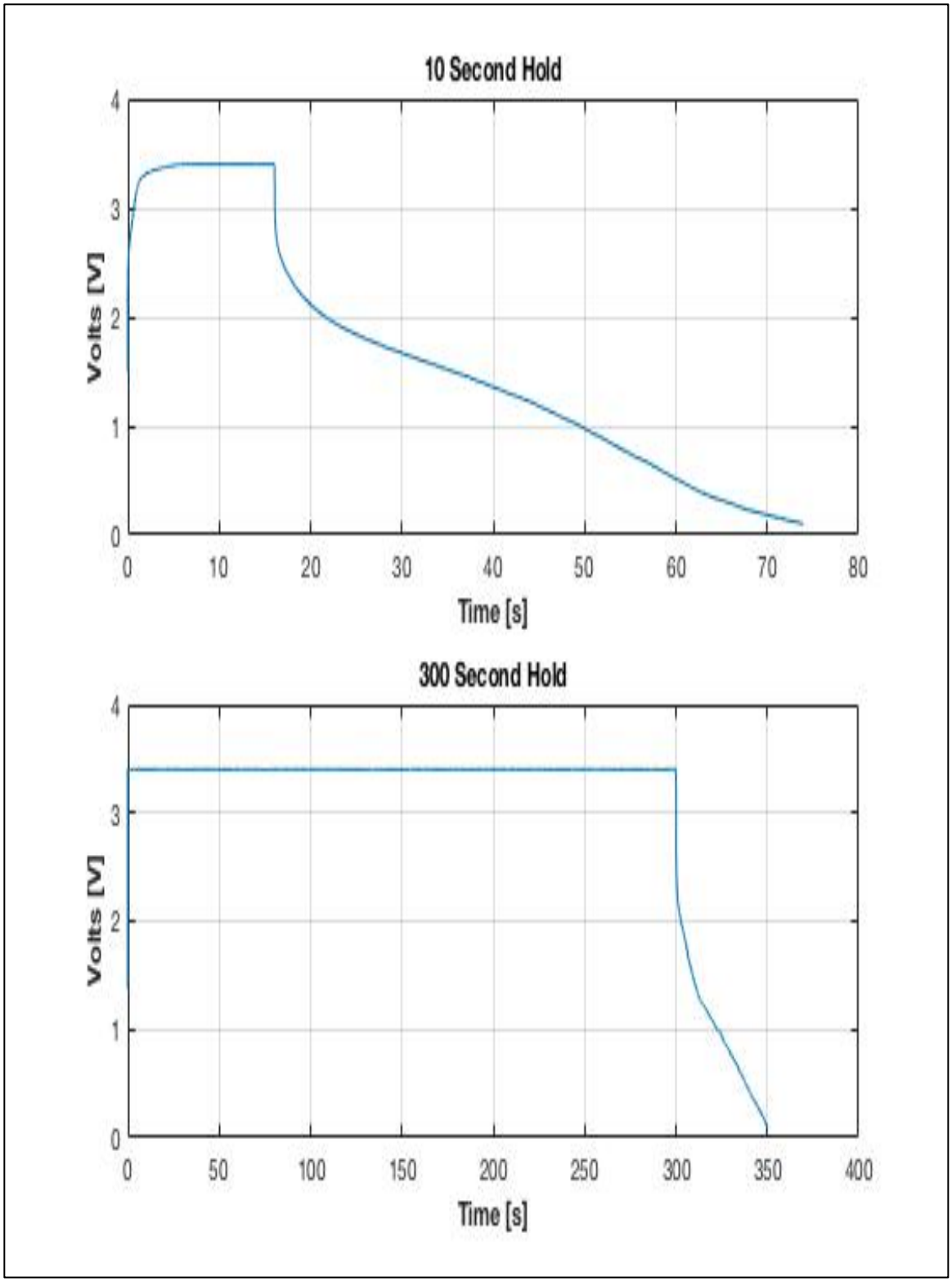

Figure 35. PC + DI/NaCl Solution for FHS Testing

Table 19 contains the performance data for the PC + DI/NaCl solution for all FHS hold times. All eight hold times were run as scheduled.

Table 19. Performance Data for PC + DI/NaCl Solution, FHS Testing

Hold Time (s)	Voltage (V)	Discharge Time (s)	Power Density (W/cm^3)	Dielectric Constant	Capacitance (F)
1	3.4	70.0	0.604	1.75 E 08	0.0418
10	3.4	57.9	0.661	1.18 E 08	0.0281
30	3.4	67.4	0.724	1.07 E 08	0.0255
60	3.4	77.4	0.745	1.13 E 08	0.0270
100	3.4	52.0	0.739	8.61 E 07	0.0206
200	3.4	50.5	0.740	8.38 E 07	0.0200
300	3.4	50.2	0.564	1.25 E 08	0.0299
1000	3.4	37	0.254	2.08 E 08	0.0201

Figure 36 shows the energy density for PC + DI/NaCl solution. FHS testing makes it difficult to predict the performance parameters at a specific discharge time because the trend line equation is based on the hold times. Conversely, the trend line equations from the Low and High Frequency testing schedules are based on discharge times so the predictions are defensible and relevant. Consideration was given to basing the FHS testing on discharge times but the point of the Murata technique was to exploit the supposed positive effects that hold times had on the NTSDM capacitor performance parameters. To that end, FHS testing was based on the hold times and the charts that follow are valuable for highlighting energy density trends as the hold times are increased.

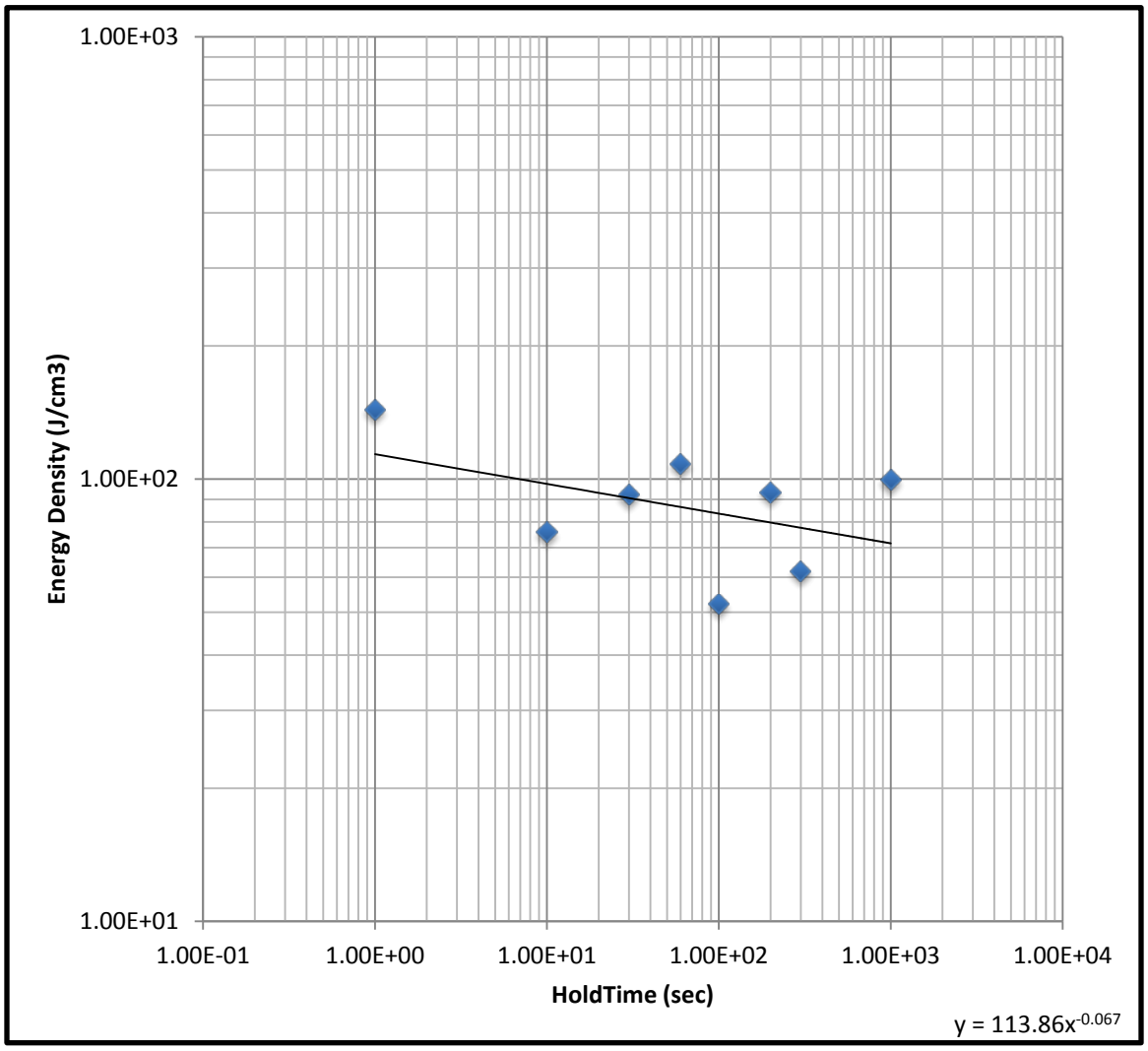

Figure 36. Energy Density for PC + DI/NaCl Solution, FHS Testing

4. PC + DI/NaCl [80/20]

a. Low Frequency Tests (PC + DI/NaCl [80/20])

No good data was obtained. Due to the immense amount of data already collected, a retest may not be necessary.

b. High Frequency Tests (PC + DI/NaCl [80/20])

Figure 37 shows the wave shapes of the PC + DI/NaCl for the High Frequency Tests. Although ten frequencies were tested, only the 50 mA and 200 mA current waveforms are shown below. The shapes for all waveforms are smooth and connected on both the charge and the discharge phase for all cycles. However, there is evidence of dramatic aliasing on both the charge and discharge phases on all cycles above 150 mA. Additionally, there were sharp declines at the onset of the discharge phase. This indicates that there was wasted energy or less area under the curve when utilizing the integral analysis tool during post-analysis processing.

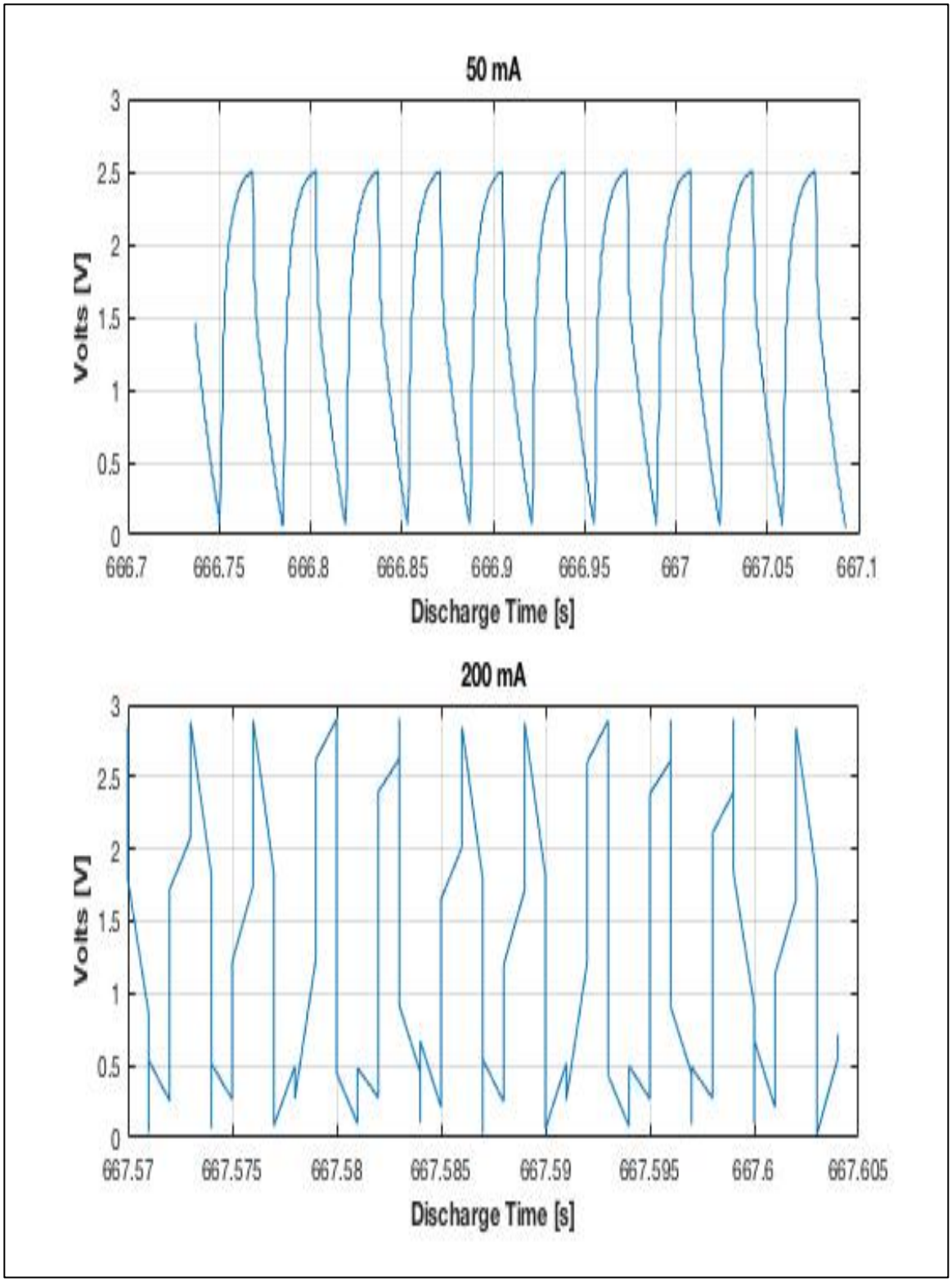

Figure 37. PC + DI/NaCl Solution for Select High Frequency Tests

Table 20 contains the performance data for the PC + DI/NaCl solution for all the High Frequency Tests. The results are the average of 10–20 cycles and tests for all currents were completed satisfactorily but with significant inconsistencies due to the aliasing.

Table 20. Performance Data for PC + DI/NaCl Solution, High Frequency Tests

Amperage (mA)	Voltage (V)	Discharge Time (s)	Power Density (W/cm^3)	Dielectric Constant	Capacitance (F)
10	2.4	4.36	5.99	7.98 E 07	1.19 E -02
20	2.5	0.653	12.0	2.31 E 07	5.51 E -03
30	2.6	0.128	16.8	8.23 E 06	1.97 E -03
40	2.5	0.0382	21.4	4.07 E 06	9.72 E -04
50	2.5	0.0163	24.7	2.32 E 06	5.55 E -04
80	2.6	0.0046	40.6	1.06 E 06	2.52 E -04
100	2.6	0.0028	57.4	8.08 E 05	1.93 E -04
150	2.7	0.0014	104.5	5.39 E 05	1.29 E -04
200	2.7	0.0010	161.1	4.75 E 05	1.13 E -04
250	3.0	0.0008	239.6	3.69 E 05	8.82 E -05

Figure 38 shows the energy density for PC + DI/NaCl solution. Further examination of the power trend line and the resulting equation predicts an energy density of 141 J/cm^3 at 100 seconds.

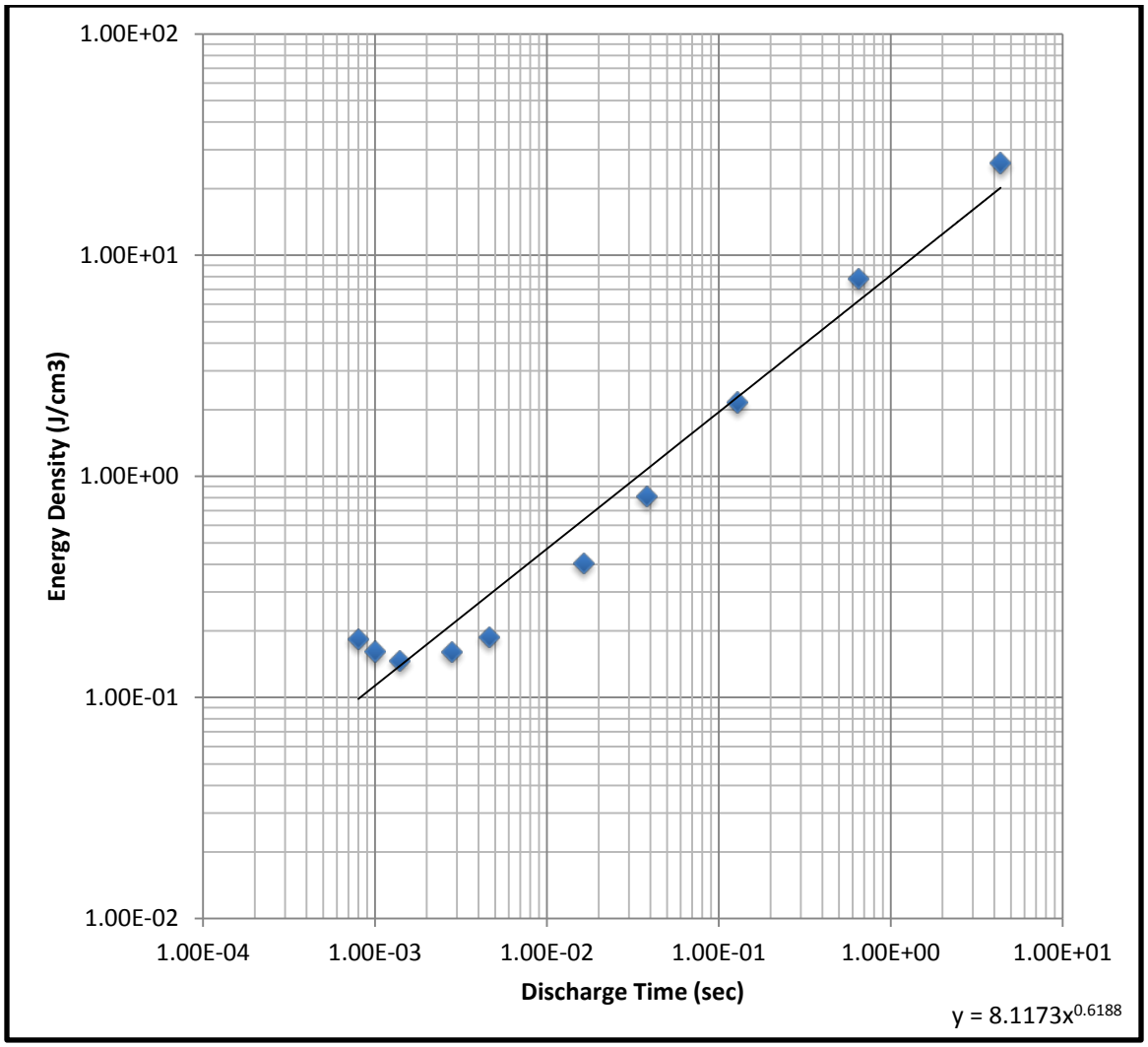

Figure 38. Energy Density for PC + DI/NaCl Solution, High Frequency Tests

c. FHS Tests (PC + DI/NaCl [80/20])

Figure 39 shows the wave shapes of the PC + DI/NaCl solution for the FHS testing. The hold times were 1, 10, 100 and 1000 seconds but only the graphs for 10 and 300 seconds are shown. The shapes for all waveforms are smooth on both the charge and the discharge phase for all cycles.

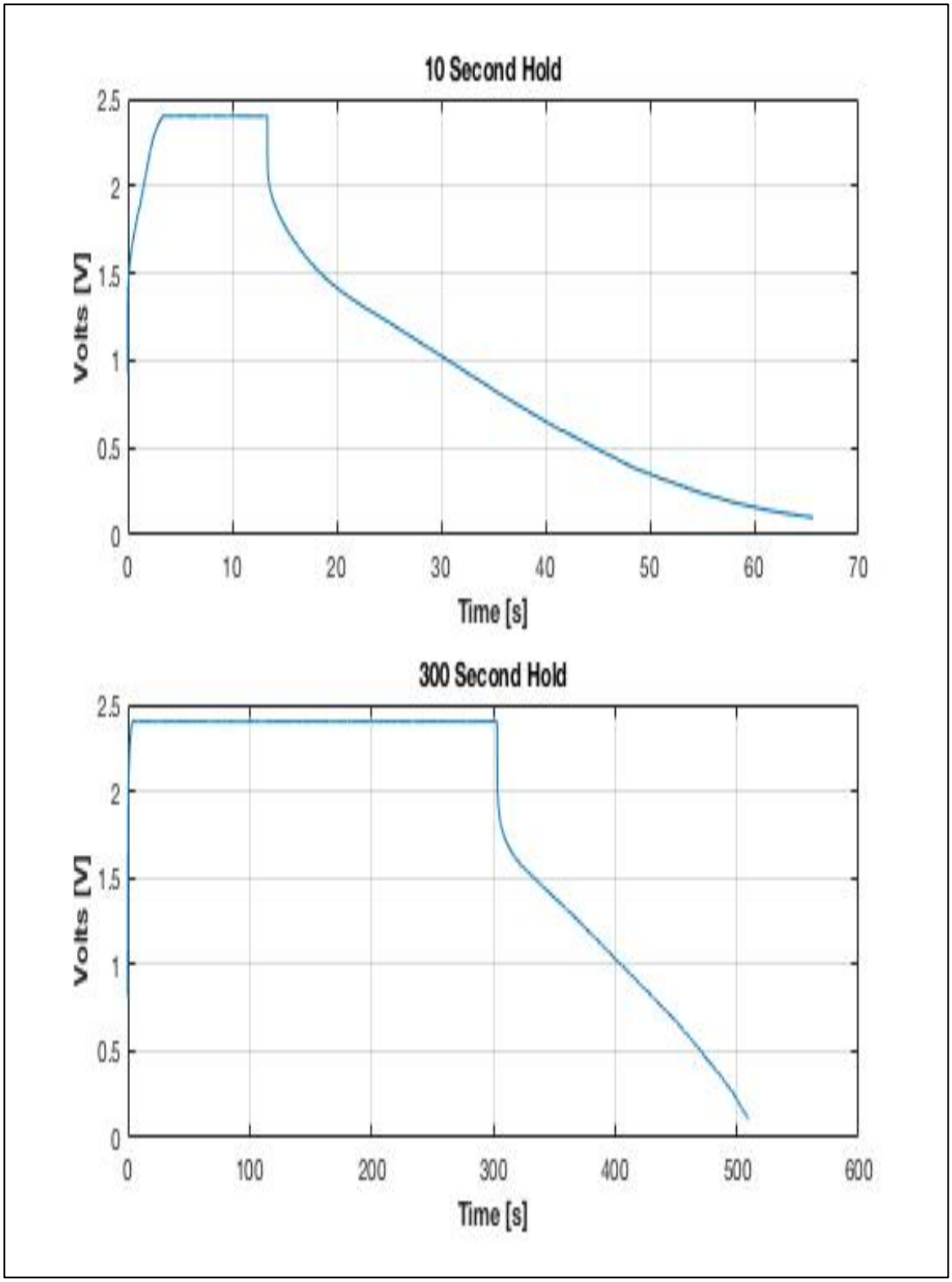

Figure 39. PC + DI/NaCl Solution for FHS Testing.

Table 21 contains the performance data for the PC + DI/NaCl solution for all FHS hold times. All eight hold times were run as scheduled.

Table 21. Performance Data for PC + DI/NaCl Solution, FHS Testing

Hold Time (s)	Voltage (V)	Discharge Time (s)	Power Density (W/cm^3)	Dielectric Constant	Capacitance (F)
1	2.4	57.8	0.330	2.54 E 08	0.061
10	2.4	52.0	0.441	1.76 E 08	0.042
30	2.4	68.0	0.514	1.72 E 08	0.041
60	2.4	87.0	0.555	1.93 E 08	0.046
100	2.4	113.0	0.571	2.42 E 08	0.058
200	2.4	162.0	0.576	1.72 E 08	0.041
300	2.4	206.4	0.564	2.12 E 08	0.051
1000	2.4	175.0	0.568	3.64 E 08	0.087

Figure 40 shows the energy density for PC + DI/NaCl solution. FHS testing makes it difficult to predict the performance parameters at a specific discharge time because the trend line equation is based on the hold times. Conversely, the trend line equations from the Low and High Frequency testing schedules are based on discharge times so the predictions are defensible and relevant. Consideration was given to basing the FHS testing on discharge times but the point of the Murata technique was to exploit the supposed positive effects that hold times had on the NTSDM capacitor performance parameters. To that end, FHS testing was based on the hold times and the charts that follow are valuable for highlighting energy density trends as the hold times are increased.

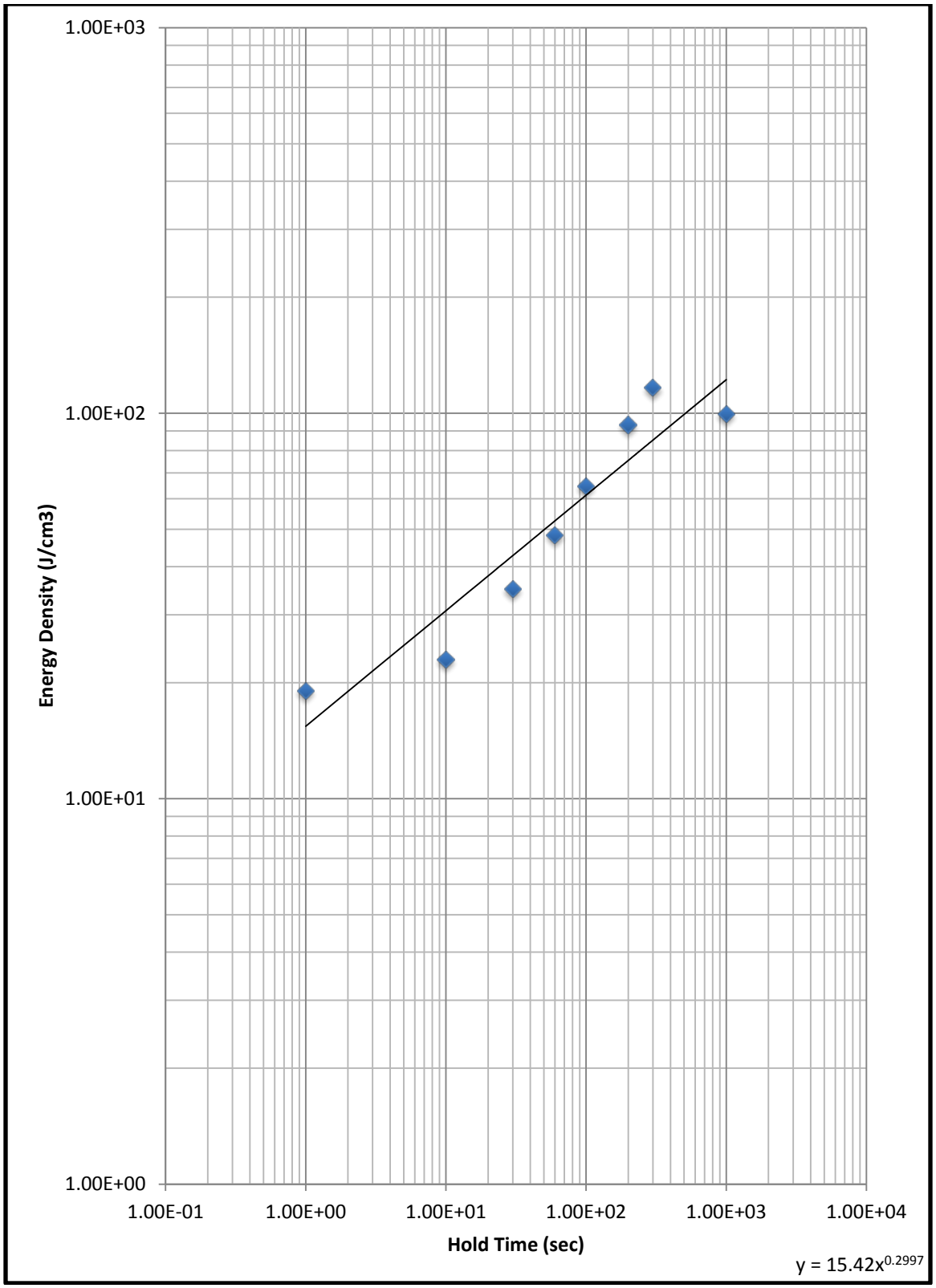

Figure 40. Energy Density for PC + DI/NaCl Solution, FHS Testing

5. PC + DI/NaCl [75/25]

a. Low Frequency Tests (PC + DI/NaCl [75/25])

Figure 41 shows the wave shapes of the PC + DI/NaCl solution for the Low Frequency Tests. Although seven frequencies were tested, only the 10 mA and 20 mA constant current waveforms are shown below. The shapes for all waveforms are smooth on both the charge and the discharge phases. There is no evidence of aliasing nor sharp declines at the onset of the discharge phase. This indicates that there was no wasted energy and the capacitor was performing at its fullest potential for the given the charge rate.

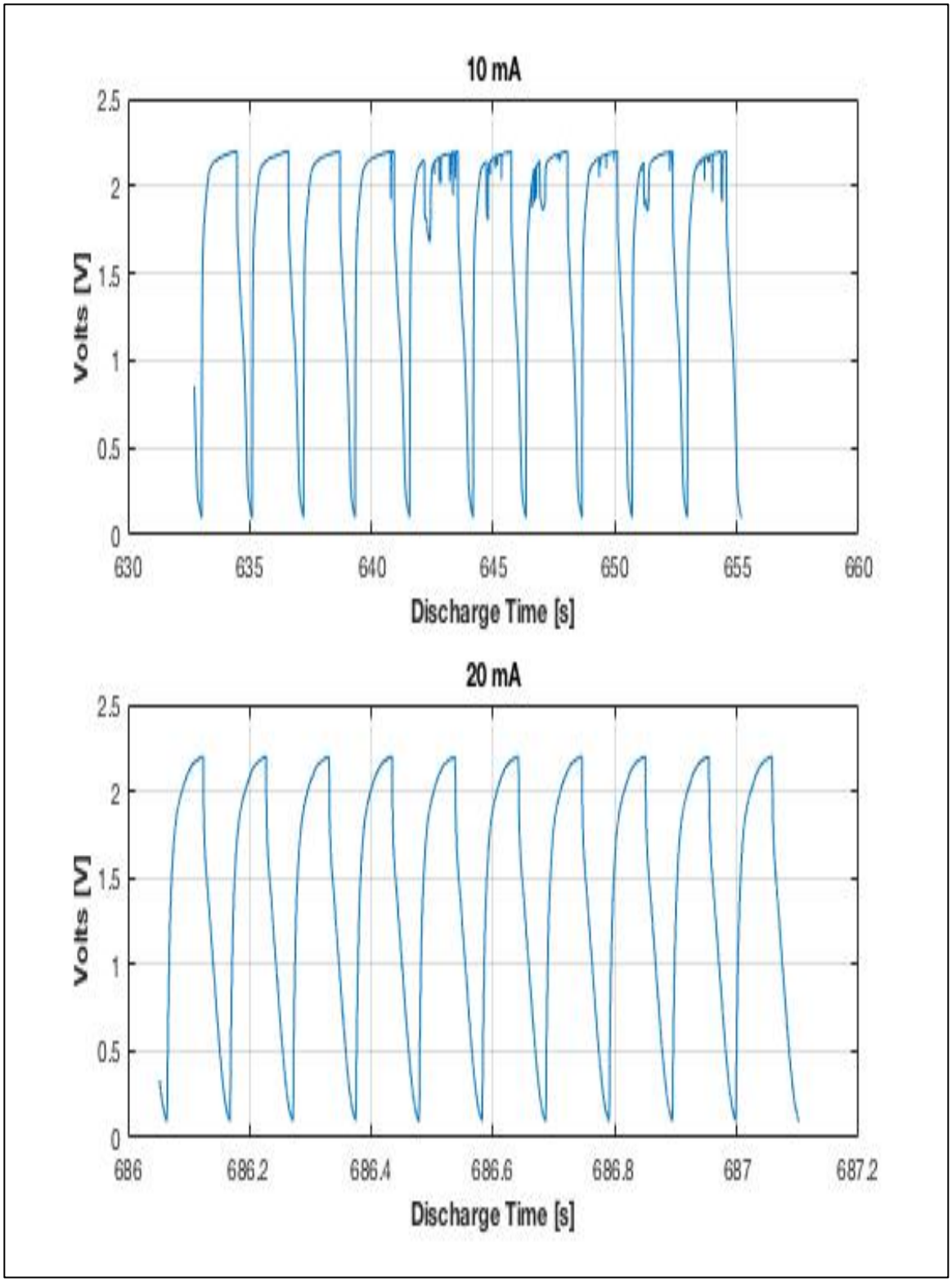

Figure 41. PC + DI/NaCl Solution for Select Low Frequency Tests

Table 22 contains the performance data for the PC + DI/NaCl solution. The results are the average of 10–20 cycles and tests for all currents were completed satisfactorily.

Table 22. Performance Data for PC + DI/NaCl Solution, Low Frequency Tests

Amperage (mA)	Voltage (V)	Discharge Time (s)	Power Density (W/cm^3)	Dielectric Constant	Capacitance (F)
5	2.2	5.62	2.90	6.62 E 07	1.58 E -02
8	2.2	1.57	3.92	3.66 E 07	8.75 E -03
10	2.2	0.603	5.01	1.51 E 07	3.60 E -03
12	2.2	0.300	6.00	8.35 E 06	1.99 E -03
15	2.2	0.120	7.22	4.58 E 06	1.09 E -03
18	2.2	0.062	8.53	3.07 E 06	7.33 E -04
20	2.2	0.044	9.44	2.62 E 06	6.25 E -04

Figure 42 shows the energy density for PC + DI/NaCl solution. Further examination of the power trend line and the resulting equation predicts an energy density of 145 J/cm^3 at 100 seconds.

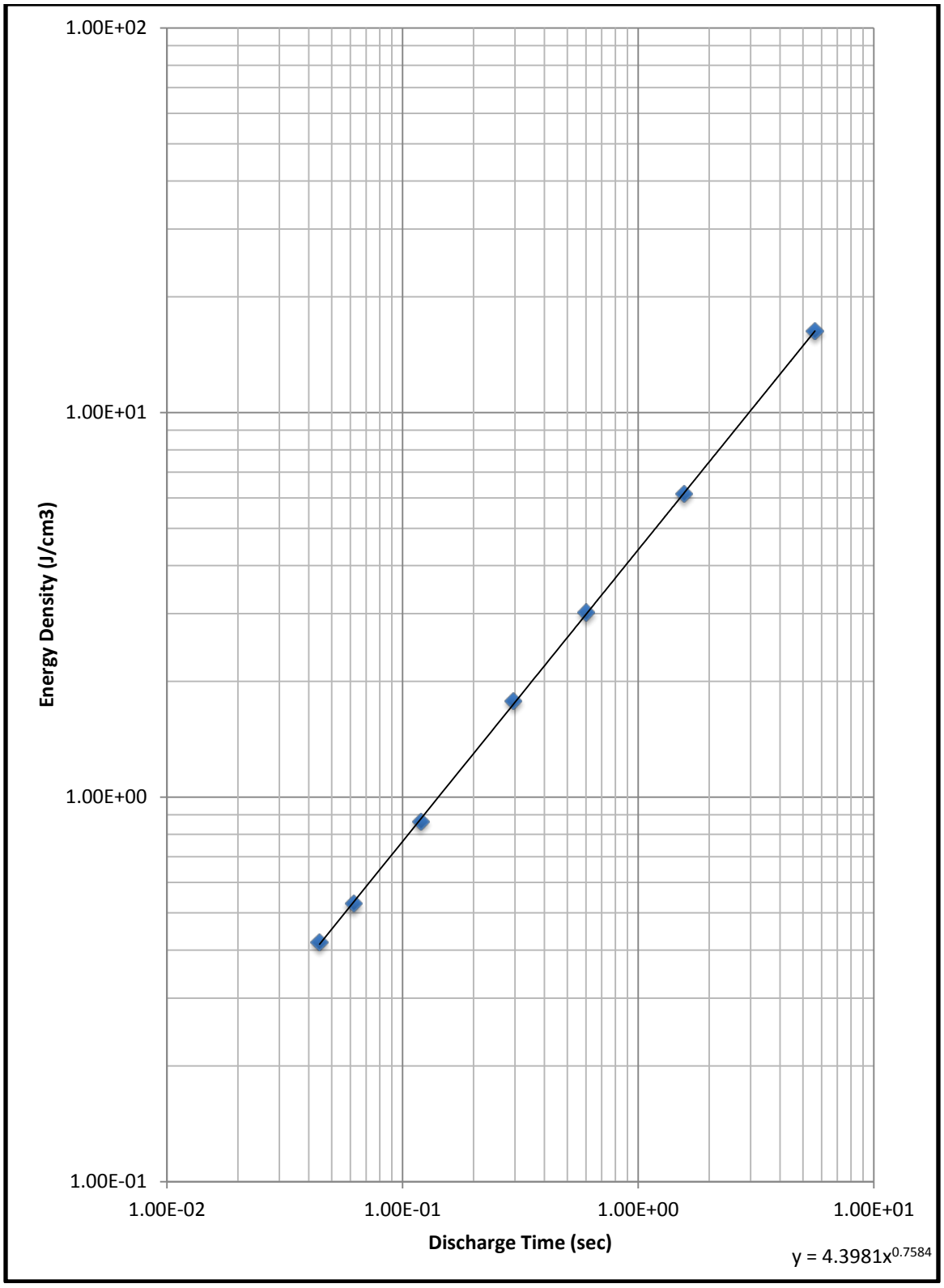

Figure 42. Energy Density for PC + DI/NaCl Solution, Low Frequency Tests

b. High Frequency Tests (PC + DI/NaCl [75/25])

Figure 43 shows the wave shapes of the PC + DI/NaCl solution for the High Frequency Tests. Although ten frequencies were tested, only the 50 mA and 200 mA current waveforms are shown below. The shapes for all waveforms are smooth and connected on both the charge and the discharge phase for all cycles. However, there is evidence of dramatic aliasing on both the charge and discharge phases on all cycles above 50 mA. Additionally, there were sharp declines at the onset of the discharge phase. This indicates that there was wasted energy or less area under the curve when utilizing the Integral analysis tool during post-analysis processing.

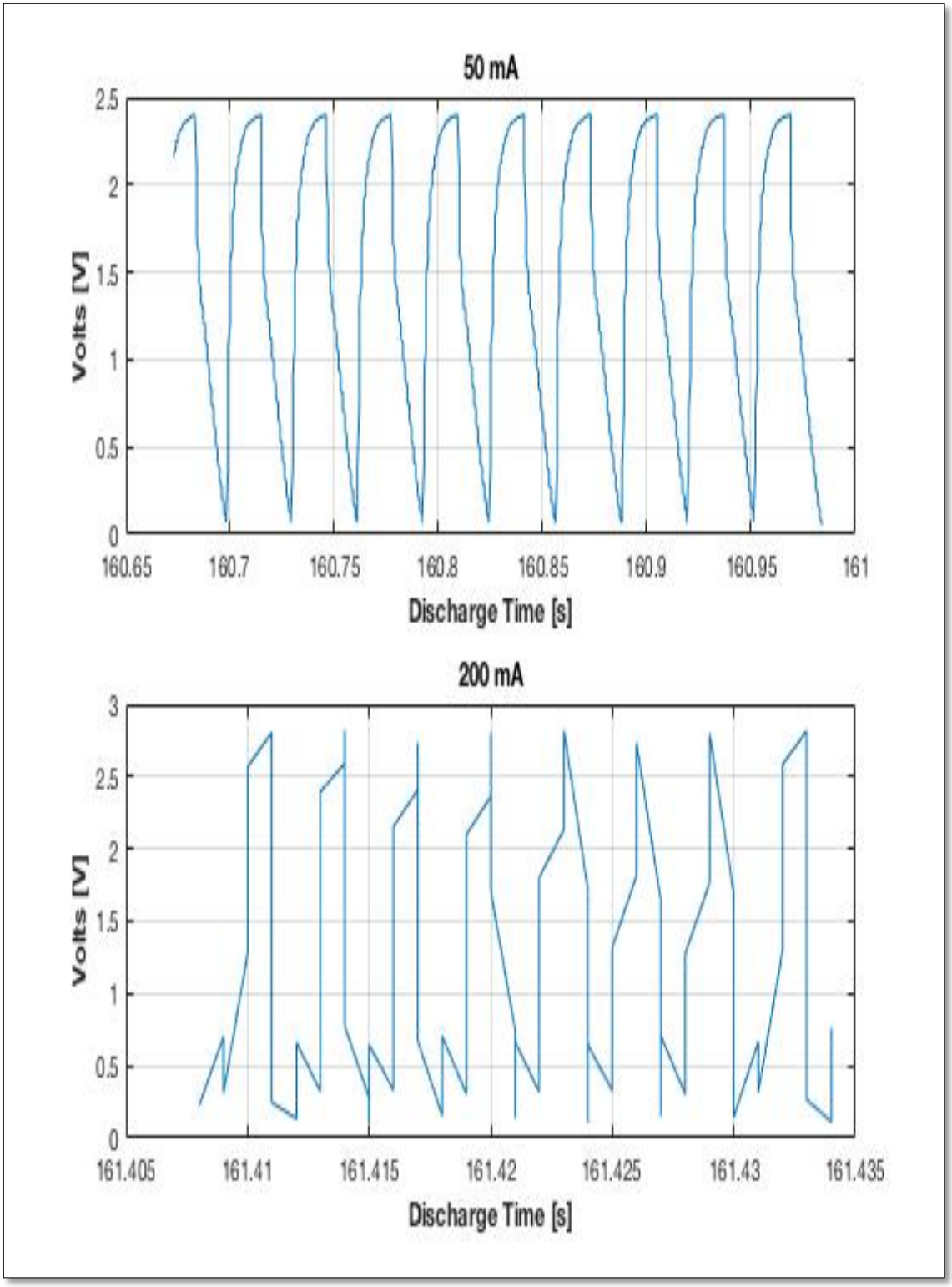

Figure 43. PC + DI/NaCl Solution for Select High Frequency Tests

Table 23 contains the performance data for the PC + DI/NaCl solution for all the High Frequency Tests. The results are the average of 10–20 cycles and tests for all currents were completed satisfactorily but with significant inconsistencies due to the aliasing.

Table 23. Performance Data for PC + DI/NaCl Solution, High Frequency Tests

Amperage (mA)	Voltage (V)	Discharge Time (s)	Power Density (W/cm^3)	Dielectric Constant	Capacitance (F)
10	3.0	.83	6.40	2.01 E 07	4.80 E -03
20	3.0	.19	11.4	1.03 E 07	2.47 E -03
30	3.0	.075	15.4	6.73 E 06	1.61 E -03
40	3.0	.037	18.8	4.86 E 06	1.16 E -03
50	3.0	.020	21.9	3.58 E 06	8.55 E -03
80	3.1	.005	33.5	1.60 E 06	3.82 E -04
100	3.1	.0024	51.6	9.01 E 05	2.15 E -04
150	3.2	.0008	148.8	2.52 E 05	6.01 E -05
200	3.5	.0006	238.8	9.79 E 04	2.34 E -05
250	3.8	.0008	292.6	1.04 E 05	2.48 E -05

Figure 44 shows the energy density for PC + DI/NaCl solution. Further examination of the power trend line and the resulting equation predicts an energy density of 158 J/cm^3 at 100 seconds.

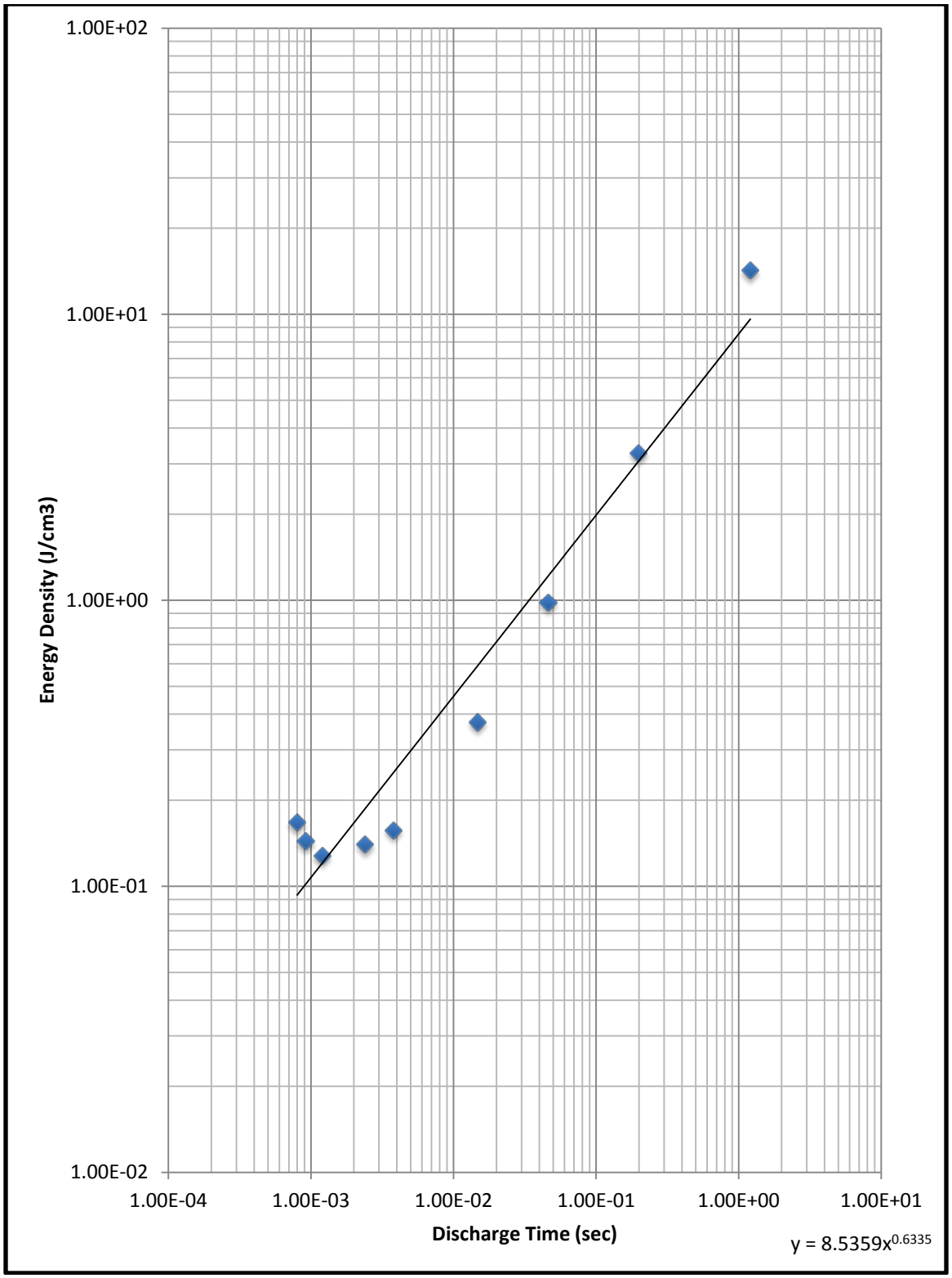

Figure 44. Energy Density for PC + DI/NaCl Solution, High Frequency Tests

c. FHS Tests (PC + DI/NaCl [75/25])

Figure 45 shows the wave shapes of the PC + DI/NaCl solution for the FHS testing. The hold times were 1, 10, 100 and 1000 seconds but only the graphs for 10 and 300 seconds are shown. The shapes for all waveforms are smooth on both the charge and the discharge phase for all cycles.

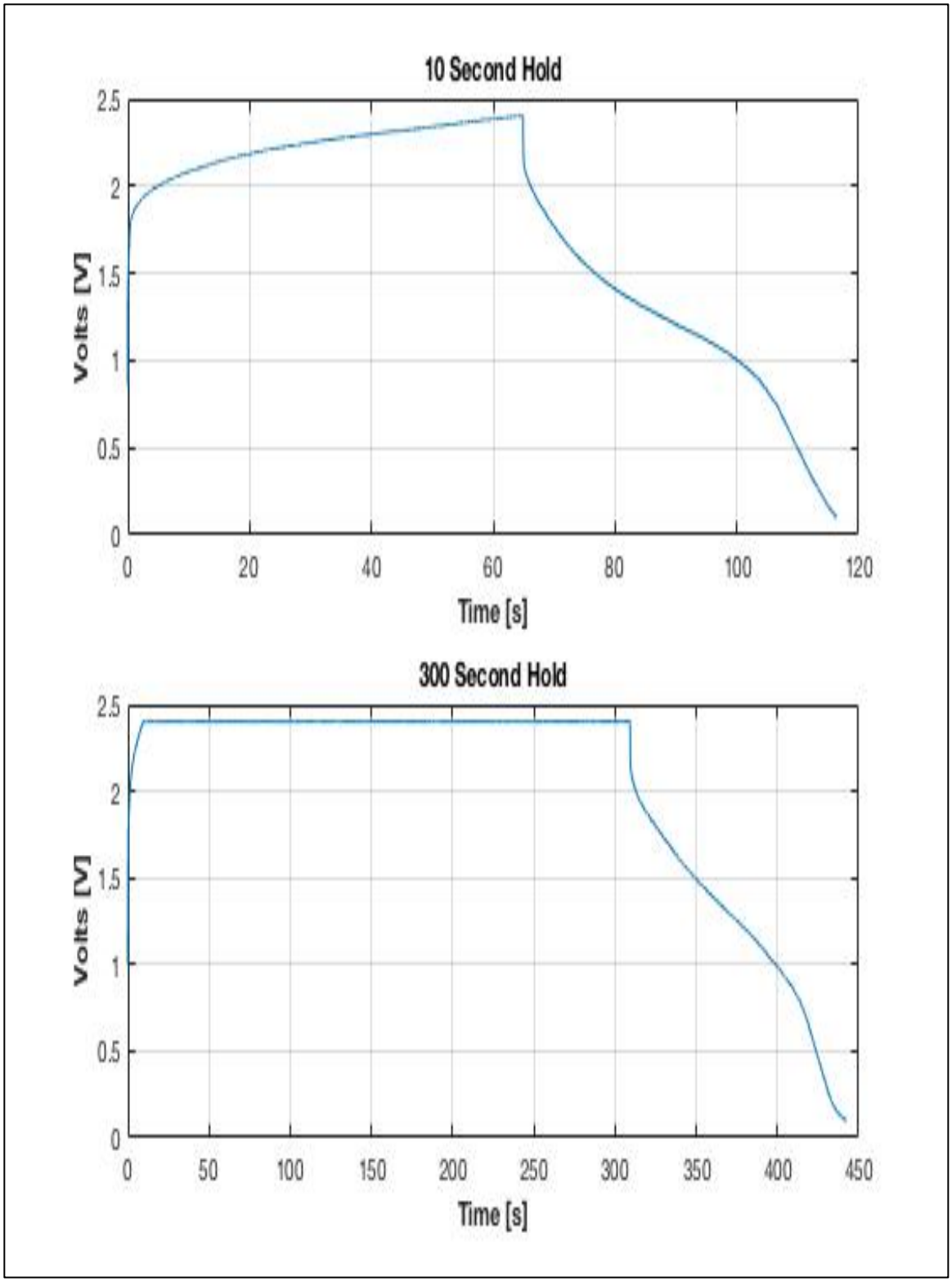

Figure 45. PC + DI/NaCl Solution for FHS Testing

Table 24 contains the performance data for the DMSO and $NaNO_3$ solution for all FHS hold times. All eight hold times were run as scheduled.

Table 24. Performance Data for PC + DI/NaCl Solution, FHS Testing

Hold Time (s)	Voltage (V)	Discharge Time (s)	Power Density (W/cm^3)	Dielectric Constant	Capacitance (F)
1	2.4	51.0	0.675	6.21 E 07	0.015
10	2.4	43.0	0.648	1.35 E 08	0.032
30	2.4	49.0	0.637	1.25 E 08	0.030
60	2.4	65.0	0.659	1.00 E 08	0.024
100	2.4	91.0	0.669	1.55 E 08	0.037
200	2.4	112.0	0.660	1.68 E 08	0.040
300	2.4	133.0	0.688	4.19 E 08	0.027
1000	2.4	240.0	0.527	6.36 E 08	0.015

Figure 46 shows the energy density for PC + DI/NaCl solution. FHS testing makes it difficult to predict the performance parameters at a specific discharge time because the trend line equation is based on the hold times. Conversely, the trend line equations from the Low and High Frequency testing schedules are based on discharge times so the predictions are defensible and relevant. Consideration was given to basing the FHS testing on discharge times but the point of the Murata technique was to exploit the supposed positive effects that hold times had on the NTSDM capacitor performance parameters. To that end, FHS testing was based on the hold times and the charts that follow are valuable for highlighting energy density trends as the hold times are increased.

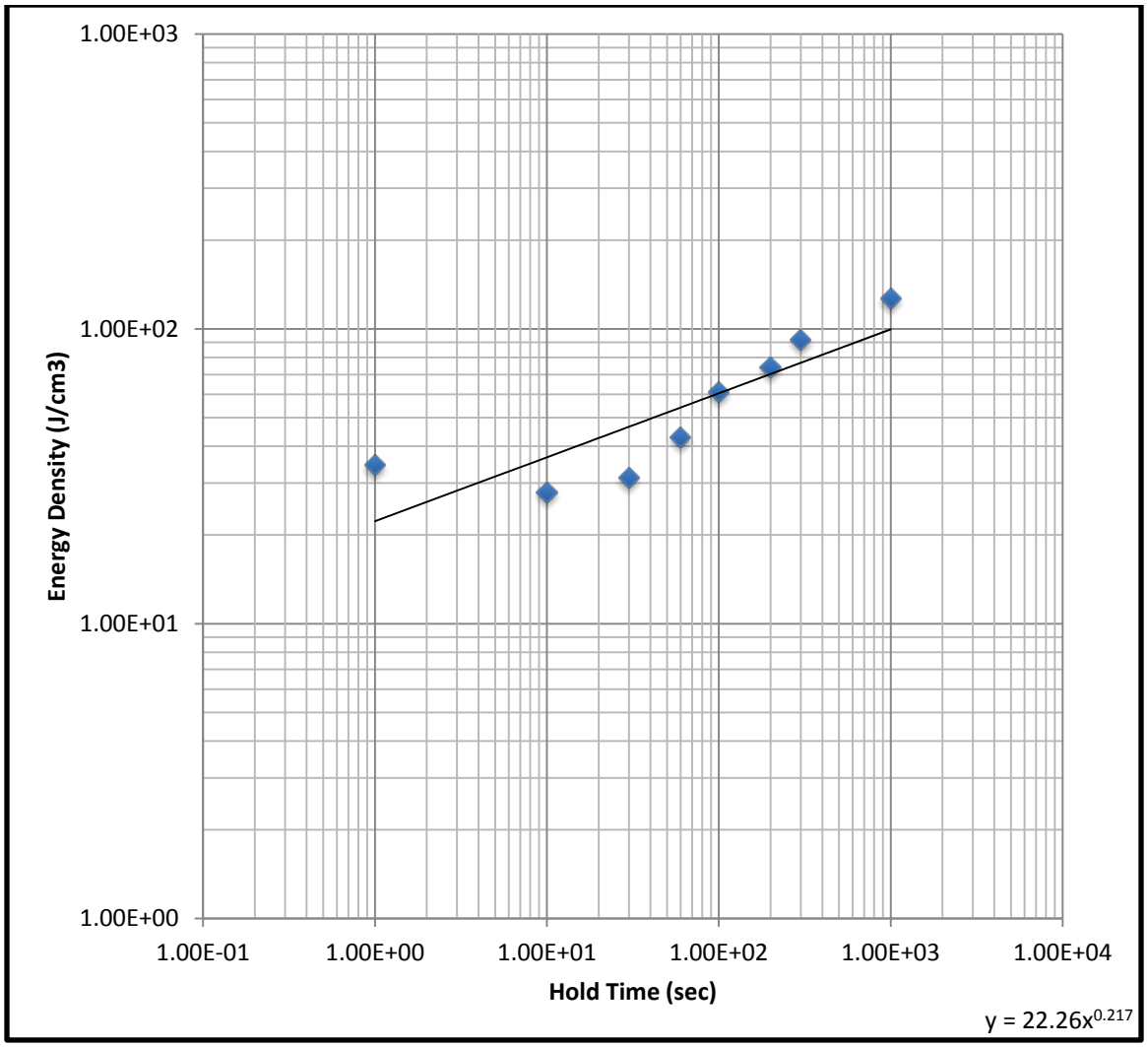

Figure 46. Energy Density for PC + DI/NaCl Solution, FHS Testing

B. DMSO

Figure 47 shows the complete testing schedule for the selected solvent.

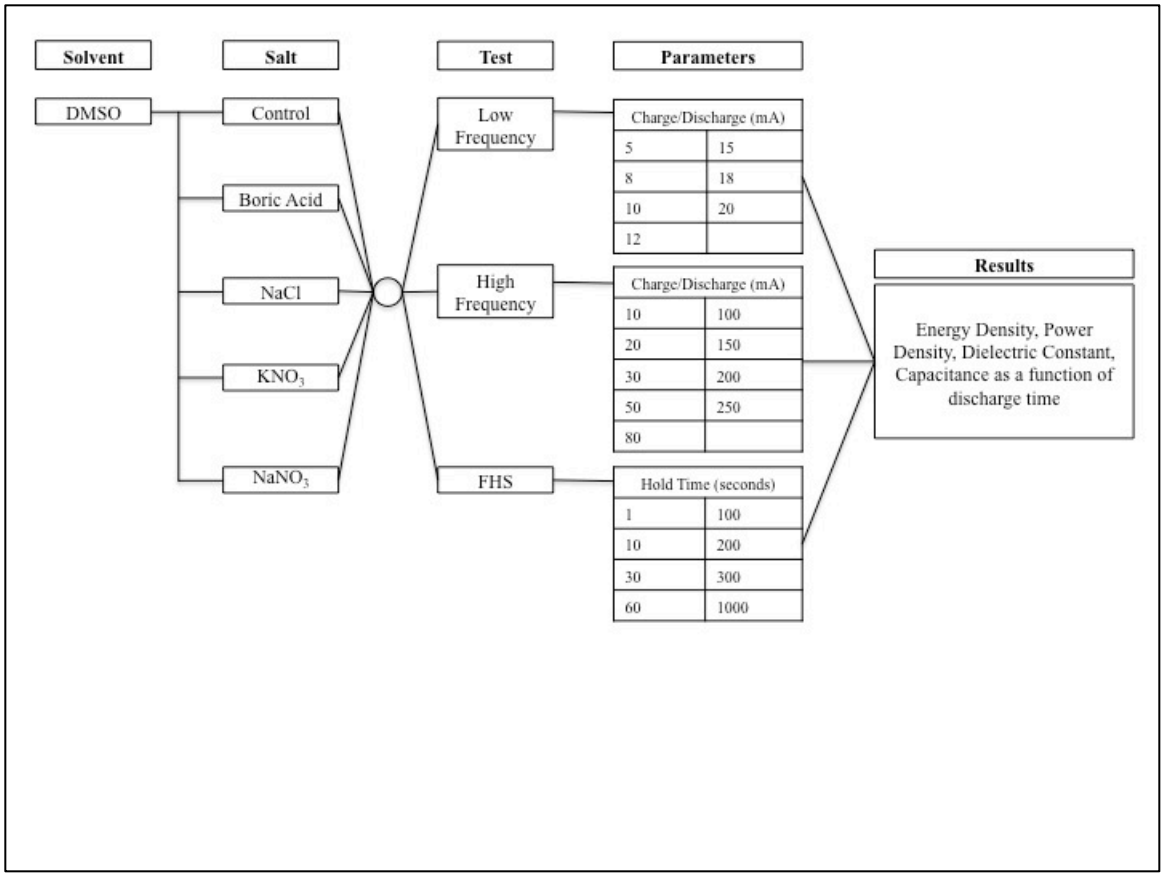

Figure 47. Complete Testing Schedule for DMSO

1. DMSO – Control

a. Low Frequency Tests (DMSO – Control)

Table 25 contains the performance data for the DMSO and control solution. The results are the average of 10–20 cycles and tests for all currents were completed satisfactorily. The capacitor reached a voltage of 3.0 volts with the specified electrolyte solution. Further examination of the power trend line and the resulting equation predicts an energy density of 74 J/cm^3 at 100 seconds.

Table 25. Performance Data for DMSO and Control Solution, Low Frequency Tests

Amperage (mA)	Energy Density (J/cm^3)	Discharge Time (s)	Power Density (W/cm^3)	Dielectric Constant	Capacitance (F)
5	2.14	3.61	3.03	4.41 E 07	.011
8	0.870	1.31	4.98	2.67 E 07	.006
10	0.568	0.79	6.14	2.02 E 07	.005
12	0.380	0.54	7.29	1.67 E 07	.004
15	0.227	0.33	9.0	1.28 E 07	.003
18	0.157	0.22	10.4	1.03 E 07	.002
20	0.124	0.17	11.6	9.02 E 06	.002

b. High Frequency Tests (DMSO – Control)

Table 26 contains the performance data for the DMSO and control solution for all the High Frequency Tests. The results are the average of 10–20 cycles and tests for all currents were completed satisfactorily but with significant inconsistencies due to the aliasing. The capacitor voltage ranged from 3.0–3.8 volts with the specified electrolyte solution. Further examination of the power trend line and the resulting equation predicts an energy density of 39 J/cm^3 at 100 seconds.

Table 26. Performance Data for DMSO and Control Solution, High Frequency Tests

Amperage (mA)	Energy Density (J/cm^3)	Discharge Time (s)	Power Density (W/cm^3)	Dielectric Constant	Capacitance (F)
10	0.545	.103	5.3	2.92 E 06	6.97 E -04
20	0.119	.019	7.6	9.70 E 05	2.32 E -04
30	0.067	.004	16.6	4.02 E 05	9.60 E -05
40	0.061	.002	30.7	2.04 E 05	4.88 E -05
50	0.066	.001	53.2	1.38 E 05	3.30 E -05
80	0.090	.001	112.1	7.00 E 05	1.67 E -05
100	0.114	8.0 E -04	142.7	7.26 E 04	1.73 E -05
150	0.156	6.0 E -04	259.8	4.92 E 04	1.18 E -05
200	0.243	6.4 E -04	384.3	5.10 E 04	1.22 E -05
250	0.342	6.0 E -04	569.8	5.27 E 04	1.26 E -05

c. FHS Tests (DMSO – Control)

Table 27 contains the performance data for the DMSO and control solution for all FHS hold times. A significant note is that only four of the normal eight hold times were run because a final testing plan was not yet created. The capacitor reached a voltage of 3.0 volts with the specified electrolyte solution.

Table 27. Performance Data for DMSO and Control Solution, FHS Testing

Hold Time (s)	Energy Density (J/cm^3)	Discharge Time (s)	Power Density (W/cm^3)	Dielectric Constant	Capacitance (F)
1	2.44	5	.488	1.56 E 07	3.74 E -03
10	4.56	9	.506	2.93 E 07	7.01 E -03
100	4.41	9	.490	3.86 E 07	9.22 E -03
1000	1.65	5	.330	2.22 E 07	5.30 E -03

2. DMSO – NaCl

a. Low Frequency Tests (DMSO – NaCl)

Table 28 contains the performance data for the DMSO and NaCl solution. The results are the average of 10–20 cycles and tests for all currents were completed satisfactorily. The capacitor reached a voltage of 3 volts with the specified electrolyte solution. Further examination of the power trend line and the resulting equation predicts an energy density of 69 J/cm^3 at 100 seconds.

Table 28. Performance Data for DMSO and NaCl Solution, Low Frequency Tests

Amperage (mA)	Energy Density (J/cm^3)	Discharge Time (s)	Power Density (W/cm^3)	Dielectric Constant	Capacitance (F)
5	5.72	2.06	2.9	3.13 E 07	.007
8	3.15	.73	4.3	1.76 E 07	.004
10	2.32	.43	5.4	1.31 E 07	.003
12	1.82	.29	6.5	1.07 E 07	.002
15	1.30	.17	7.7	8.05 E 07	.002
18	0.970	.11	9.0	6.25 E 07	.001
20	0.810	.08	9.9	5.43 E 06	.001

b. High Frequency Tests (DMSO – NaCl)

Table 29 contains the performance data for the DMSO and NaCl solution for all the High Frequency Tests. The results are the average of 10–20 cycles and tests for all currents were completed satisfactorily but with significant inconsistencies due to the aliasing. The capacitor reached a voltage of 3.0 volts with the specified electrolyte solution. Further examination of the power trend line and the resulting equation predicts an energy density of 13 J/cm^3 at 100 seconds.

Table 29. Performance Data for DMSO and NaCl Solution, High Frequency Tests

Amperage (mA)	Energy Density (J/cm^3)	Discharge Time (s)	Power Density (W/cm^3)	Dielectric Constant	Capacitance (F)
10	2.78	.51	5.5	1.41 E 07	3.36 E -03
20	0.0909	.09	9.9	5.95 E 06	1.42 E -03
30	0.282	.03	9.7	3.09 E 06	7.38 E -04
40	0.233	.01	18.0	1.92 E 06	4.59 E -04
50	0.159	.0068	23.4	1.25 E 06	2.99 E -04
80	0.100	.0021	50.4	4.53 E 05	1.08 E -04
100	0.103	.0012	85.5	3.03 E 05	7.24 E -05
150	0.130	.0008	162.4	1.65 E 05	3.94 E -05
200	0.172	.0006	286.6	7.79 E 04	1.86 E -05
250	0.195	.0006	326.2	8.03 E 04	1.92 E -05

c. FHS Tests (DMSO – NaCl)

Table 30 contains the performance data for the DMSO and NaCl solution for all FHS hold times. The capacitor reached a voltage of 3.0 volts with the specified electrolyte solution.

Table 30. Performance Data for DMSO and NaCl Solution, FHS Testing

Hold Time (s)	Energy Density (J/cm^3)	Discharge Time (s)	Power Density (W/cm^3)	Dielectric Constant	Capacitance (F)
1	12.77	28	.46	1.07 E 08	.026
10	14.77	31	.48	1.08 E 08	.026
30	16.50	38	.43	1.53 E 08	.037
60	17.02	41	.42	1.72 E 08	.041
100	21.05	42	.50	1.40 E 08	.034
200	17.56	47	.37	2.12 E 08	.050
300	16.67	51	.33	2.52 E 08	.060
1000	19.13	44	.43	1.78 E 08	.043

3. DMSO – Boric

a. Low Frequency Tests (DMSO – Boric)

Table 31 contains the performance data for the DMSO and Boric acid solution. The results are the average of 10–20 cycles and tests for all currents were completed satisfactorily. Further examination of the power trend line and the resulting equation predicts an energy density of 35 J/cm^3 at 100 seconds.

Table 31. Performance Data for DMSO and Boric Acid Solution, Low Frequency Tests

Amperage (mA)	Energy Density (J/cm^3)	Discharge Time (s)	Power Density (W/cm^3)	Dielectric Constant	Capacitance (F)
5	1.06	.46	2.31	7.83 E 06	1.87 E -03
8	0.411	.12	3.55	3.25 E 06	7.76 E -04
10	0.243	.057	4.23	2.04 E 06	4.88 E -04
12	0.157	.030	5.32	1.29 E 06	3.09 E -04
15	0.099	.014	6.89	7.93 E 05	1.90 E -04
18	0.075	.0084	8.87	5.49 E 05	1.31 E -04
20	0.066	.0066	10.01	4.37 E 05	1.04 E -04

b. High Frequency Tests (DMSO – Boric)

Table 32 contains the performance data for the DMSO and Boric acid solution for all the High Frequency Tests. The results are the average of 10–20 cycles and tests for all currents were completed satisfactorily but with significant inconsistencies due to the aliasing. The capacitor voltage ranged from 3.0–6.5 volts with the specified electrolyte solution. Further examination of the power trend line and the resulting equation predicts an energy density of 1 J/cm^3 at 100 seconds.

Table 32. Performance Data for DMSO and Boric Acid Solution, High Frequency Tests

Amperage (mA)	Energy Density (J/cm^3)	Discharge Time (s)	Power Density (W/cm^3)	Dielectric Constant	Capacitance (F)
10	0.438	.097	4.5	3.34 E 06	7.97 E -04
20	0.082	.009	9.3	6.68 E 05	1.60 E -04
30	0.272	.003	90.8	2.43 E 05	5.80 E -05
40	0.056	.0016	35.2	1.29 E 05	3.07 E -05
50	0.062	.0012	51.9	9.50 E 04	2.27 E -05
80	0.089	.0008	111.9	6.13 E 04	1.46 E -05
100	0.118	.0008	147.6	6.28 E 04	1.50 E -05
150	0.177	.0009	260.5	4.30 E 04	1.03 E -05
200	0.289	.0006	481.6	4.34 E 04	1.04 E -05
250	0.347	.0006	577.7	4.49 E 04	1.07 E -05

c. FHS Tests (DMSO – Boric)

Table 33 contains the performance data for the DMSO and Boric acid solution for all FHS hold times. All eight hold times were run as scheduled. The capacitor reached a voltage of 3.0 volts with the specified electrolyte solution.

Table 33. Performance Data for DMSO and Boric Acid Solution, FHS Testing

Hold Time (s)	Energy Density (J/cm^3)	Discharge Time (s)	Power Density (W/cm^3)	Dielectric Constant	Capacitance (F)
1	7.35	19	.39	8.14 E 07	.020
10	8.71	22	.40	9.38 E 07	.022
30	9.96	25	.40	1.09 E 08	.026
60	9.91	25	.40	1.09 E 08	.026
100	10.16	27	.38	1.19 E 08	.028
200	12.52	34	.37	1.54 E 08	.037
300	12.77	40	.32	1.83 E 08	.044
1000	21.47	63	.34	2.93 E 08	.070

4. DMSO – KNO_3

a. Low Frequency Tests (DMSO – KNO_3)

Table 34 contains the performance data for the DMSO and KNO_3 solution. The results are the average of 10–20 cycles and tests for all currents were completed satisfactorily. The capacitor reached a voltage of 3.0 volts with the specified electrolyte solution. Further examination of the power trend line and the resulting equation predicts an energy density of 23 J/cm^3 at 100 seconds.

Table 34. Performance Data for DMSO and KNO_3 Solution, Low Frequency Tests

Amperage (mA)	Energy Density (J/cm^3)	Discharge Time (s)	Power Density (W/cm^3)	Dielectric Constant	Capacitance (F)
5	10.82	3.61	3.0	4.41 E 07	1.05 E -02
8	6.52	1.31	5.0	2.67 E 07	6.37 E -03
10	4.85	0.79	6.1	2.02 E 07	4.83 E -03
12	3.93	0.54	7.3	1.67 E 07	3.98 E -03
15	2.95	0.33	9.0	1.28 E 07	3.07 E -03
18	2.26	0.22	10.4	1.03 E 07	2.47 E -03
20	1.99	0.17	11.6	9.02 E 06	2.16 E -03

b. High Frequency Tests (DMSO – KNO_3)

Table 35 contains the performance data for the DMSO and KNO_3 solution for all the High Frequency Tests. The results are the average of 10–20 cycles and tests for all currents were completed satisfactorily but with significant inconsistencies due to the aliasing. The capacitor voltage ranged from 3.0–3.8 volts with the specified electrolyte solution. Further examination of the power trend line and the resulting equation predicts an energy density of 39 J/cm^3 at 100 seconds.

Table 35. Performance Data for DMSO and KNO_3 Solution, High Frequency Tests

Amperage (mA)	Energy Density (J/cm^3)	Discharge Time (s)	Power Density (W/cm^3)	Dielectric Constant	Capacitance (F)
10	5.18	.097	4.5	3.34 E 06	7.97 E -04
20	1.99	.009	9.3	6.68 E 05	1.60 E -04
30	1.06	.003	90.8	2.43 E 05	5.80 E -05
40	0.654	.0016	35.2	1.29 E 05	3.07 E -05
50	0.438	.0012	51.9	9.50 E 04	2.27 E -05
80	0.196	.0008	111.9	6.13 E 04	1.46 E -05
100	0.148	.0008	147.6	6.28 E 04	1.50 E -05
150	0.132	.0009	260.5	4.30 E 04	1.03 E -05
200	0.154	.0006	481.6	4.34 E 04	1.04 E -05
250	0.195	.0006	577.7	4.49 E 04	1.07 E -05

c. FHS Tests (DMSO – KNO_3)

Table 36 contains the performance data for the DMSO and KNO_3 solution for all FHS hold times. All eight hold times were run as scheduled. The capacitor reached a voltage of 3.0 volts with the specified electrolyte solution.

Table 36. Performance Data for DMSO and KNO_3 Solution, FHS Testing

Hold Time (s)	Energy Density (J/cm^3)	Discharge Time (s)	Power Density (W/cm^3)	Dielectric Constant	Capacitance (F)
1	14.88	32	.465	1.15 E 08	.028
10	17.63	37	.477	1.35 E 08	.032
30	11.72	29	.406	1.25 E 08	.030
60	1.08	31	.390	1.35 E 08	.032
100	26.43	56	.472	2.10 E 08	.050
200	16.64	40	.416	1.68 E 08	.040
300	12.14	35	.347	1.58 E 08	.038
1000	21.24	51	.416	2.04 E 08	.049

5. DMSO – $NaNO_3$

a. Low Frequency Tests (DMSO – $NaNO_3$)

Table 37 contains the performance data for the DMSO and $NaNO_3$ solution. The results are the average of 10–20 cycles and tests for all currents were completed satisfactorily. The capacitor reached a voltage of 3.0 volts with the specified electrolyte solution. Further examination of the power trend line and the resulting equation predicts an energy density of 74 J/cm^3 at 100 seconds.

Table 37. Performance Data for DMSO and $NaNO_3$ Solution, Low Frequency Tests

Amperage (mA)	Energy Density (J/cm^3)	Discharge Time (s)	Power Density (W/cm^3)	Dielectric Constant	Capacitance (F)
5	10.0	2.98	3.4	3.51 E 07	8.38 E -03
8	6.5	1.25	5.2	2.41 E 07	5.76 E -03
10	5.1	.80	6.3	1.97 E 07	4.71 E -03
12	4.2	.56	7.5	1.69 E 07	4.03 E -03
15	3.2	.35	9.0	1.36 E 07	3.25 E -03
18	2.5	.24	10.5	1.14 E 07	2.72 E -03
20	2.2	.19	11.4	1.02 E 07	2.44 E -03

b. High Frequency Tests (DMSO – $NaNO_3$)

Table 38 contains the performance data for the DMSO and $NaNO_3$ solution for all the High Frequency Tests. The results are the average of 10–20 cycles and tests for all currents were completed satisfactorily but with significant inconsistencies due to the aliasing. The capacitor voltage ranged from 3.0–3.8 volts with the specified electrolyte solution. Further examination of the power trend line and the resulting equation predicts an energy density of 43 J/cm^3 at 100 seconds.

Table 38. Performance Data for DMSO and $NaNO_3$ Solution, High Frequency Tests

Amperage (mA)	Energy Density (J/cm^3)	Discharge Time (s)	Power Density (W/cm^3)	Dielectric Constant	Capacitance (F)
10	5.3	.83	6.40	2.01 E 07	4.80 E -03
20	2.2	.19	11.4	1.03 E 07	2.47 E -03
30	1.6	.075	15.4	6.73 E 06	1.61 E -03
40	.7	.037	18.8	4.86 E 06	1.16 E -03
50	.4	.020	21.9	3.58 E 06	8.55 E -03
80	.2	.005	33.5	1.60 E 06	3.82 E -04
100	.1	.0024	51.6	9.01 E 05	2.15 E -04
150	.1	.0008	148.8	2.52 E 05	6.01 E -05
200	.1	.0006	238.8	9.79 E 04	2.34 E -05
250	.2	.0008	292.6	1.04 E 05	2.48 E -05

c. FHS Tests (DMSO – $NaNO_3$)

Table 39 contains the performance data for the DMSO and $NaNO_3$ solution for all FHS hold times. All eight hold times were run as scheduled. The capacitor reached a voltage of 3.0 volts with the specified electrolyte solution.

Table 39. Performance Data for DMSO and $NaNO_3$ Solution, FHS Testing

Hold Time (s)	Energy Density (J/cm^3)	Discharge Time (s)	Power Density (W/cm^3)	Dielectric Constant	Capacitance (F)
1	15.55	10	1.56	9.76 E 07	.023
10	15.60	29	0.54	1.11 E 08	.026
30	29.33	51	0.58	1.52 E 08	.036
60	33.21	57	0.58	1.75 E 08	.042
100	24.79	60	0.58	1.85 E 08	.044
200	42.45	72	0.59	2.16 E 08	.052
300	53.21	57	0.93	2.52 E 08	.060
1000	50.50	100	0.58	3.10 E 08	.074

C. NMP

Figure 48 shows the complete testing schedule for the selected solvent.

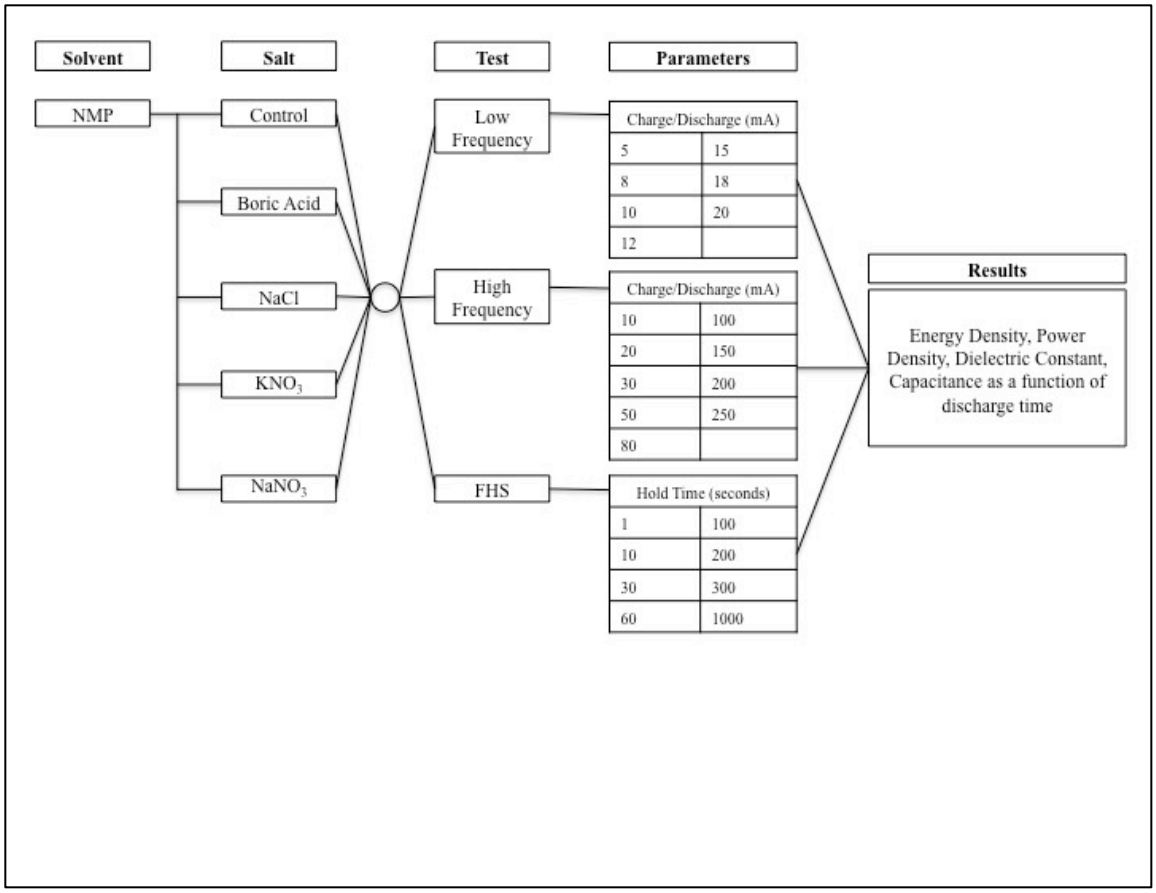

Figure 48. Complete Testing Schedule for NMP

1. NMP – Control

a. Low Frequency Tests (NMP – Control)

Table 40 contains the performance data for the NMP and control solution. The results are the average of 10–20 cycles and tests for all currents were completed satisfactorily. The capacitor voltage ranged from 2.0–2.5 volts with the specified electrolyte solution. Further examination of the power trend line and the resulting equation predicts an energy density of 29 J/cm^3 at 100 seconds.

Table 40. Performance Data for NMP and Control Solution, Low Frequency Tests

Amperage (mA)	Energy Density (J/cm^3)	Discharge Time (s)	Power Density (W/cm^3)	Dielectric Constant	Capacitance (F)
5	0.0156	0.0058	2.7	8.45 E 06	2.02 E -05
8	0.0172	0.0035	4.9	7.26 E 04	1.74 E -05
10	0.0153	0.0028	5.4	6.83 E 04	1.63 E -05
12	0.0200	0.0034	6.2	6.42 E 04	1.53 E -05
15	0.0234	0.0020	11.7	6.09 E 04	1.46 E -05
18	0.0256	0.0018	14.2	5.98 E 04	1.43 E -05
20	0.0268	0.0016	16.7	5.53 E 04	1.32 E -05

b. High Frequency Tests (NMP – Control)

Table 41 contains the performance data for the NMP and control solution for all the High Frequency Tests. The results are the average of 10–20 cycles and tests for all currents were completed satisfactorily but with significant inconsistencies due to the aliasing. The capacitor voltage ranged from 2.2–3.6 volts with the specified electrolyte solution. Further examination of the power trend line and the resulting equation predicts an energy density of 1 J/cm^3 at 100 seconds.

Table 41. Performance Data for NMP and Control Solution, High Frequency Tests

Amperage (mA)	Energy Density (J/cm^3)	Discharge Time (s)	Power Density (W/cm^3)	Dielectric Constant	Capacitance (F)
10	0.020	0.003	6.56	6.52 E 04	1.56 E -05
20	0.024	0.0016	15.1	5.45 E 04	1.30 E -05
30	0.025	0.001	25.1	5.20 E 04	1.24 E -05
40	0.031	0.0006	38.8	4.49 E 04	1.07 E -05
50	0.036	0.0006	60.0	4.66 E 04	1.11 E -05
80	0.056	0.0006	103.7	4.01 E 04	9.58 E -05
100	0.066	0.0006	109.3	4.27 E 04	1.02 E -05
150	0.089	0.0006	148.7	4.75 E 04	1.13 E -05
200	0.110	0.0006	183.9	5.37 E 04	1.28 E -05
250	0.136	0.0006	225.8	6.13 E 04	1.47 E -05

c. FHS Tests (NMP – Control)

Data was not collected for this testing method due to severe instability of the NMP at all voltages and hold times. When attempting low voltages currents, the sample would short and was rendered useless for additional testing.

2. NMP – NaCl

a. Low Frequency Tests (NMP – NaCl)

Table 42 contains the performance data for the NMP and NaCl solution. The results are the average of 10–20 cycles and tests for all currents were completed satisfactorily. The capacitor reached a voltage of 7.5 volts with the specified electrolyte solution. Further examination of the power trend line and the resulting equation predicts an energy density of 69 J/cm^3 at 100 seconds.

Table 42. Performance Data for NMP and NaCl Solution, Low Frequency Tests

Amperage (mA)	Energy Density (J/cm^3)	Discharge Time (s)	Power Density (W/cm^3)	Dielectric Constant	Capacitance (F)
5	0.171	0.0510	3.42	3.13 E 07	3.28 E-05
8	0.151	0.0120	13.1	1.76 E 07	2.61 E-05
10	0.153	0.0082	18.6	1.31 E 07	1.95 E-05
12	0.158	0.0068	23.2	1.07 E 07	1.70 E-05
15	0.163	0.0068	23.9	8.05 E 07	1.56 E-05
18	0.143	0.0044	32.4	6.25 E 07	1.50 E-05
20	0.147	0.0039	38.0	5.43 E 06	1.45 E-05

b. High Frequency Tests (NMP – NaCl)

Table 43 contains the performance data for the NMP and NaCl solution for all the High Frequency Tests. The results are the average of 10–20 cycles and tests for all currents were completed satisfactorily but with significant inconsistencies due to the aliasing. The capacitor voltage ranged from 2.8–8.0 volts with the specified electrolyte solution. Further examination of the power trend line and the resulting equation predicts an energy density of 23 J/cm^3 at 100 seconds.

Table 43. Performance Data for NMP and NaCl Solution, High Frequency Tests

Amperage (mA)	Energy Density (J/cm^3)	Discharge Time (s)	Power Density (W/cm^3)	Dielectric Constant	Capacitance (F)
10	0.024	0.0056	4.28	2.12 E 04	5.06 E -05
20	0.024	0.0019	12.7	8.74 E 04	2.09 E -05
30	0.282	0.0034	83.0	6.26 E 04	1.50 E -05
40	0.062	0.0068	9.2	6.28 E 04	1.50 E -05
50	0.075	0.0012	62.7	1.07 E 05	2.57 E -05
80	0.106	0.0008	132.7	5.05 E 04	1.21 E -05
100	0.138	0.0008	173.0	5.13 E 04	1.22 E -05
150	0.237	0.0008	296.6	4.07 E 04	9.72 E -06
200	0.345	0.0006	574.6	4.12 E 04	9.84 E -06
250	0.463	0.0006	771.5	4.15 E 04	9.92 E -06

c. FHS Tests (NMP – NaCl)

Table 44 contains the performance data for the NMP and NaCl solution for all FHS hold times. A significant note is that only four of the normal eight hold times were run because a final testing plan was not yet created. The capacitor reached a voltage of 9 volts with the specified electrolyte solution.

Table 44. Performance Data for NMP and NaCl Solution, FHS Testing

Hold Time (s)	Energy Density (J/cm^3)	Discharge Time (s)	Power Density (W/cm^3)	Dielectric Constant	Capacitance (F)
1	1.76	4.10	0.43	1.46 E 07	3.49 E -03
10	6.56	12.76	0.51	3.25 E 07	7.78 E -03
30	13.39	22.99	0.58	4.95 E 07	1.18 E -02
60	14.69	25.43	0.58	5.79 E 07	1.38 E -02
100	10.11	19.80	0.51	5.40 E 07	1.29 E -02
200	6.70	14.60	0.46	4.68 E 07	1.12 E -02
300	3.82	9.30	0.41	3.25 E 07	7.77 E -03
1000	1.97	5.0	0.39	3.53 E 07	8.43 E -03

3. NMP – Boric

a. Low Frequency Tests (NMP – Boric)

Table 45 contains the performance data for the NMP and Boric acid solution. The results are the average of 10–20 cycles and tests for all currents were completed satisfactorily. Further examination of the power trend line and the resulting equation predicts an energy density of 35 J/cm^3 at 100 seconds.

Table 45. Performance Data for NMP and Boric Acid Solution, Low Frequency Tests

Amperage (mA)	Energy Density (J/cm^3)	Discharge Time (s)	Power Density (W/cm^3)	Dielectric Constant	Capacitance (F)
5	0.171	0.051	3.4	7.20 E 04	1.72 E -05
8	0.151	0.012	13.1	1.09 E 05	2.61 E -05
10	0.153	0.008	18.6	8.16 E 04	1.95 E -05
12	0.158	0.007	23.2	7.11 E 04	1.70 E -05
15	0.163	0.007	23.9	6.54 E 04	1.56 E -05
18	0.143	0.004	32.4	6.27 E 04	1.51 E -05
20	0.147	0.004	38.0	6.06 E 04	1.45 E -05

b. High Frequency Tests (NMP – Boric)

Table 46 contains the performance data for the NMP and Boric acid solution for all the High Frequency Tests. The results are the average of 10–20 cycles and tests for all currents were completed satisfactorily but with significant inconsistencies due to the aliasing. The capacitor voltage ranged from 3.0–6.5 volts with the specified electrolyte solution. Further examination of the power trend line and the resulting equation predicts an energy density of 0.03 J/cm^3 at 100 seconds.

Table 46. Performance Data for NMP and Boric Acid Solution, High Frequency Tests

Amperage (mA)	Energy Density (J/cm^3)	Discharge Time (s)	Power Density (W/cm^3)	Dielectric Constant	Capacitance (F)
10	0.180	0.0040	19.1	5.27 E 04	1.26 E -05
20	0.272	0.0030	44.6	4.79 E 04	1.14 E -05
30	0.436	0.0044	90.8	6.39 E 05	1.53 E -05
40	0.575	0.0046	99.0	1.01 E 05	2.41 E -05
50	0.557	0.0037	125.1	1.26 E 05	3.01 E -05
80	0.557	0.0042	157	1.97 E 05	4.71 E -05
100	0.854	0.0010	205.4	2.22 E 04	5.31 E -05
150	0.496	0.0020	397.1	9.38 E 04	2.24 E -05
200	0.443	0.0006	739.0	4.68 E 04	1.12 E -05
250	0.374	0.0004	934.8	4.38 E 04	1.05 E -05

c. FHS Tests (NMP – Boric)

Table 47 contains the performance data for the NMP and Boric acid solution for all FHS hold times. All eight hold times were run as scheduled. The capacitor reached a voltage of 3.0 volts with the specified electrolyte solution.

Table 47. Performance Data for NMP and Boric Acid Solution, FHS Testing

Hold Time (s)	Energy Density (J/cm^3)	Discharge Time (s)	Power Density (W/cm^3)	Dielectric Constant	Capacitance (F)
1	0.918	2.66	0.35	1.20 E 07	2.88 E-03
10	1.894	4.71	0.40	1.83 E 07	4.38 E-03
30	2.316	6.04	0.38	2.47 E 07	5.90 E-03
60	3.027	7.98	0.38	3.70 E 07	8.05 E-03
100	2.900	7.60	0.38	3.31 E 07	7.91 E-03
200	2.290	5.60	0.41	2.46 E 07	5.89 E-03
300	2.597	6.30	0.41	2.45 E 07	5.85 E-03
1000	2.205	5.00	0.44	1.59 E 07	3.81 E-03

4. NMP – KNO_3

a. Low Frequency Tests (NMP - KNO_3)

Data was not collected for this testing method due to severe instability of the NMP and KNO_3 solution at all voltages. When attempting low voltages currents, the sample would short and was rendered useless for additional testing.

b. High Frequency Tests (NMP – KNO_3)

Table 48 contains the performance data for the NMP and KNO_3 solution for all the High Frequency Tests. The results are the average of 10–20 cycles and tests for all currents were completed satisfactorily but with significant inconsistencies due to the aliasing. The capacitor voltage ranged from 3.7–5.8 volts with the specified electrolyte solution. Further examination of the power trend line and the resulting equation predicts an energy density of 12 J/cm^3 at 100 seconds.

Table 48. Performance Data for NMP and KNO_3 Solution, High Frequency Tests

Amperage (mA)	Energy Density (J/cm^3)	Discharge Time (s)	Power Density (W/cm^3)	Dielectric Constant	Capacitance (F)
10	2.928	0.505	5.79	1.53 E 07	3.66 E -03
20	1.393	0.123	11.2	7.42 E 06	1.77 E -03
30	0.493	0.029	16.9	2.61 E 06	6.23 E -04
40	0.275	0.012	23.7	1.38 E 06	3.29 E -04
50	0.190	0.006	31.6	8.65 E 05	2.07 E -04
80	0.201	0.002	111.5	3.26 E 05	7.78 E -05
100	0.162	0.0012	135.2	1.91 E 05	4.55 E -05
150	0.193	0.0008	241.2	1.11 E 05	2.66 E -05
200	0.234	0.0006	389.4	6.17 E 04	1.48 E -05
250	0.315	0.0006	524.7	6.38 E 04	1.53 E -05

c. FHS Tests (NMP – KNO_3)

Table 49 contains the performance data for the NMP and KNO_3 solution for all FHS hold times. Four hold times were run as scheduled. This schedule differed from other FHS testing schedules because limited results were obtained with the original schedule. Exploratory testing with this specific combination produced favorable results for the following hold times: 10, 60, 180 and 600 seconds. The capacitor reached a voltage of 3.2 volts with the specified electrolyte solution.

Table 49. Performance Data for NMP and KNO_3 Solution, FHS Testing

Hold Time (s)	Energy Density (J/cm^3)	Discharge Time (s)	Power Density (W/cm^3)	Dielectric Constant	Capacitance (F)
10	7.602	0.01	760.2	7.44 E 07	0.0178
60	9.588	21.0	0.46	8.78 E 07	0.0201
180	25.95	46.0	0.56	1.32 E 08	0.0315
600	13.44	22	0.61	1.07 E 08	0.0255

5. NMP – $NaNO_3$

a. Low Frequency Tests (NMP – $NaNO_3$)

Table 50 contains the performance data for the NMP and $NaNO_3$ solution. The results are the average of 10–20 cycles and tests for all currents were completed satisfactorily. The capacitor reached a voltage of 3 volts with the specified electrolyte solution. Further examination of the power trend line and the resulting equation predicts an energy density of 74 J/cm^3 at 100 seconds.

Table 50. Performance Data for NMP and $NaNO_3$ Solution, Low Frequency Tests

Amperage (mA)	Energy Density (J/cm^3)	Discharge Time (s)	Power Density (W/cm^3)	Dielectric Constant	Capacitance (F)
5	7.98	2.98	3.4	3.51 E 07	8.38 E -03
8	3.18	1.25	5.2	2.41 E 07	5.76 E -03
10	1.79	.80	6.3	1.97 E 07	4.71 E -03
12	1.02	.56	7.5	1.69 E 07	4.03 E -03
15	0.50	.35	9.0	1.36 E 07	3.25 E -03
18	0.27	.24	10.5	1.14 E 07	2.72 E -03
20	0.19	.19	11.4	1.02 E 07	2.44 E -03

b. High Frequency Tests (NMP – $NaNO_3$)

Table 51 contains the performance data for the NMP and $NaNO_3$ solution for all the High Frequency Tests. The results are the average of 10–20 cycles and tests for all currents were completed satisfactorily but with significant inconsistencies due to the aliasing. The capacitor voltage ranged from 3.0–3.8 volts with the specified electrolyte solution. Further examination of the power trend line and the resulting equation predicts an energy density of 43 J/cm^3 at 100 seconds.

Table 51. Performance Data for NMP and $NaNO_3$ Solution, High Frequency Tests

Amperage (mA)	Energy Density (J/cm^3)	Discharge Time (s)	Power Density (W/cm^3)	Dielectric Constant	Capacitance (F)
10	2.59	.83	6.4	2.01 E 07	4.80 E -03
20	0.38	.19	11.4	1.03 E 07	2.47 E -03
30	0.12	.075	15.4	6.73 E 06	1.61 E -03
40	0.08	.037	18.8	4.86 E 06	1.16 E -03
50	0.08	.020	21.9	3.58 E 06	8.55 E -03
80	0.10	.005	33.5	1.60 E 06	3.82 E -04
100	0.13	.0024	51.6	9.01 E 05	2.15 E -04
150	0.18	.0008	148.8	2.52 E 05	6.01 E -05
200	0.26	.0006	238.8	9.79 E 04	2.34 E -05
250	0.34	.0008	292.6	1.04 E 05	2.48 E -05

c. FHS Tests (NMP – $NaNO_3$)

Table 52 contains the performance data for the NMP and $NaNO_3$ solution for all FHS hold times. All eight hold times were run as scheduled. The capacitor reached a voltage of 3 volts with the specified electrolyte solution.

Table 52. Performance Data for NMP and $NaNO_3$ Solution, FHS Testing

Hold Time (s)	Energy Density (J/cm^3)	Discharge Time (s)	Power Density (W/cm^3)	Dielectric Constant	Capacitance (F)
1	15.55	10	1.56	9.76 E 07	.023
10	15.60	29	0.54	1.11 E 08	.026
30	29.33	51	0.58	1.52 E 08	.036
60	33.21	57	0.58	1.75 E 08	.042
100	24.79	60	0.58	1.85 E 08	.044
200	42.45	72	0.59	2.16 E 08	.052
300	53.21	57	0.93	2.52 E 08	.060
1000	50.50	100	0.58	3.10 E 08	.074

D. PROPYLENE CARBONATE

Figure 49 shows the complete testing schedule for PC.

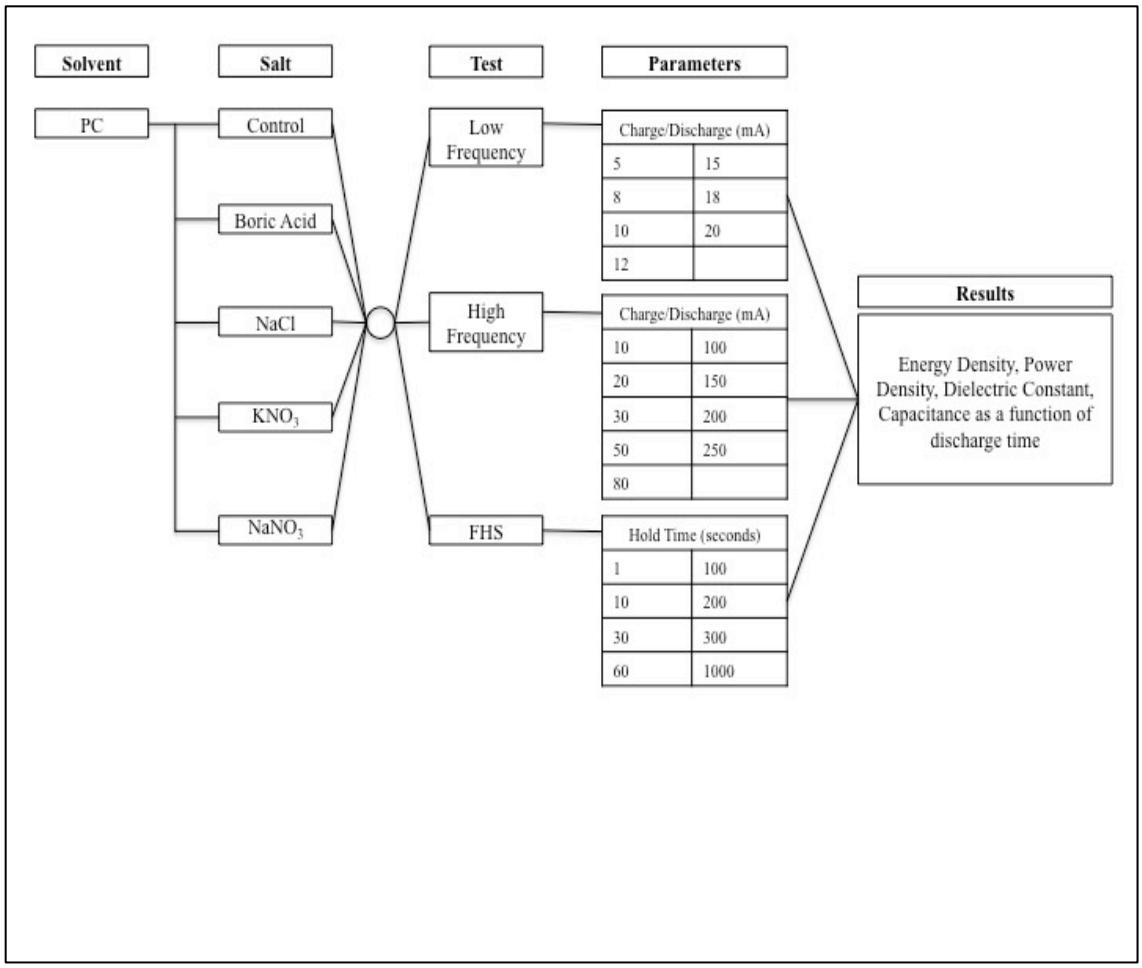

Figure 49. Complete Testing Schedule for PC

1. PC – Control

a. Low Frequency Tests (PC – Control)

Table 53 contains the performance data for the PC and control solution. The results are the average of 10–20 cycles and tests for all currents were completed satisfactorily. The capacitor voltage ranged from 7.0–8.0 volts with the specified electrolyte solution. Further examination of the power trend line and the resulting equation predicts an energy density of 0.04 J/cm^3 at 100 seconds.

Table 53. Performance Data for PC and Control Solution, Low Frequency Tests

Amperage (mA)	Energy Density (J/cm^3)	Discharge Time (s)	Power Density (W/cm^3)	Dielectric Constant	Capacitance (F)
5	0.140	0.0139	10.1	5.29 E 04	1.26 E -05
8	0.158	0.0094	16.9	4.63 E 04	1.11 E -05
10	0.173	0.0081	21.7	4.52 E 04	1.08 E -05
12	0.185	0.0066	27.8	4.47 E 04	1.07 E -05
15	0.199	0.0055	36.3	4.44 E 04	1.06 E -05
18	0.213	0.0045	47.5	4.33 E 04	1.04 E -05
20	0.124	0.0044	28.3	4.33 E 04	1.04 E -05

b. High Frequency Tests (PC – Control)

Table 54 contains the performance data for the PC and control solution for all the High Frequency Tests. The results are the average of 10–20 cycles and tests were only completed for 10 and 20 mA. The PC and control solution would short at higher charge currents. The capacitor voltage ranged from 7.2–7.5 volts with the specified electrolyte solution. Further examination of the power trend line and the resulting equation predicts an energy density of 0.5 J/cm^3 at 100 seconds.

Table 54. Performance Data for PC and Control Solution, High Frequency Tests

Amperage (mA)	Energy Density (J/cm^3)	Discharge Time (s)	Power Density (W/cm^3)	Dielectric Constant	Capacitance (F)
10	0.163	0.0075	21.6	4.79 E 04	1.14 E -06
20	0.216	0.0043	49.3	4.42 E 04	1.06 E -05

c. FHS Tests (PC – Control)

Data was not collected for this testing method due to severe instability of the PC and control solution at all voltages and hold times. When attempting low voltages currents, the sample would short and was rendered useless for additional testing.

2. PC – NaCl

a. Low Frequency Tests (PC – NaCl)

Table 55 contains the performance data for the PC and NaCl solution. The results are the average of 10–20 cycles and tests for all currents were completed satisfactorily. The capacitor voltage ranged from 7.5–8.2 volts with the specified electrolyte solution. Further examination of the power trend line and the resulting equation predicts an energy density of .0033 J/cm^3 at 100 seconds.

Table 55. Performance Data for PC and NaCl Solution, Low Frequency Tests

Amperage (mA)	Energy Density (J/cm^3)	Discharge Time (s)	Power Density (W/cm^3)	Dielectric Constant	Capacitance (F)
5	0.145	0.015	9.9	5.93 E 04	1.42 E-05
8	0.171	0.010	17.7	4.95 E 04	1.18 E-05
10	0.185	0.008	23.0	4.71 E 04	1.13 E-05
12	0.194	0.007	28.9	4.67 E 04	1.12 E-05
15	0.214	0.006	37.7	4.61 E 04	1.10 E-05
18	0.226	0.005	42.8	4.52 E 04	1.08 E-05
20	0.239	0.005	52.9	4.49 E 04	1.08 E-05

b. High Frequency Tests (PC – NaCl)

Table 56 contains the performance data for the PC and NaCl solution for all the High Frequency Tests. The results are the average of 10–20 cycles and tests for all currents were completed satisfactorily but with significant inconsistencies due to the aliasing. The capacitor voltage ranged from 2.8–8.0 volts with the specified electrolyte solution. Further examination of the power trend line and the resulting equation predicts an energy density of 0.5 J/cm^3 at 100 seconds.

Table 56. Performance Data for PC and NaCl Solution, High Frequency Tests

Amperage (mA)	Energy Density (J/cm^3)	Discharge Time (s)	Power Density (W/cm^3)	Dielectric Constant	Capacitance (F)
10	0.024	0.0056	4.3	2.12 E 04	5.06 E -05
20	0.024	0.0019	12.6	8.74 E 04	2.09 E -05
30	0.282	0.0034	83.0	6.26 E 04	1.50 E -05
40	0.062	0.0068	9.2	6.28 E 04	1.50 E -05
50	0.075	0.0012	62.7	1.07 E 05	2.57 E -05
80	0.106	0.0008	132.7	5.05 E 04	1.21 E -05
100	0.138	0.0008	173.0	5.13 E 04	1.22 E -05
150	0.237	0.0008	296.6	4.07 E 04	9.72 E -06
200	0.345	0.0006	574.6	4.12 E 04	9.84 E -06
250	0.463	0.0006	771.5	4.15 E 04	9.92 E -06

c. FHS Tests (PC – NaCl)

Data was not collected for this testing method due to severe instability of the PC and NaCl solution at all voltages and hold times. When attempting low voltages currents, the sample would short and was rendered useless for additional testing.

3. PC – Boric

a. Low Frequency Tests (PC – Boric)

Table 57 contains the performance data for the PC and Boric acid solution. The results are the average of 10–20 cycles and tests for all currents were completed satisfactorily. The capacitor voltage ranged from 7.5–8.1 volts with the specified electrolyte solution. Further examination of the power trend line and the resulting equation predicts an energy density of 0.15 J/cm^3 at 100 seconds.

Table 57. Performance Data for PC and Boric Acid Solution, Low Frequency Tests

Amperage (mA)	Energy Density (J/cm^3)	Discharge Time (s)	Power Density (W/cm^3)	Dielectric Constant	Capacitance (F)
5	0.163	0.0202	8.1	1.31 E 05	3.14 E -05
8	0.174	0.0013	142.2	7.32 E 04	1.75 E -05
10	0.185	0.0884	20.9	6.35 E 04	1.52 E -05
12	0.195	0.0074	26.3	5.87 E 04	1.40 E -05
15	0.207	0.0060	34.5	5.53 E 04	1.32 E -05
18	0.220	0.0052	42.6	5.36 E 04	1.28 E -05
20	0.228	0.0047	48.7	5.25 E 04	1.26 E -05

b. High Frequency Tests (PC – Boric)

Table 58 contains the performance data for the NMP and Boric acid solution for all the High Frequency Tests. The results are the average of 10–20 cycles and tests were only completed for all but the last three test currents (150, 200 and 250 mA). The PC and Boric acid solution shorted at higher charge currents. The capacitor voltage ranged from 10.1–11.2 volts with the specified electrolyte solution. Further examination of the power trend line and the resulting equation predicts an energy density of 0.6 J/cm^3 at 100 seconds.

Table 58. Performance Data for PC and Boric Acid Solution, High Frequency Tests

Amperage (mA)	Energy Density (J/cm^3)	Discharge Time (s)	Power Density (W/cm^3)	Dielectric Constant	Capacitance (F)
10	0.27	0.0101	27.0	5.84 E04	1.31 E-05
20	0.35	0.0054	64.5	4.93 E04	1.18 E-05
30	0.48	0.0050	96.1	5.52 E04	1.32 E-05
40	0.62	0.0050	123.0	7.73 E04	1.85 E-05
50	0.72	0.0050	144.8	1.05 E05	2.50 E-05
80	0.78	0.0040	195.4	1.67 E05	4.00 E-05
100	0.92	0.0041	226.6	2.09 E05	5.00 E-05
150	0.89	0.0020	279.4	3.14 E05	7.50 E-05
200	0.45	0.0060	749.4	4.66 E04	1.11 E-05
250	0.40	0.0060	668.8	4.65 E04	1.11 E-05

c. FHS Tests (PC – Boric)

Data was not collected for this testing method due to severe instability of the PC and Boric acid solution at all voltages and hold times. When attempting low voltages currents, the sample would short and was rendered useless for additional testing.

4. PC – KNO_3

a. Low Frequency Tests (PC – KNO_3)

Table 59 contains the performance data for the PC and Boric acid solution. The results are the average of 10–20 cycles and tests for all currents were completed satisfactorily. The capacitor voltage ranged from 7.5–8.2 volts with the specified electrolyte solution. Further examination of the power trend line and the resulting equation predicts an energy density of 0.0062 J/cm^3 at 100 seconds.

Table 59. Performance Data for PC and Boric Acid Solution, Low Frequency Tests

Amperage (mA)	Energy Density (J/cm^3)	Discharge Time (s)	Power Density (W/cm^3)	Dielectric Constant (n/a)	Capacitance (F)
5	0.15	0.0158	9.4	6.38 E 04	1.52 E -05
8	0.17	0.0102	16.5	5.63 E 04	1.35 E -05
10	0.18	0.0082	21.9	5.29 E 04	1.26 E -05
12	0.19	0.0071	27.1	5.15 E 04	1.23 E -05
15	0.21	0.0058	35.8	5.03 E 04	1.20 E -05
18	0.22	0.0051	44.1	4.93 E 04	1.18 E -05
20	0.23	0.0045	51.8	4.81 E 04	1.15 E -05

b. High Frequency Tests (PC - KNO_3)

Table 60 contains the performance data for the PC and KNO_3 solution for all the High Frequency Tests. The results are the average of 10–20 cycles and tests for all currents were completed satisfactorily but with significant inconsistencies due to the aliasing. The capacitor voltage ranged from 3.7–5.8 volts with the specified electrolyte solution. Further examination of the power trend line and the resulting equation predicts an energy density of 8 E-06 J/cm^3 at 100 seconds.

Table 60. Performance Data for PC and KNO_3 Solution, High Frequency Tests

Amperage (mA)	Energy Density (J/cm^3)	Discharge Time (s)	Power Density (W/cm^3)	Dielectric Constant (n/a)	Capacitance (F)
10	0.28	0.0104	27.2	6.13 E 04	1.46 E -05
20	0.32	0.0054	58.7	5.08 E 04	1.21 E -05
30	0.52	0.0053	98.0	6.28 E 04	1.50 E -05
40	0.62	0.0050	123.8	8.37 E 04	2.00 E -05
50	0.73	0.0055	134.3	1.05 E 05	2.50 E -05
80	0.78	0.0040	195.9	1.67 E 05	4.00 E -05
100	0.92	0.0040	230.4	2.09 E 05	5.00 E -05

c. FHS Tests (PC – KNO_3)

Data was not collected for this testing method due to severe instability of the PC and KNO_3 solution at all voltages and hold times. When attempting low voltages currents, the sample would short and was rendered useless for additional testing.

5. PC – $NaNO_3$

a. Low Frequency Tests (PC – $NaNO_3$)

Table 61 contains the performance data for the PC and $NaNO_3$ solution. The results are the average of 10–20 cycles and tests for all currents were completed satisfactorily. The capacitor voltage ranged from 1.0–8.1 volts with the specified electrolyte solution. Further examination of the power trend line and the resulting equation predicts an energy density of 0.4 J/cm^3 at 100 seconds.

Table 61. Performance Data for PC and $NaNO_3$ Solution, Low Frequency Tests

Amperage (mA)	Energy Density (J/cm^3)	Discharge Time (s)	Power Density (W/cm^3)	Dielectric Constant (n/a)	Capacitance (F)
5	0.26	0.1577	1.7	3.80 E 06	9.08 E -04
8	0.17	0.0102	16.1	6.71 E 04	1.60 E -05
10	0.18	0.0083	21.9	5.53 E 04	1.32 E -05
12	0.19	0.0070	27.3	5.15 E 04	1.23 E -05
15	0.21	0.0058	35.9	4.96 E 04	1.18 E -05
18	0.22	0.0050	44.9	4.80 E 04	1.15 E -05
20	0.23	0.0046	50.7	4.71 E 04	1.13 E -05

b. High Frequency Tests (PC – $NaNO_3$)

Table 62 contains the performance data for the PC and $NaNO_3$ solution for all the High Frequency Tests. The results are the average of 10–20 cycles and tests for all currents were completed satisfactorily but with significant inconsistencies due to the aliasing. The capacitor voltage ranged from 10.1–11.2 volts with the specified electrolyte solution. Further examination of the power trend line and the resulting equation predicts an energy density of 0.5 J/cm^3 at 100 seconds.

Table 62. Performance Data for PC and $NaNO_3$ Solution, High Frequency Tests

Amperage (mA)	Energy Density (J/cm^3)	Discharge Time (s)	Power Density (W/cm^3)	Dielectric Constant (n/a)	Capacitance (F)
10	0.27	0.0102	26.8	6.22 E 04	1.49 E -05
20	0.31	0.0450	6.9	4.90 E 04	1.17 E -05
30	0.50	0.0052	95.7	6.19 E 04	1.48 E -05
40	0.58	0.0050	115.9	8.37 E 04	2.00 E -05
50	0.73	0.0050	145.0	1.05 E 05	2.50 E -05
80	0.78	0.0040	195.7	1.67 E 05	4.00 E -05
100	0.91	0.0040	227.4	2.09 E 05	5.00 E -05
150	0.55	0.0020	275.9	3.14 E 05	7.50 E -05
200	0.26	0.0006	440.4	4.67 E 04	1.12 E -05
250	0.40	0.0006	673.2	4.65 E 04	1.11 E -05

c. FHS Tests (PC – $NaNO_3$)

Data was not collected for this testing method due to severe instability of the PC and $NaNO_3$ solution at all voltages and hold times. When attempting low voltages currents, the sample would short and was rendered useless for additional testing.

IV. DISCUSSION

In this chapter, the results are discussed with a focus on performance parameters relevant for potential use in such Navy applications as the Railgun, EMALS and FEL. To support the energy requirements of these weapons systems, the Navy requires high-energy delivery, in a relatively short amount of time [38], [39]. This energy requirement corresponds to the high-power density of the capacitor. To support this discussion, the pertinent information has been outlined in the empirical findings section and tests have been distilled to graphs that display Power Density (W/cm^3) v. Discharge Time (seconds) for each of the four salt solutions dissolved in the Propylene Carbonate (PC), (NMP) and (DMSO).

A. EMPIRICAL FINDINGS

Several significant points were discovered as a result of the NTSDM testing conducted in the thesis:

1. Higher voltages were attained for all pure OPS salt solutions when compared to aqueous salt solutions. The average range of the OPS solutions was 2.4–5.0 volts with the highest voltage occurring at 7.0 volts. The highest voltage attained with aqueous salt solutions was 2.3 volts [2]. This is consistent with both the general energy storage device theory and the hypothesis. Exploratory testing concentrated on finding OPS that possessed higher breakdown voltages than aqueous solvents. The breakdown voltages for the OPS were established during low frequency testing in order to directly compare the values to aqueous solvents.

2. There was no correlation between maximum voltage and energy density. The highest energy densities were associated with relatively low operating voltages. For example, the mixture of PC and DI/NaCl (75/25) mixed solution produced the highest energy density of 158 J/cm^3 at only 3.0 volts. The highest operating voltage for this mixture was 3.8 volts but operating voltages as high as 7.0 volts were attained throughout the thesis. The energy densities attained from the 7.0 volts ranged from 1–5 J/cm^3.

These results are not consistent with the hypothesis or the general energy storage device theory that states energy density will increase with an increase in voltage squared, Equation 6.

$$Energy\ Density_{General} = \frac{1}{2}CV^2 \quad (6)$$

The issue was that the capacitance also decreased at an average of 2–3 orders of magnitude that effectively nullified any impacts the increased voltage had on the energy density.

3. None of the pure OPS salt solutions had energy densities as high as those obtained with aqueous salt solutions used in previous studies. The highest energy density obtained was 74 J/cm^3 from both the DMSO/$NaNO_3$ and NMP/$NaNO_3$ salt solutions. The lowest energy density obtained was 0.16 J/cm^3 from the NMP / $NaNO_3$ salt solution. The highest energy density obtained from the aqueous solutions was 160 J/cm^3 [2].

   These results are not consistent with the hypothesis or the general energy storage device theory for the same reason explained in Point 3 above.

4. None of the pure OPS salt solutions had power densities as high as those obtained with aqueous salt solutions used in previous studies. This was based on a discharge time of ~0.01 seconds since this is relevant to Navy applications. The highest power density obtained was 29 W/cm^3 from the PC + DI/NaCl (85/15) mixed solution. The lowest power density obtained was 1.7 W/cm^3 from the PC/$NaNO_3$ salt solution. The highest power density obtained from the aqueous solutions was 90 W/cm^3 [2].

   This observation was not correlated to the general energy storage device theory since research on OPS is relatively new and unsupported. Additionally, these observations are not consistent with the hypothesis since it was postulated that increased power density would result from increased energy density. Since the energy density was significantly lower than expected, the power density values were lower than realized in previous studies.

5. The energy and power densities varied far less for OPS salt solutions than for aqueous salt solutions. This observation was not consistent with general energy storage device theory since most commercial capacitor results (seen in Ragone Chart, Figure 50) span as many as three decades [40]. This same argument is used to describe why this observation does not support the hypothesis. Previous energy group results span over three decades but also attained power densities that far exceed commercial energy storage devices. Although the capacitors in this thesis attained higher energy densities than both the previous work and commercial capacitors, they failed to achieve comparable power densities.

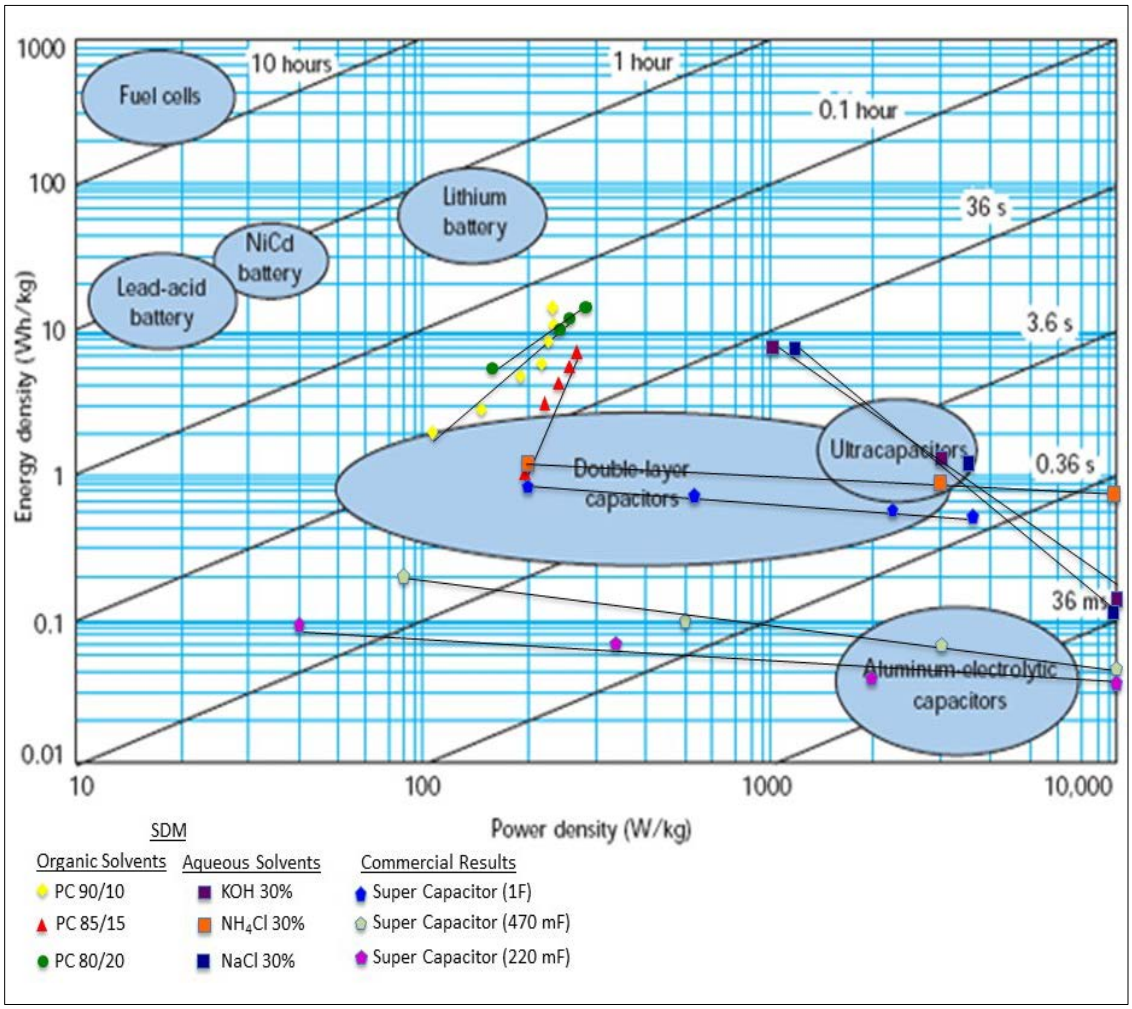

Figure 50. Comparison of Best Thesis Capacitors and Commercially Produced Energy Storage Devices. Adapted from [2], [21].

6. When compared to all solutions, the mixture of PC and DI/NaCl (95/05) mixed salt solutions had the highest operating voltages ranging from 7.0–8.3 volts. This observation was not correlated to the general energy storage device theory since research on OPS is relatively new and unsupported. This is consistent with the hypothesis in that a relationship was discovered between the PC and the concentration of DI/NaCl added to the mixture. The highest DI/NaCl salt concentration, 25%, produced the lowest voltage while the lowest DI/NaCl salt concentration, 5%, produced the highest. It was observed that salt solutions lowered the operating voltage but increased energy density.

7. The FHS tests produced the longest discharge time of 240 seconds. This was for the PC and DI/NaCl (75/25) mixed salt solution at a 1000 second hold. This observation is consistent with the hypothesis for two reasons. The first reason is that the 1000-second hold allows for ample time for the alignment and formation of large salt ions dipoles into an optimum array that will maximize energy storage. The second reason is that the 25% salt solution is the highest amount of salt dissolved into any OPS. The dissolved salts support the formation of large salt dipoles and when coupled with long hold time will yield high energy densities and long discharge times.

8. For many of the solutions, energy density increased as the discharge time decreased. This observation is not consistent with general energy storage device theory as previous group results all indicate that general energy storage device theory should increase as discharge time increases. Additionally, several commercial capacitors were tested using similar equipment and techniques used in this thesis and the results were similar to previous group work. This is an interesting phenomenon that warrants additional research.

9. There was no correlation between the highest energy and power densities attained from the same solution. The highest energy density attained was in the mixture of PC and DI/NaCl (75/25) at 158 J/cm^3 with a corresponding power density of 52 W/cm^3. Similarly, the highest power density obtained was 397.1 W/cm^3 from the NMP / Boric acid solution with a corresponding energy density of 0.5 J/cm^3. This was an

observation that did not tie directly to the general energy storage device theory pertaining to energy storage devices nor the hypothesis set forth in this thesis.

B. LOW FREQUENCY TESTS

For this discussion, the best and worst parameters were based on the highest and lowest power densities observed for all Low Frequency Test currents. Figure 51 shows the power densities resulting from the tested solvents and solutions conducted at Low Frequency Test currents. Although there was some overlap of regions, each solvent and their respective salt solutions produced distinguishable regions and groups.

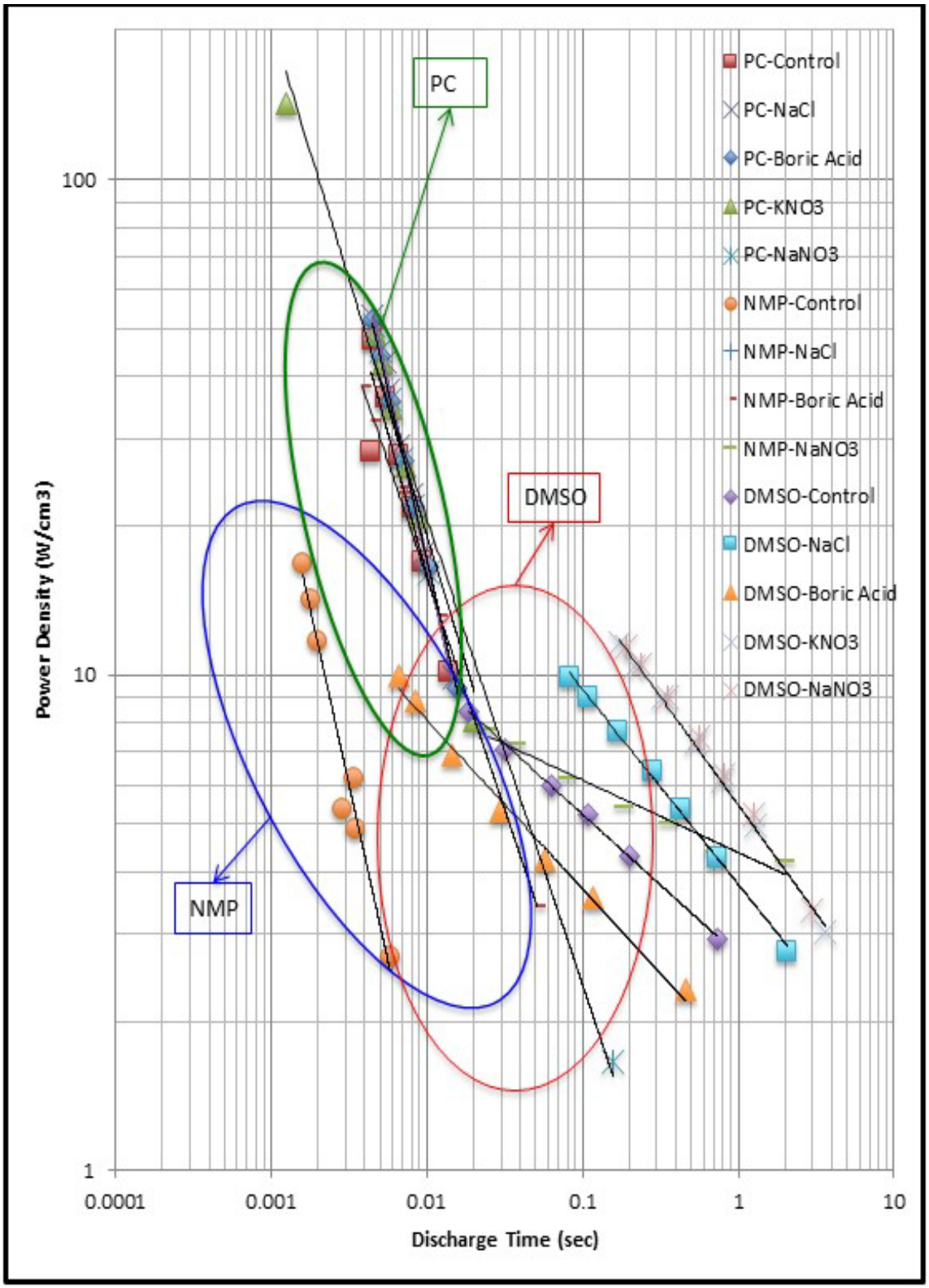

Figure 51. Power Density (W/cm^3) from Low Frequency Tests

Figure 52 provides a focused, expanded look at the data from PC mixed with the various salts (green-circled area from Figure 51). This was done to analyze whether or not the data points were reliable based on the discharge times. Since the discharge times in this group were greater than 0.002 seconds, the power densities were considered reliable. The reliability of the data is reinforced by the linear results. For the most part, the PC mixed with the various salts produce a salt identity nearly independent of discharge times and power densities. The range of power densities in this group ranged from 10–53 W/cm^3.

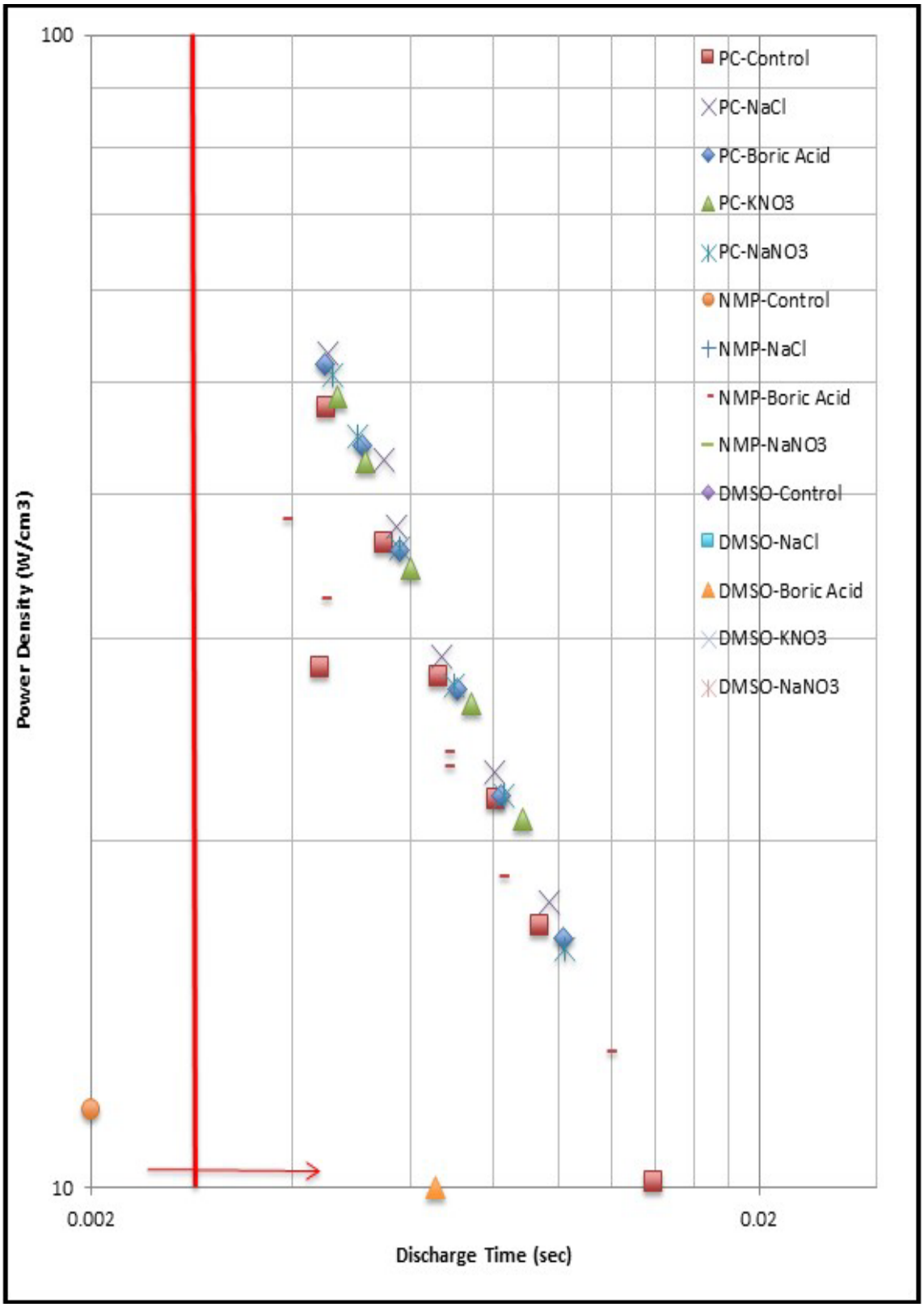

Figure 52. Focused Look at Circled Green Area from Figure 45

Tables 63–67 show the power densities of the tested solvent and salt solutions. Based on the data, the PC combined with any salt produced higher power densities than any of the other pure solvent/salt combinations. Another observation was that NMP and DMSO yielded similar power densities at the lower currents (5 mA, 8 mA and 10 mA) for three of the salt solutions-Control, NaCl and Boric Acid. For the same salt solutions, NMP's power density was two to three times higher than the other two solvents. When mixed with the $NaNO_3$ solution, NMP and DMSO produced nearly identical results. The final observation was that the NMP and KNO_3 salt solution did not work together. This salt solution combination was tested on multiple anodized foils and produced no results. It was noted that visually, no salt had dissolved when KNO_3 was added to the NMP.

Table 63. Power Density of Tested Solvent and Control Solutions

	PC	NMP	DMSO
Control	Power Density (W/cm^3)		
	10.1	2.7	2.9
	16.9	4.9	4.3
	21.7	5.4	5.2
	27.8	6.2	6.0
	36.3	11.7	7.1
	47.5	14.2	8.5
	28.3	16.7	9.1

Table 64. Power Density of Tested Solvent and NaCl Solutions

	PC	NMP	DMSO
NaCl	Power Density (W/cm^3)		
	9.9	3.4	2.8
	17.7	13.1	4.3
	23.0	18.6	5.4
	28.9	23.2	6.4
	37.5	23.9	7.7
	42.8	32.4	9.0
	52.9	38.0	9.9

Table 65. Power Density of Tested Solvent and Boric Acid Solutions

	PC	NMP	DMSO
Boric	Power Density (W/cm^3)		
	9.4	3.4	2.3
	16.5	13.1	3.6
	21.9	18.6	4.2
	27.1	23.2	5.3
	35.8	23.9	6.9
	44.1	32.4	8.9
	51.8	38.0	10.0

Table 66. Power Density of Tested Solvent and KNO_3 Solutions

	PC	NMP	DMSO
KNO_3	Power Density (W/cm^3)		
	8.1	0.0	3.0
	142	0.0	5.0
	20.9	0.0	6.1
	26.3	0.0	7.3
	34.5	0.0	9.0
	42.6	0.0	10.4
	48.7	0.0	11.6

Table 67. Power Density of Tested Solvent and $NaNO_3$ Solutions

	PC	NMP	DMSO
$NaNO_3$	Power Density (W/cm^3)		
	1.7	4.2	3.4
	16.1	4.4	5.2
	21.9	5.0	6.3
	27.3	5.4	7.5
	35.9	6.2	9.0
	44.9	7.3	10.5
	50.7	7.8	11.4

Based on these results, the low frequency test results are categorized into two groups based on whether or not the OPS salt solution was accepted or rejected for further study, development and possible implementation. The acceptance criterion was based on

the highest energy density obtained for each OPS salt solution combined with the power density at the 0.01-second discharge point.[3] It was determined that energy densities less than 5 J/cm^3 and power densities less than 10 W/cm^3 were not considered for subsequent experimentation. These metrics are based on competing with the energy and power density values obtained from previous group studies as well as a comparison to comparable commercial energy storage devices. The pure solvent salt solutions results are shown in Table 68 and the mixed solution containing PC + DI/NaCl are shown in Table 69.

Table 68. Low Frequency Testing Acceptance Criteria Pure Solvent Solutions

Solvent	Salt	Energy Density (J/cm^3)	Power Density (W/cm^3)	Accept / Reject
PC	Control	0.1	10.1	Reject
	Boric Acid	0.2	9.4	Reject
	NaCl	0.2	9.9	Reject
	KNO_3	0.2	8.1	Reject
	$NaNO_3$	0.3	1.7	Reject
NMP	Control	.01	2.7	Reject
	Boric Acid	.02	13.1	Reject
	NaCl	5.3	13.1	Accept
	KNO_3	No Good Data		Reject
	$NaNO_3$	8.0	6.2	Reject
DMSO	Control	6.0	9.1	Reject
	Boric Acid	4.8	6.8	Reject
	NaCl	19.5	10.0	Accept
	KNO_3	27.5	11.6	Accept
	$NaNO_3$	21.8	11.4	Accept

[3] The Navy is interested in short pulse weapons systems that require significant power discharged in the range of 0.01 seconds.

Table 69. Low Frequency Testing Acceptance Criteria Mixed Solvent Solution

Solvent	Concentration (PC / DI+NaCl)	Energy Density (J/cm^3)	Power Density (W/cm^3)	Accept / Reject
PC + DI/NaCl	95 / 05	1.2	9.0	Reject
	90 / 10	0.2	8.4	Reject
	85 / 15	17.2	13.3	Accept
	80 / 20	38.4	No Good Data	Reject
	75 / 25	16.3	8.5	Reject

C. HIGH FREQUENCY TESTS

Figure 53 shows the highest and highest power densities resulting from the tested solvents and solutions conducted at High Frequency Test currents. Although there was some overlap of regions, each solvent and their respective salt solutions produced distinguishable regions and groups.

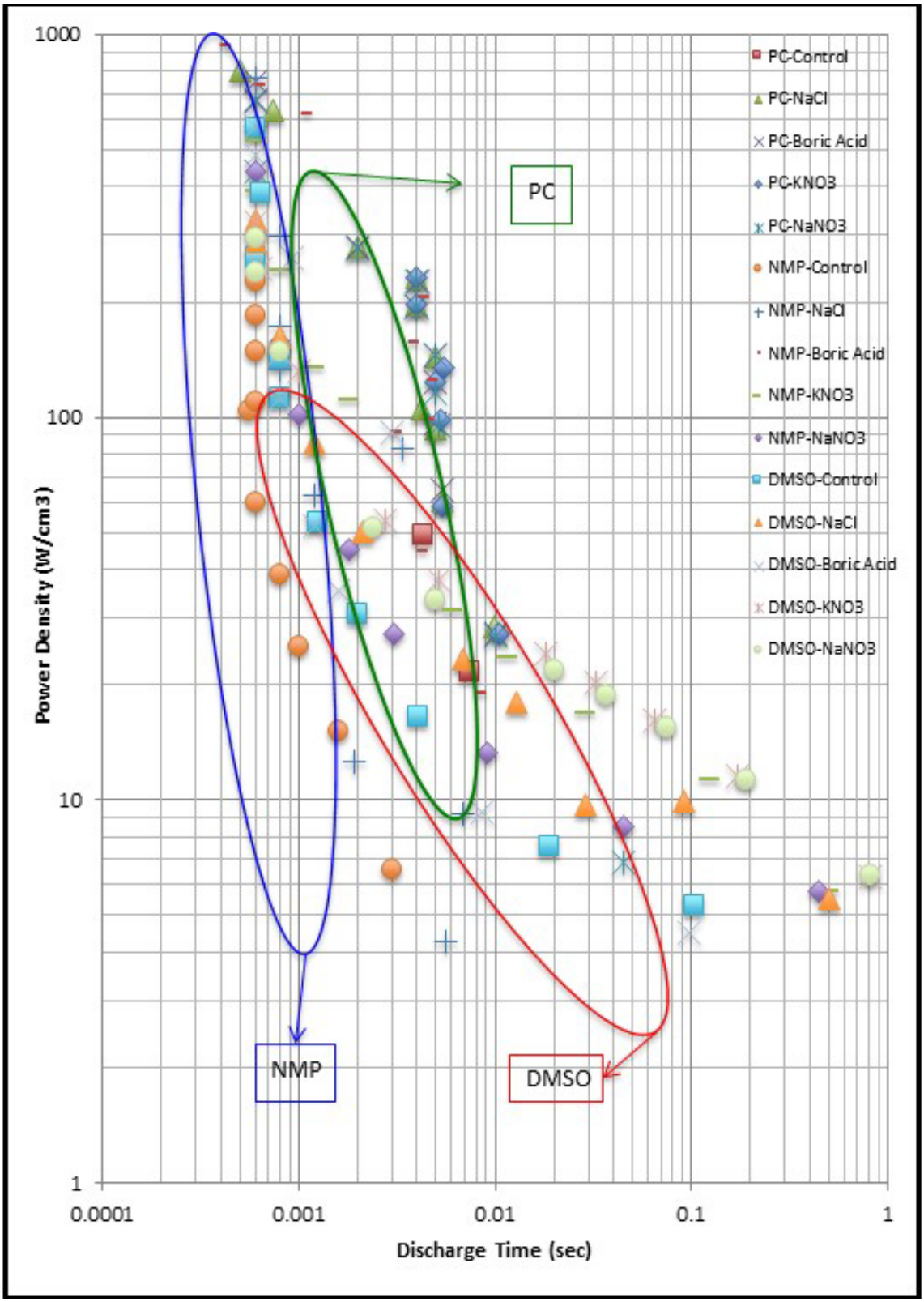

Figure 53. Power Density (W/cm^3) from High Frequency Tests

Figure 54 shows a zoomed in perspective of the blue and green-circled areas from Figure 53. This was done to analyze whether or not the data points were reliable based on the discharge times. The data for discharge times less than 0.002 seconds (red vertical line), is considered unreliable. As a matter of fact, all the data points resulting from most of the NMP and PC testing may be unreliable and further consideration and analysis of additional performance parameters is required. This includes the peak power density obtained from the NMP/Boric Acid solution, 935 W/cm^3. The power densities to the right of the red vertical line ranged from 13–228 W/cm^3.

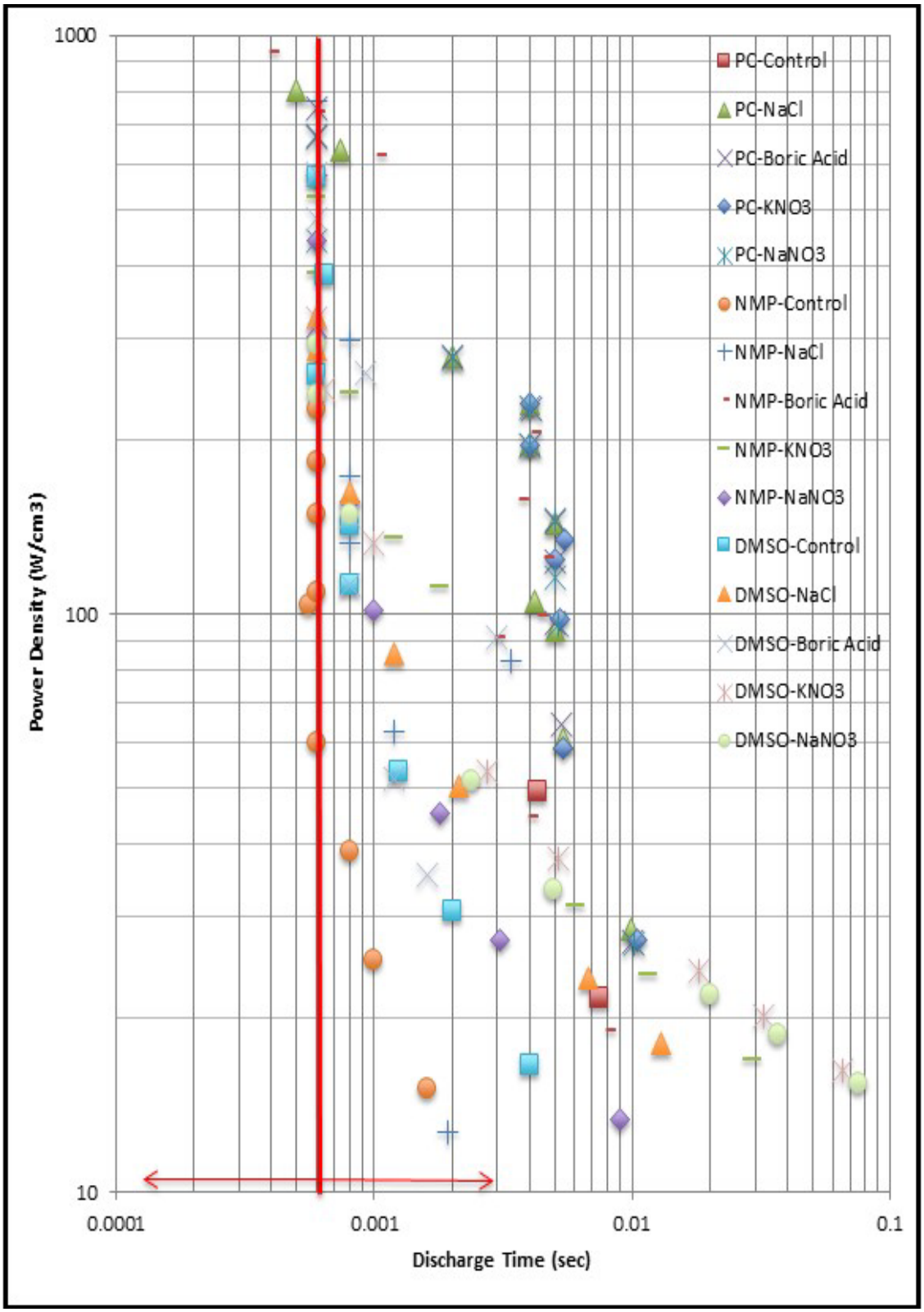

Figure 54. Focused Look at Circled Blue and Green Area from Figure 47

Tables 70–74 show the power densities of the tested solvent and salt combinations for the High Frequency tests. The PC combined with any salt produced a higher power density compared to the other solvents and salt combinations at the High Frequency testing current of: 20 mA, 30 mA and 50 mA. At currents above 50 mA, NMP combined with any salt yielded a higher power density than any other solvent and salt combinations. Another observation was that all three solvents followed a similar discharge pattern. The power density maintained a smooth exponential decay at the longer discharge times and then yielded a straight-line discharge for approximately one decade. This occurred at the High Frequency testing currents. The final observation was that the PC mixed with the control solution did not work above 50 mA. The higher currents shorted the capacitor and cause irrevocable damage to the TiO_2 sample that prevented subsequent testing with that particular sample.

Table 70. Power Density of Tested Solvents and Control Solution

	PC	NMP	DMSO
Control	Power Density (W/cm^3)		
	21.6	6.6	5.3
	49.3	15.1	7.6
	0.0	25.1	16.6
	0.0	38.8	30.7
	0.0	60.0	53.2
	0.0	104	112
	0.0	109	143
	0.0	149	260
	0.0	184	384
	0.0	226	570

Table 71. Power Density of Tested Solvents and NaCl Solution

	PC	NMP	DMSO
NaCl	Power Density (W/cm^3)		
	28.5	4.3	5.5
	60.8	12.7	9.9
	93.4	83.0	9.7
	106	9.2	18.0
	144	62.7	23.4
	197	133	50.4
	231	173	85.5
	279	297	162
	633	575	287
	802	772	326

Table 72. Power Density of Tested Solvents and Boric Acid Solution

	PC	NMP	DMSO
Boric Acid	Power Density (W/cm^3)		
	27.0	19.1	4.5
	64.5	44.6	9.3
	96.1	90.8	90.8
	123.0	99.0	35.2
	145	125	51.9
	195	157	112
	227	205	148
	279	621	261
	749	739	482
	669	935	578

Table 73. Power Density of Tested Solvents and KNO_3 Solution

	PC	NMP	DMSO
KNO_3	Power Density (W/cm^3)		
	27.2	5.8	6.3
	58.7	11.2	11.5
	98.0	16.9	16.2
	124	23.7	20.2
	134	31.3	24.1
	196	112	37.6
	230	135	53.5
		241	132
		389	244
		525	325

Table 74. Power Density of Tested Solvents and $NaNO_3$ Solution

	PC	NMP	DMSO
$NaNO_3$	Power Density (W/cm^3)		
	26.8	5.8	6.4
	6.9	8.5	11.4
	95.7	13.3	15.4
	116	27.3	18.8
	145	45.3	21.9
	196	101	33.5
	227	156	51.6
	276	301	149
	440	440	239
	673	573	293

Based on the results obtained above, the high frequency test results are categorized into two groups based on whether or not the OPS salt solution was accepted or rejected for further study, development and possible implementation. The acceptance criterion was based on the highest energy density obtained for each OPS salt solution combined with the power density at the 0.01-second discharge point.[4] It was determined

[4] The Navy is interested in short pulse weapons systems that require significant power discharged in the range of 0.01 seconds.

that energy densities less than 5 J/cm^3 and power densities less than 10 W/cm^3 were not considered for subsequent experimentation. These metrics are based on competing with the energy and power density values obtained from previous group studies as well as a comparison to comparable commercial energy storage devices. The pure solvent salt solutions results are shown in Table 75 and the mixed solution containing PC + DI/NaCl are shown in Table 76.

Table 75. High Frequency Testing Acceptance Criteria Pure Solvent Solutions

Solvent	Salt	Energy Density (J/cm^3)	Power Density (W/cm^3)	Accept / Reject
PC	Control	0.2	21.6	Reject
	Boric Acid	0.9	27.0	Reject
	NaCl	0.8	28.5	Reject
	KNO_3	0.9	27.2	Reject
	$NaNO_3$	0.3	26.8	Reject
NMP	Control	0.1	6.6	Reject
	Boric Acid	0.9	19.6	Reject
	NaCl	0.5	4.3	Reject
	KNO_3	3.0	23.7	Reject
	$NaNO_3$	2.6	13.2	Reject
DMSO	Control	0.5	7.6	Reject
	Boric Acid	0.4	4.5	Reject
	NaCl	2.7	18.0	Reject
	KNO_3	5.2	16.2	Accept
	$NaNO_3$	5.3	15.4	Accept

Table 76. High Frequency Testing Acceptance Criteria Mixed Solvent Solution

Solvent	Concentration (PC / DI+NaCl)	Energy Density (J/cm^3)	Power Density (W/cm^3)	Accept / Reject
PC + DI/NaCl	95 / 05	0.9	26.0	Reject
	90 / 10	10.8	17.9	Accept
	85 / 15	6.9	28.8	Accept
	80 / 20	26.1	24.7	Accept
	75 / 25	14.2	21.2	Accept

D. FHS TESTING

Despite the relatively large energy densities associated with the FHS testing, the subsequent long discharge times produced extremely low power densities. The power density results from FHS testing ranged from 0.5–0.9 W/cm^3 for all solvent and salt solution combinations. This indicates that for this set of capacitors, and possibly all SDM based capacitors FHS type of testing may be unsuitable when high power is required.

E. DISCUSSION OF VARIABLES

1. Viscosity and Density

This thesis postulates that the viscosities and densities of the various non-aqueous solvents play a significant role in capacitor performance. The density of water was used because it is an established and well-documented reference. Table 77 compares the viscosity of the tested non-aqueous solvents and water. The first observation was that water was the less viscous liquid of the group. During testing, the breakdown voltage of water was 2.3 volts, NMP was 3.8 volts, DMSO was 4.0 volts and PC was 9 volts. Therefore, as the density of the liquid increased, so did the breakdown voltage.

Table 77. Kinematic Viscosity and Density of Water and Tested Solvents, at $20^{o}C$

	Kinematic Viscosity (mPa)	Density (g/ml)
Water	1.0016	0.9982
NMP	1.67	1.025
DMSO	1.99	1.095
PC	2.5	1.2

The second observation was that the more dense fluid would require a longer time for the existing salt ions to form the large dipoles. Once the large dipoles were formed, they could maintain the ideal dipole orientation for a longer time. This observation was made when analyzing the FHS tests at the 300-second hold cycle for three non-aqueous solvents mixed with the NaCl salt solution. The results were NMP yielded an energy density of 3.8 J/cm^3 and a hold time of 9.3 second; DMSO yielded an energy density of 16.7 J/cm^3 and a discharge time of 51 seconds; and PC yielded an energy density of 91.5 J/cm^3 a discharge time of 133 seconds. Based on this small sample, the energy density and discharge time increased as a function of density.

2. Drying Salts

When a bottle of NH_4F is not properly stored in the desiccant holder. This allowed moisture to contaminate the NH_4F and cause errant results. In order to prevent the introduction of water into a test system (solvent and salt solution), all chemicals intended for testing would remain in a vacuum chamber with desiccant material for a period of at least 24 hours.

It was then postulated that the exploratory and initial testing results obtained for this thesis might be unreliable because the salts utilized for this work were exposed to the atmosphere and no attempt was made to remove the moisture before testing. When the salts were needed for testing they were immediately transferred from the vacuum to the non-aqueous solvent to minimize the absorption of atmospheric moisture into the system.

The dried salts, when mixed in the various non-aqueous solvents, had significantly lowered the operating voltages but also stabilized the waveforms so there was no distortion on either the charge or the discharge phase at lower frequencies. This was an improvement over the salts that contained moisture because the charge and discharge waveforms were inconsistent and not smooth. Lastly, there was a slight increase in discharge time but it is difficult to attribute the increase solely to the dried salts.

3. Dissolving Salts

The selected salts, when mixed with the non-aqueous solvents, did not form a saturated ionic solution. Failing to dissolve a significant amount of salt prevented the formation and alignment of large salt dipoles and thus limited the capacitors ability to create energy. Despite the various methods used to create a saturated ionic salt solution; no one method successfully dissolved the salt. Methods to dissolve salts included adding heat, manual agitation, ultrasonic agitation and time [41]–[43].

V. CONCLUSIONS AND FUTURE WORK

This thesis advanced the study of the Novel Paradigm Supercapacitors (NPS) by analyzing performance of NTSDM in which, for the first time, non-aqueous and mixed non-aqueous based ionic salt solutions were used. The engineering goal focused on the development of second-generation NTSDM that operated at higher voltages than aqueous solutions. In turn, operation at higher voltages potentially produces higher energy and power densities. Similar to previous group research, the NTSDM consisted of a titanium dioxide array of nanotubes that allowed for the storage and subsequent alignment and formation of large ionic salt dipoles. The NPS were tested for capacitive performance as a function of frequency. The effectiveness of the system was determined by evaluating the energy density, power density, capacitance, and dielectric constant.

The three non-aqueous solvents evaluated in this study successfully attained operating voltages in the range of 3.0–5.0 volts. These voltages are significantly higher than realized in previous studies. However, the higher voltages did not result in higher energy densities as the best results attained were in the range of 90–155 J/cm^3. The power densities were initially favorable with a range of 700–950 W/cm^3 but with discharge times of 0.0004–0.0006 seconds. Previous research concluded that the limitations associated with the testing equipment and analyzing software precluded reliable data that correlated to discharge times of less than 0.002 seconds. Therefore, the large power densities associated with these short discharge times were considered unreliable. The remaining reliable energy and power densities were significantly lower than results attained in previous group studies. However, all results were still higher than the existing results presented in capacitive energy storage/power delivery research.

It was assumed that none of the non-aqueous solvents successfully dissolved any of the salts. It was also noted that all non-aqueous solvents have realized saturation concentrations far below that of water. According to SDM theory, dipole length and the salt concentration are critical to the production of high NTSDM dielectric values. The absence of significant concentrations of dissolved salt significantly lowered the dielectric value of the solutions studied in this work, relative to the values obtained in earlier

studies using only aqueous solutions. As a consequence, there did not exist a sufficient amount of formed large dipoles to facilitate maximum energy storage. In an effort to combine high salt concentrations with high breakdown voltages, liquid mixtures were tried. Specifically, a non-aqueous solvent was mixed with a saturated salt solution of distilled water and NaCl. DI and NaCl produce a saturated solution at 35.7 g of NaCl to 100 g of DI [43]. PC was selected as the non-aqueous solvent due to it possessing the highest tested voltages of 7.0–9.0 volts with the control solution. The DI/NaCl solution was added to the PC in varied concentrations with the ideal amount of DI/NaCl solution at approximately 15–20%. Maximum values obtained in this range were: energy density-143 J/cm^3, longest discharge time-240 seconds and voltage-7 volts.[5] In particular, the maximum obtained voltage was far better than a single water solution.

The results were not on par with the extremely high performance parameters established by the NPS energy group for aqueous salt solution based NTSDM. Despite this fact, there is value in continuing research in the use of non-aqueous solvents as long as a higher priority is placed on saturating a selected solvent with an ionic salt solution. This is the best way to test the theory that the obtained higher voltage will result in a higher energy and power density.

It was assumed that the various methods to dissolve the salts failed simply because the selected non-aqueous solvents would not dissolve the selected salts. Despite these failures, NMP, DMSO and PC provided positive results with regard to increasing the operating voltage of the ionic salt solution and should remain at the center of future research. The challenge is discovering a set of complimentary salts that will dissolve in the selected non-aqueous solvents. Another way to address the saturation issue is to discover additional methods to dissolve salts. Other methods could include electrolysis, boiling, agitation for longer periods of time and compounding mixtures [44]. Compounding mixtures is popular when using a DMSO salt saturated solution to preserve coral reef DNA [45]. Expounding on how DMSO is used to preserve coral reef DNA, an

[5] The highest attained energy density was 158 J/cm^3. However, that number was an extrapolated value based on the linear fit curve. Since the linear fit curve was based on a reliable set of data points, it is believed that this is an achievable number.

initial solution of ethylenediaminetetraacetic acid (EDTA) is mixed with nanopure water and NaOH to make neutral pH solution [44]. DMSO is then added with NaCl to make the salt saturated solution. Similar to all the salts used throughout this thesis, the solubility limits were not documented so NaCl was added until precipitates formed in the solution.

The other issue requiring additional research is the leakage rate of the NTSDM capacitors created with the stated ionic salt solutions. The capacitors analyzed during this thesis were charged and then immediately discharged for all tests. Future tests would include charging the capacitor and then removing the energy source for a period of time. At the end of the wait period, the capacitor would be discharged. In theory, the large salt dipoles should transition from their organized states back to their original unaligned states of disorder. It is assumed that the performance parameters would decrease due to the leakage of the capacitor.

THIS PAGE INTENTIONALLY LEFT BLANK

LIST OF REFERENCES

[1] S. Fromille, "Novel concept for high dielectric constant composite electrolyte dielectrics," M.S. thesis, Dept. Mech. Eng., Naval Postgraduate School, Monterey, CA, 2013.

[2] S. M. Lombardo, "Characterization of anodized titanium-based novel paradigm supercapacitors: impact of salt identity and frequency on dielectric values, power and densities," M.S. thesis, Dept. Mech. Eng., Naval Postgraduate School, Monterey, CA, 2017.

[3] Office of Naval Research. (n.d.). Electromagnetic railgun. [Online]. Available: https://www.onr.navy.mil/en/Media-Center/Fact-Sheets/Electromagnetic-Railgun. Accessed May 13, 2007.

[4] Navy Live. (April 12, 2015). Concept to completion: Laser weapon system begins with Einstein's deduction. [Online]. Available: http://navylive.dodlive.mil/2015/04/12/concept-to-completion-laser-weapon-system-begins-with-einsteins-deduction/. Accessed May 13, 2017.

[5] Office of Naval Research. (n.d.). Historic leap: Navy shipboard laster operates in Persian Gulf. [Online]. Available: https://www.onr.navy.mil/Media-Center/Press-Releases/2014/LaWS-shipboard-laser-uss-ponce.aspx. Accessed May 13, 2017.

[6] Kyle Mizokami. (October 19, 2016). The Zumwalt destroyer is here, now what about the railgun? [Online]. Available: http://www.popularmechanics.com/military/navy-ships/a23440/zumwalt-destroyer-railgun/. Accessed May 13, 2017.

[7] J. Mugg. (August 10, 2016). US Navy's railgun dream could be denied by two big problems. [Online]. Available: http://nationalinterest.org/blog/the-buzz/us-navys-railgun-dream-could-be-denied-by-two-big-problems-17301. Accessed May 13, 2017.

[8] T. Casey. (November 5, 2013). Navy's new "all-electric" destroyer is a seagoing microgrid. [Online]. Available: https://cleantechnica.com/2013/11/05/us-navy-launches-new-all-electric-zumwalt-destroyer/. Accessed May 13, 2017.

[9] M. C. Stewart, "Comparison of two railgun power supply architectures to quantify the energy dissipated after the projectile leaves the railgun," M.S. thesis, Dept. Elect. & Comp. Eng., Naval Postgraduate School, Monterey, CA, 2016.

[10] General Atomics and Affiliated Companies. (n.d.). EMALS – Launching aircraft with the power of the railgun. [Online]. Available: http://www.ga.com/emals-subsystems. Accessed May 13, 2017.

[11] A. M. Still, “Electromagnetic launchers for use in aircraft launch at sea,” M.S. thesis, Cockrell School of Eng., University of Texas, Austin, TX, 1998.

[12] U.S. House, Committee on the Armed Forces. *Oversight of the electromagnetic aircraft launch system (EMALS).* (H. Rpt. H.A.S.C. No. 111-83). Washington, DC: Government Printing Office, 2009.

[13] Office of Naval Research. (n.d.). Free Electron Laser. [Online]. Available: https://www.onr.navy.mil/en/Media-Center/Fact-Sheets/Free-Electron-Laser. Accessed May 13, 2017.

[14] C. Dillow. (January 20, 2011). The Navy’s megawatt laster weapon takes a big leap forward with powerful new electron injector. [Online]. Available: http://www.popsci.com/technology/article/2011-01/navys-free-electron-laser-weapon-takes-big-leap-forward-powerful-new-electron-injector. Accessed May 13, 2017.

[15] S. Ackerman. (February 18, 2011). Unexpectedly, Navy’s superlaster blasts away a record. [Online]. Available: https://www.wired.com/2011/02/unexpectedly-navys-superlaser-blasts-away-a-record/. Accessed May 13, 2017.

[16] U.S. Navy: Energy, Environment and Climate Change. (n.d.). Energy. [Online]. Available: http://greenfleet.dodlive.mil/energy/. Accessed May 13, 2017.

[17] M. Jayalakshmi and K. Balasubramanian, “Simple capacitors to supercapacitors-an overview,” *Int.J.Electrochem.Sci*, vol. 3, pp. 1196–1217, Sep. 2008.

[18] J. Phillips et al., “Toward a universal model of high energy density capacitors,” unpublished.

[19] S. Fromille and J. Phillips, “Super dielectric materials,” *Materials*, vol. 7, 8197–8212, 2014. doi: 10.3390/ma7128197

[20] MIT: Electricity and Magnetism Course Notes. (n.d.). Guide 5: Chapter 5 – Capacitance and Dielectrics. [Online]. Available: http://web.mit.edu/viz/EM/visualizations/coursenotes/modules/guide05.pdf. Accessed May 13, 2017.

[21] Joules – Joint Operation for Ultra Low Emission Shipping. (n.d.). Technologies – Storage, distribution, electrical, convertors. [Online]. Available: http://www.joules-project.eu/Joules/technologies/storage_distribution_electrical_convertors. Accessed May 17, 2017.

[22] L.L. Zhang and Zhao, X.S, “Carbon-based materials as supercapacitor electrodes,” *Chemical Society reviews*, vol. 38, no. 9, p. 2520, 2009.

[23] J. W. Gandy, “Characterization of micron-scale nanotubular super dielectric materials,” M.S. thesis, Dept. Mech. Eng., Naval Postgraduate School, Monterey, CA, 2015.

[24] C. Pecharromán,F. Esteban-Betegón, and R. Jiménez, “Electric Field Enhancement and Conduction Mechanisms in Ni/BaTiO 3 Percolative Composites,” *Ferroelectrics*, vol. 400, no. 1, pp. 81–88, 2010.

[25] P. Lunkenheimer et al, “Colossal dielectric constants in transition-metal oxides. The European physical journal,” *Special topics*, vol. 180, no. 1, pp.61–89, 2009.

[26] P. Lunkenheimer et al, “Nonintrinsic origin of the colossal dielectric constants inCaCu3Ti4O12,” *Physical Review B: Condensed Matter and Materials Physics*, vol. 70, no. 17, 2004.

[27] P. Lunkenheimer et al, “Origin of apparent colossal dielectric constants,” *Physical Review B: Condensed Matter and Materials Physics*, vol. 66, no. 5, 2002.

[28] F. J. Q. Cortes and J. Phillips, “Tube-super dielectric materials: electrostatic capacitors with energy density greater than 200 J·cm-3,” *Materials,* vol. 8, 6208–6227, 2015. doi: 10.3390/ma8095301

[29] N. L. Jenkins, “Optimal super dielectric material,” M.S. thesis, Dept. Mech. Eng., Naval Postgraduate School, Monterey, CA, 2015.

[30] Engineering and Technology History Wiki. (n.d.). Capacitors. [Online]. Available: http://ethw.org/Capacitors. Accessed May 13, 2017.

[31] J. Phillips and H. Zea. “Procedure for Creating Anodized TiO_2 Samples,” unpublished.

[32] Purdue University. (n.d.). Radiological and environmental management. Scanning electron microscope. [Online]. Available: https://www.purdue.edu/ehps/rem/rs/sem.htm. Accessed May 5, 2017.

[33] Bio-Logic. (n.d.). VMP-3000, The ultimate electrochemical workstation. [Online]. Available: http://www.bio-logic.net/wp-content/uploads/2015-biologic-vmp300.pdf. Accessed May 5, 2017.

[34] Targray. (n.d.). LiPF6 battery electrolyte solutions. [Online]. Available: http://www.targray.com/li-ion-battery/electrolyte. Accessed May 5, 2017.

[35] “Electrolytes for lithium batteries and fuel cells.” *Center for Nanomaterials Design and Assembly.* (n.d.). [Online]. Available: https://www.pa.msu.edu/cmp/CORE-CM/Baker.pdf. Accessed May 13, 2017.

[36] Lithium-ion battery. (n.d.). *Wikipedia.* [Online]. Available: https://en.wikipedia.org/wiki/Lithium-ion_battery. Accessed: May 05, 2017.

[37] Murata. (n.d.). Murata supercapacitor technical note-No. C2M1CXS-053L. [Online]. Available: http://www.murata.com/~/media/webrenewal/products/capacitor/edlc/techguide/electrical/c2m1cxs-053.ashx. Accessed May 5, 2017.

[38] "Electric ship weapon system: directed energy weapons," class notes for Electrical Power Engineering. Dept. of Mech. And Aerosp. Eng., Naval Postgraduate School, Monterey, CA, fall 2015.

[39] M. Fabey. (January 23, 2017). U. S. Navy develops stronger lasers. [Online]. Available: https://defensesystems.com/articles/2017/01/23/fabeylaser.aspx Accessed May 5, 2017.

[40] T. Christen and M. W. Carlen, "Theory of Ragone plots," *J. of Power Sources,* vol. 91, iss. 2, pp. 210–216, Dec. 2000.

[41] Fluka. (n.d.). 71376, 71378, 71386 Sodium chloride (Halite, Common Salt or Table Salt, Rock Salt). [Online]. Available: https://www.sigmaaldrich.com/content/dam/sigma-aldrich/docs/Sigma/Datasheet/6/71376dat.pdf. Accessed May 13, 2017.

[42] Chem1-General Chemistry Virtual Textbook. (n.d.). Solubility equilibria of salts. [Online]. Available: http://www.chem1.com/acad/webtext/solut/solut-6a.html. Accessed May 13, 2017.

[43] H. L. Clever, M. E. Derrick and S. A. Johnson. (March 4, 1992). The solubility of some sparingly soluble salts of zinc and cadmium in water and aqueous electrolyte solutions. [Online]. Available: https://www.nist.gov/sites/default/files/documents/srd/jpcrd444.pdf. Accessed May 13, 2017.

[44] L.A. May et al., "Saline-saturated DMSO-EDTA as a storage medium for microbial DNA analysis from coral mucus swab samples," in NOAA Technical Memorandum, Feb 2011. NOS NCCOS 127.

[45] Roberts Lab: School of Aquatic and Fishery Sciences | University of Washington. (n.d.). Salt saturated DMSO for DNA preservation. [Online]. Available: http://faculty.washington.edu/sr320/?p=11628. Accessed May 21, 2017.

INITIAL DISTRIBUTION LIST

1. Defense Technical Information Center
   Ft. Belvoir, Virginia

2. Dudley Knox Library
   Naval Postgraduate School
   Monterey, California